CR-166178

SANITARY ENGINEERING RESEARCH LABORATORY
COLLEGE OF ENGINEERING
AND
SCHOOL OF PUBLIC HEALTH
UNIVERSITY OF CALIFORNIA
BERKELEY

REMOTE SENSING OF WATER QUALITY IN RESERVOIRS AND LAKES IN SEMI-ARID CLIMATES

by

Harold M. Anderson
Alexander J. Horne

NASA Grant Number
NSG-2003

December 1975

Sanitary Engineering Research Laboratory
College of Engineering
School of Public Health
University of California
Berkeley

SERL Report No. 75-1

TABLE OF CONTENTS

TABLE OF CONTENTS (continued)

LIST OF TABLES

LIST OF FIGURES

LIST OF FIGURES (continued)

LIST OF FIGURES (continued)

LIST OF FIGURES (continued)

ABSTRACT

Lakes and reservoirs in semi-arid zones are usually warm with abundant sunlight for much of the year. Such conditions are ideal for the growth of nuisance plants—particularly blue-green algae. In addition, erosion is often high since ground cover is sparse in dry drainage basins. This report describes a new system of monitoring lake water quality more effectively than conventional techniques.

Laboratory measurements *of natural populations of nuisance types of aquatic algae and higher plants irradiated with simulated sunlight produced characteristic reflected energy spectra (spectral signatures). It was possible to distinguish the spectral signature of blue-green algae—major nuisance types—from that of normally beneficial types such as diatoms, green algae, and the higher aquatic plant duckweed. Blue-green algae in particular reflected large quantities of light in the near infrared (NIR = 700-1050 nm) and more overall light per unit biomass (chlorophyll a) than other algae, but about as much as duckweed. Artificially induced collapse of the planktonic blue-green alga's buoyancy mechanism (which also occurs naturally) reduced reflectance over the whole spectrum (400-1050 nm). It is hypothesised that the spectral signature of planktonic blue-green algae is greatly dependent upon its cellular architecture—specifically the gas vacuoles which provide many air-cell protoplasm interfaces. The high reflectance of duckweed and most plant leaves is similar to that of planktonic blue-green algae for analogous reasons. Within broad ranges, NIR reflectance corresponded to chlorophyll a concentrations but "infinite thickness and thinness" prevented precise levelopment of this technique with out instrumentation.*

Overlake measurements *using aerial cameras (remote sensing) combined with water truth collected from boats most economically provided wide-band photographs rather than precise spectra. With use of false color infrared film (400-950 nm), the reflected spectral signatures seen from hundreds to thousands of meters above the lake merged to produce various color tones. Such colors were easily and inexpensively obtained and could be recognized by lake management personnel without any prior training. It was noted that the characteristic spectral signatures of various algal types were also recognizable—in part by the color tone produced by remote sensing. Fiery red indicates large concentrations of nuisance blue-green algae; pink, lesser quantities of blue-greens or masses of the aquatic duckweed plant; diatoms and green algae show faint white at abnormally high concentrations but are indistinguishable from the water in recreational lakes and reservoirs. Periphyton (generally green algae) and macrophytes show dark areas with a faint red tint. Turbidity, primarily due to reservoir edge erosion as the systems filled, was easily distinguished on color IR film.*

Patchiness *(spatial heterogeneity) provided an additional method of recognizing planktonic algae species. Blue-green algae almost always occurred in patches, sometimes showing microstructure—small-scale (1-20 m) patterning similar in appearance to a giant thumbprint. Green algae and diatoms showed no visible patchiness in the recreational waters studied, but exhibited faint patterns when highly concentrated as in sewage*

oxidation ponds. Patchiness in blue-green algae was visible on color IR film at chlorophyll concentrations greater than 10 ug/l--approximately a threshold for onset of nuisance conditions. An increase of two magnitudes in chlorophyll a was necessary for recognition of non-gas vacuolated algae.

Color IR pictures can be processed in time to study general accumulations of nuisance plants, but monochrome TV-type scanning provided instantaneous information. If the NIR band is used for scanning, the pattern produced can be used to identify blue-green algae and periphyton. However, for unknown reasons algal surface concentrations in the Southern California reservoirs were much lower than in other years, and were usually below the sensitivity of the method. This was not the case at Clear Lake, where remote sensing has proven very useful in the design and implementation of algal controls. The period 0800 to 0900 hours is most suitable for recognition of phytoplanktonic spectral signatures, but frequent morning fog over the Southern California reservoirs reduced filming time considerably and was the major drawback in economic use of the technique.

I. INTRODUCTION

NEED FOR THE STUDY

In reservoirs, as distinct from natural lakes, algal nuisance blooms are less acceptable because modern reservoirs are usually designed to allow heavy multipurpose use including recreation. However, due to their smaller size and more regular morphometry, reservoirs are generally more easily managed from the viewpoint of algal control. Nevertheless, algal controls are expensive and must be used economically.

As part of the California Water Plan several large multipurpose reservoirs have recently been created, all situated in the Los Angeles area. Even though some of these reservoirs are not yet full there is evidence of algal nuisance, and the optimal management for nuisance control is uncertain. (It should be noted that these reservoirs are limnologically unique because lakes in regions with Mediterranean climate do not normally have a continuous inflow of relatively nutrient-rich water.)

Nuisance scums of blue-green algae, excessive growths of aquatic weeds (macrophytes), shoreline periphyton (attached algae), and siltation constitute threats to the maximum life and use of multipurpose reservoirs. Taste and odor problems, restricted recreational use, and decreased water storage capacity are the natural consequences of these threats. Extensive biological and limnological monitoring programs provide a means to assess impaired water quality before it presents a threat to full water use, but the cost paid for such a service is often high [1-3].

User agencies (e.g. California Department of Water Resources) are aware of the shortcomings of conventional monitoring. For example, standard biological monitoring techniques often fail to observe complex algal distributions which arise under the influence of wind-induced water movements [4]. Indeed, when conventional limnological techniques are used, substantial horizontal variations in blue-green algal biomass in large bodies of water often go unobserved [5,6]. The wasteful use of expensive algal controls (e.g. $CuSO_4$) during treatment operations is often the result. Reservoir siltation, on the other hand, can usually be accurately monitored, but often little is known about the fate of the sediment after it enters the lake [1]. Goldman *et al.* note that an overall view of the complex deposition patterns of sediment and the effect of increasing sediment load on accelerated eutrophication processes is needed [7].

In California, design and construction of new reservoirs used primarily for recreation and drinking water are expected to increase during at least the next 30 years. As noted in the 1968 Annual Report of the California Department of Water Resources (DWR):

> "California is currently in the midst of constructing an unprecedented water project for one essential reason—the State has no alternative. Eighty percent of the people in California live in metropolitan areas from Sacramento to the Mexican border; however, 70 percent of the State's water supply originates North of the

> latitude of San Francisco Bay. Throughout the State, the bulk of rainfall occurs in a few winter months, while the summers, when water needs are greatest, are long and dry. The solution to California's maldistribution of water resources has been one of conserving the sporadic stream runoff in surface storage reservoirs and transporting supplies to areas of use. Progressively, larger storage works and longer conveyance systems have been required to meet the continuing growth in demands for water." [8]

As the need for water increases, large new reservoirs will undoubtedly have to be built in areas less favorable to siltation and biological control, inasmuch as many of the more suitable sites have already been used. Thus the cost of monitoring water quality will reach an excessively high level unless suitable alternative systems are developed. Coupled with this is the fact that as clear water reservoirs age, water quality often deteriorates [9]. It is not certain, however, if this is an inevitable consequence or merely a result of inadequate management of the reservoir system. Many natural lakes show cycles of oligotrophy and eutrophy, depending on the state of their watershed. Possibly management techniques to mimic whichever state is desired in the reservoirs and lakes can be determined and used. To do this a wide-ranging informational base is needed. This study hopefully provides a part of this foundation.

PURPOSE AND SCOPE

The initial objective of this study on the Southern California reservoirs was to provide a potential user agency (e.g. California DWR) with a method of recording rapidly the extent and nature of surface phenomena on reservoirs. Nuisance scums of blue-green algae, excessive growths of aquatic weeds, and mud flows are probably identifiable using remote sensing, a technique which needs some further development to be used in both the immediate and long-term management of these reservoirs. The two subsidiary aims in working with these reservoirs were to test the practicality of using:

1. Photographic observations which record changes in surface phenomena with time in relation to existing lake management methods. Use of conventional color infrared and four-band photography involves a time lag of 1-3 days for processing.

2. Instantaneous observations which record immediately, for example, the presence of nuisance algal scums and the effect of copper treatments. TV-video-type sensing using a multichannel scanner involves a zero time lag.

The art of remote sensing and research into applications of remote sensing in terrestrial environmental studies have reached an advanced state of development in recent years. Studies undertaken by NASA and others indicate potential uses for remote sensing techniques in monitoring water quality [2, 5-7, 10-14]. But as yet a comprehensive knowledge of how aquatic phenomena, over a wide range of concentrations, affect the spectral response of water bodies does not exist [14]. At the same time, preliminary observations of a joint study undertaken by Ames Research Center (NASA), the University of California at Berkeley, and Clear Lake

Algal Research Unit (CLARU) have established that nuisance concentrations of certain aquatic species (notably blue-green algae) are easily recognized in remote sensing imagery [5, 6].

Agencies in charge of water quality control are concerned with the appearance of nuisance species and high concentrations of aquatic algae. With some additional knowledge of algal spectral signatures, remote sensing techniques might be preferable to conventional limnological techniques in monitoring water quality of lakes and reservoirs of the semi-arid zone. To this end, the following specific objectives were set:

1. Determine the feasibility of providing user agencies with a provisional manual on remote sensing of aquatic phenomena in reservoirs, including information on techniques presently in use and information on the general state of the art.

2. Further define the reflected light spectral characteristics (spectral signatures) of aquatic phenomena present at nuisance levels. a) Determine if nuisance blue-green algae can be differentiated from other algae on the basis of their spectral response. b) Determine the usefulness of the infrared wavelength band in identifying surface blooms (and concentration) of nuisance phytoplankton.

3. Determine whether or not more conventional imaging devices commonly available at low cost to the public can be used in reservoir studies to give useful water quality data without an extended time lag.

Four studies jointly conducted by Ames Research Center (NASA) and the Sanitary Engineering Research Laboratory of the University of California (SERL) were completed on large multipurpose reservoirs in the Los Angeles area. NASA-Ames provided the aerial reconnaissance using multispectral photography or light filtered closed-circuit television. Concurrent with aerial reconnaissance, ground truth measurements of algal biomass, algal species, light penetration, and turbidity were accomplished using SERL personnel and equipment. Imagery and knowledge gained from the Clear Lake study were used as a basis for comparison with the results of the Southern California study. Some of the previously unpublished material assembled from the Clear Lake study is also presented in this report. Analysis of ground truth samples and imagery was carried out at SERL, as was the research into the nature of light reflectance by nuisance levels of aquatic phenomena.

The four reservoirs used in the California State Water Project were: Perris Lake (Riverside County), Castaic Lake (Los Angeles County), Silverwood Lake (San Bernardino County), and Pyramid Lake (Los Angeles County). Even though 1974 was the first year of simultaneous operation of all four reservoirs, evidence of algal nuisance was already present and optimal management for nuisance control was uncertain. Hence it was felt that these reservoirs might provide the ideal test location for the use of remote sensing in aquatic systems where water quality standards must be kept high.

ORGANIZATION

The project is part of the general research on lake eutrophication in California lakes and estuaries under the faculty investigatorship of Dr. A. J. Horne, and was a cooperative effort between the Sanitary Engineering Research Laboratory (SERL) at the University of California in Berkeley and the Ames Research Center (NASA). Funds for the study were derived from an extension of NASA's original grant No. NSG-2003 (NASA funding source 176-53-11) entitled "Remote sensing and large-scale movements of nuisance algal blooms in eutrophic water bodies as related to water truth measurements."

ACKNOWLEDGMENTS

Many individuals directly concerned with California's water quality contributed toward this study. The authors wish to thank the California Department of Water Resources (Southern California Division); Mr. R. C. Brown, DWR, Sacramento for assistance with photographic reproductions; Ames Research Center; the Clear Lake Algal Research Unit (CLARU); and Lake County for their assistance. In particular, the collaboration of Mr. C. J. W. Carmiggelt and Mr. W. D. Hansen was greatly appreciated. Special appreciation is also extended to Mr. H. J. Naftzger (Research Assistant, SERL), Dr. John Elder (Research Fellow, SERL), Mr. R. Wrigley (Research Scientist, NASA-Ames), Mr. Steve Klooster (Research Scientist, NASA-Ames), Mr. C. Wezernak (Research Scientist, Environmental Research Institute of Michigan), Ziba Photography, Berkeley, and Ms. R. Guidi for their assistance in technical data interpretation and cooperation in report preparation.

II. RECOMMENDATIONS

Remote sensing techniques were demonstrably useful in determining the presense, extent, and location of blue-green algae in water bodies. Therefore, as a tool for water quality evaluation, photographic remote sensing could benefit water-use agencies. This study indicates that unless lakes have massive blue-green algal blooms, the closed-circuit television system is of little value, even though results could be obtained instantaneously. Further studies are recommended to:

1. Delineate the ways in which reflectance varies with concentration of blue-green, green, diatoms, and dinoflagellate algae. Such experiments should also determine reflectance when a mixture of the above components is present.

2. Define how the physiological state of algae from different groups affects spectral response. Ideally, this would necessitate the use of controlled laboratory situations where nutrient, light, and chemical stresses could be more accurately monitored.

3. Produce a model system for aerial monitoring (remote sensing) of water quality based upon the present study. Such a program would undoubtedly also use conventional limnological monitoring to test which system is a more effective early warning signal for nuisance algae.

4. Extend the research on reflected light signatures of water bodies processing nuisance algal problems to areas outside the semi-arid region of California. This should determine the usefulness of this system in other environments. Such a program would compare the *in situ* light scattering properties of a variety of lakes by both aerial photographic and spectroradiometeric means. This approach takes into account subtle changes in water conditions which cannot be reproduced in a laboratory situation (e.g. changes in dissolved color causing changes in spectral signatures).

5. Determine feasibility of using inexpensive cameras for water quality monitoring. High resolution aerial photographs are the ideal system. Conventional 35 or 70 mm hand-held cameras could be adopted when cost is a limiting factor. A color infrared film with a simplified dye development similar to that of Polaroid films would be especially useful. The photographic industry could be consulted in this matter, where real time data collection was essential, as for example prior to copper sulfate treatment or algal harvesting by skimmers.

III. DESCRIPTION OF STUDY AREA

CASTAIC LAKE

Castaic Lake is the southern terminus of the West Branch of the State Water Project. Located in the Tehachapi Mountains of Los Angeles County, the reservoir in 1974 had a gross holding capacity of about 400 x 10^6 m^3, a surface area of about 890 ha, and a shoreline of about 46 km. At normal operation, the surface elevation is 432 m and the majority of the basin varies in depth from 35 to 93 m. The mean depth is 45 m.

The lake is composed of two arms which extend northeasterly (Elizabeth arm) and northwesterly (Castaic arm) from the dam. Above the Castaic arm is a small dam owned by the Los Angeles Department of Water and Power. The dam impounds a body of water known as the Castaic Lake forebay. Below the dam is an afterbay known as Castaic Lagoon (cf. Figure 1).

The shoreline around Castaic Lake is dentate, has steep slopes, and is marked with many coves. Natural inflow is limited to the Elizabeth arm where a small creek feeds into the lake with periodic water flows. Inflow from the State aqueduct arrives at the north end of Castaic arm and outflow takes place at the southern end. Because of the location of inlets and outlets, the water tends to be short-circuited through the Castaic arm and the arms form two distinct limnological basins. The nutrient-rich waters of the Castaic arm generally tend to be more productive than the nutrient-depleted waters of the Elizabeth arm during the many warm, dry summer months.

LAKE PERRIS

Lake Perris, located in the Perris Valley, Riverside County, is the southern terminus of the East Branch of the State Water Project. The reservoir has a maximum holding capacity of approximately 153 x 10^6 m^3, a surface area of 931 ha, and 16 km of shoreline. Lake Perris is shallow ($\sim$ 35 m at its maximum depth near the dam) and has only a gradual slope running east to west. Depths in the eastern portion are very shallow, averaging only 6 m. Surface elevation is 484 m at normal operation. Mean depth is 16.5 m (cf. Figure 2).

The lake is used at a regulatory and emergency storage reservoir. No natural flows feed it and inflow and outflow are again restricted to one end (deep west end and near the dam). This reservoir is the latest to be filled beginning in 1973 and was full by April 1974.

Strong afternoon winds (Santa Ana winds) in late summer affect circulation patterns a great deal and biomass is often concentrated on either the northwestern or southwestern side of Alessandro Island (see Figure 2). The eastern shore already has a growth of macrophytes (pondweed) and periphyton (mainly *Spirogyra*) on its rocky shallow shore. This southern climate is, given adequate nutrients, an ideal place for algal growths. However, except for the first few months of operation, this lake was relatively free of algal problems.

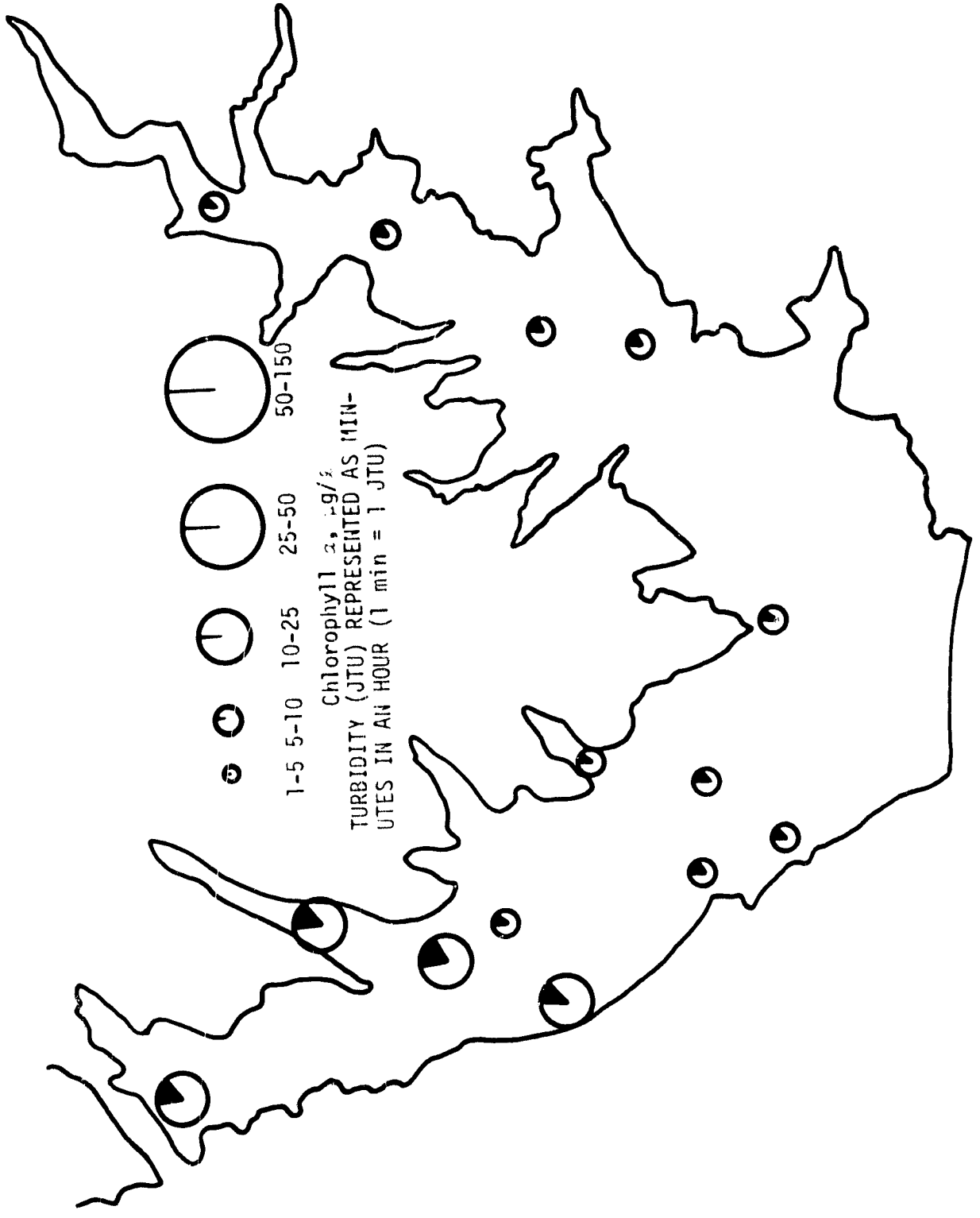

FIGURE 1. SKETCH MAP OF CASTAIC LAKE, 2 NOVEMBER 1974

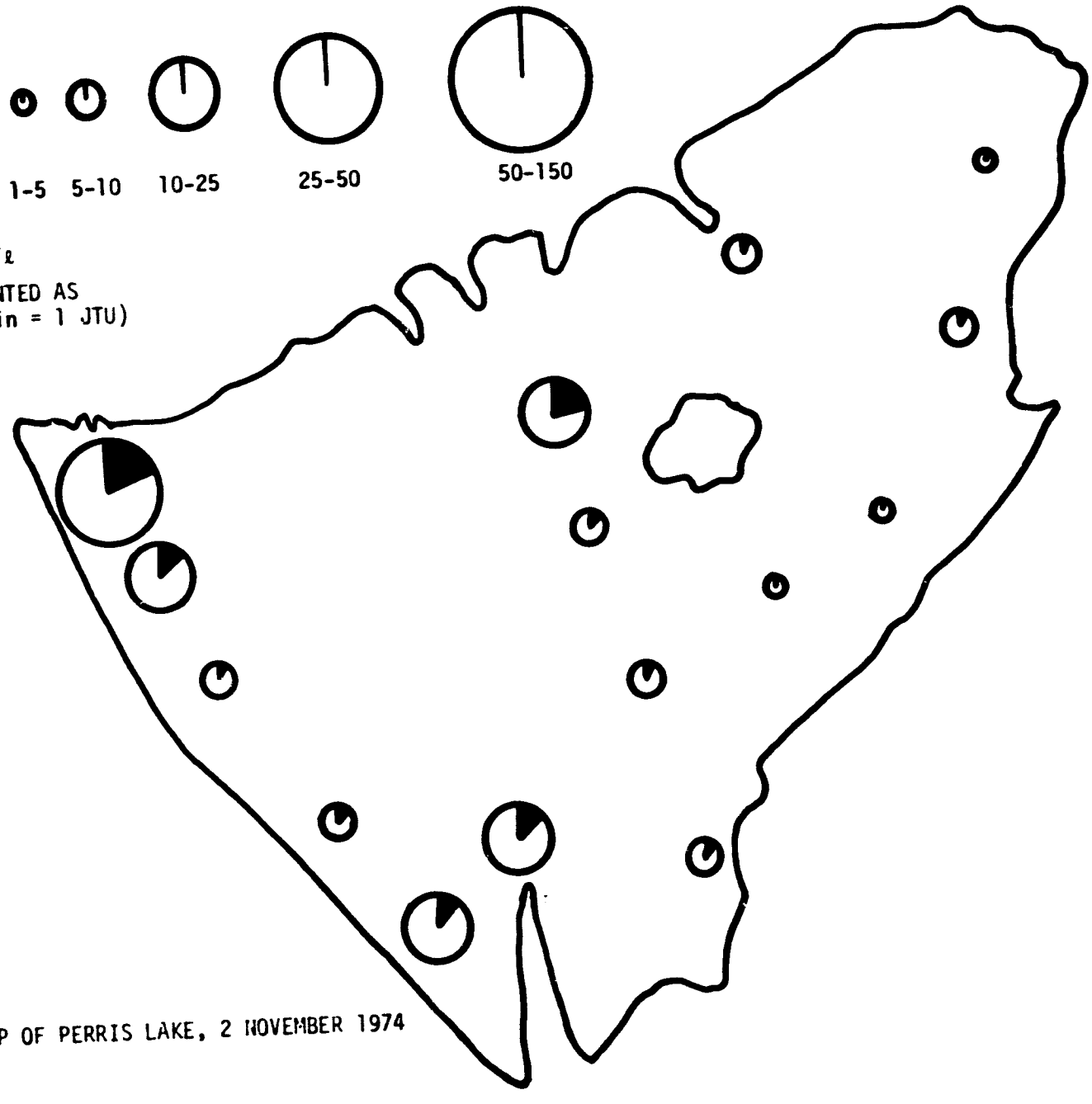

FIGURE 2. SKETCH MAP OF PERRIS LAKE, 2 NOVEMBER 1974

SILVERWOOD LAKE

Silverwood Lake is located at the 1020 m elevation of the San Bernardino Mountains. It has a maximum holding capacity of 93 x 10^6 m^3, a surface area of 394 ha, and 20.9 km of generally steep shoreline. Mean depth is 23.5 m (Figure 3). The climate is generally cooler than that of Perris or Castaic. Although freezing weather and snow are not uncommon from December through March, the reservoir does not freeze over.

Silverwood is operated as an in-line flow-through reservoir. Water which must traverse 100 miles of the Mohave Desert enters to the north and exits south. Silt deposition from storms is high and nutrient levels are generally also high.

PYRAMID LAKE

Pyramid Lake, located on the West Branch of the California aqueduct, has a maximum storage capacity of 2.21 x 10^8 m^3, a surface area of 550 ha, and a 34 km shoreline. Located in the Tehachapi Mountains (780 m surface elevation), Pyramid Lake has a climate similar to that of Silverwood. Water enters from the north by way of Gorman Creek improvement channel and exits from the south via the Angeles Tunnel. The lake is highly dentate with generally steep sides and a relatively flat sloping bottom. Mean depth is 40.6 m (Figure 4).

A characteristic of all the reservoirs is a continuous inflow of relatively nutrient-rich Sacramento River delta waters. Compounding this problem is the fact that the reservoirs, with the exception of Perris, have native influent streams which are relatively poor in quality, characterized by high hardness, alkalinity, sulfates, and boron. Erodable hills also contribute to the large sediment load, especially when fluctuations in water depth are great as during filling. Since at least two of the four reservoirs are located in regions where the climate is warm all year, the potential for nuisance algal blooms exists. All of the reservoirs are intended for intense recreational use and as drinking water. It is clear that such blooms are imcompatible with the proposed use. Optimal management programs are of utmost importance if the full potential of the reservoirs is to be utilized.

CLEAR LAKE

Although Clear Lake, California, was not part of the study area, remote sensing imagery of this highly eutrophic lake as part of the original NASA grant has been taken regularly for 2 years. Because widely ranging algal concentrations are often encountered on the lake, excellent imagery illustrating conditions not found in the reservoirs is referred to in the report. For this reason, a description of the lake is in order.

Clear Lake, which now belies its name, is better called by the Pomo Indian name Lupiyoma (= large water). It lies at an elevation of about 400 m in a valley in the northern coastal range of California and consists of a large, shallow Upper Arm and two smaller basins—Oaks Arm and Lower Arm (see Figure 6). Details of the physical parameters of the basins are given in Table II. Rainfall occurs only between September and April and

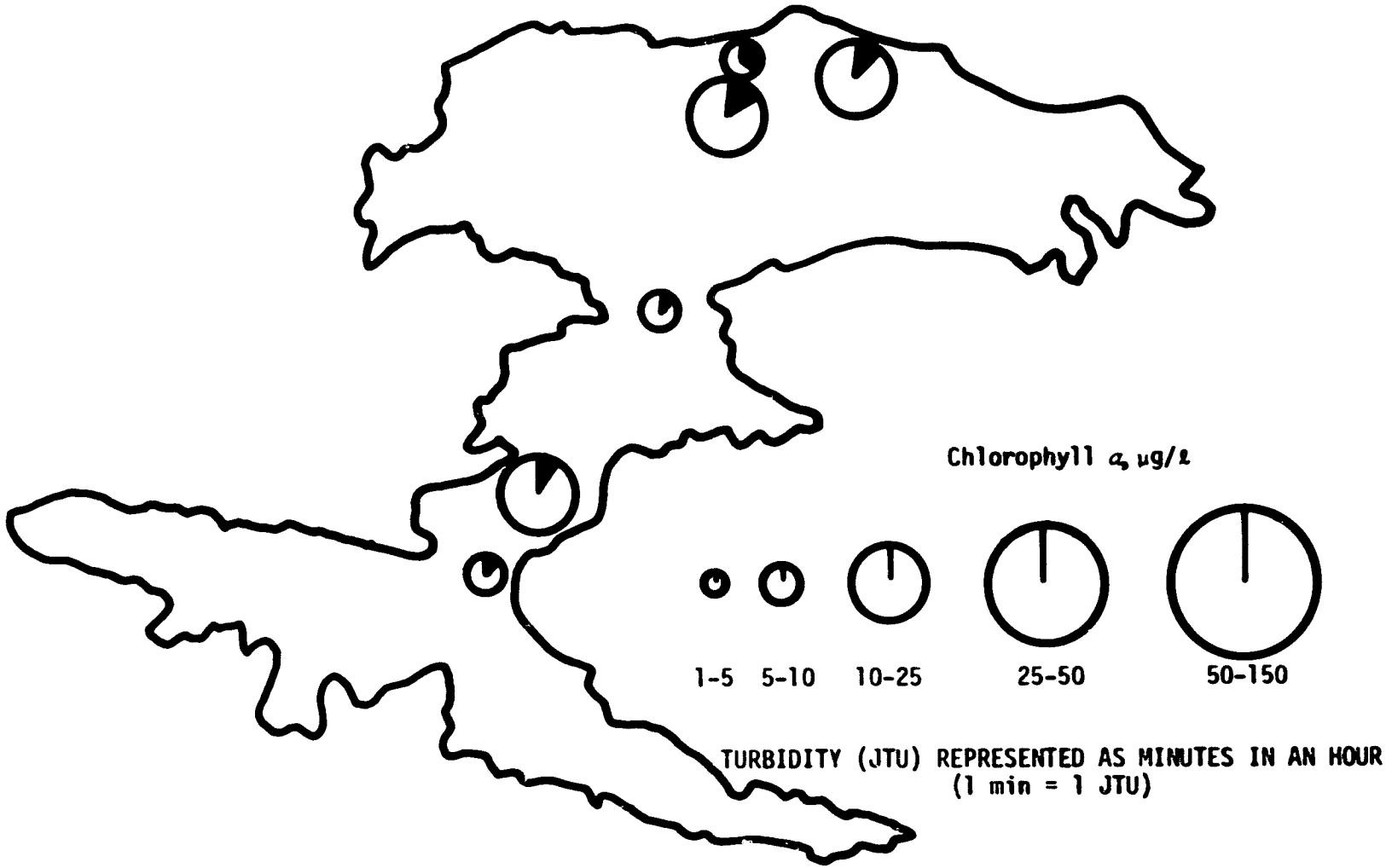

FIGURE 3. SKETCH MAP OF SILVERWOOD LAKE, 11 JULY 1974

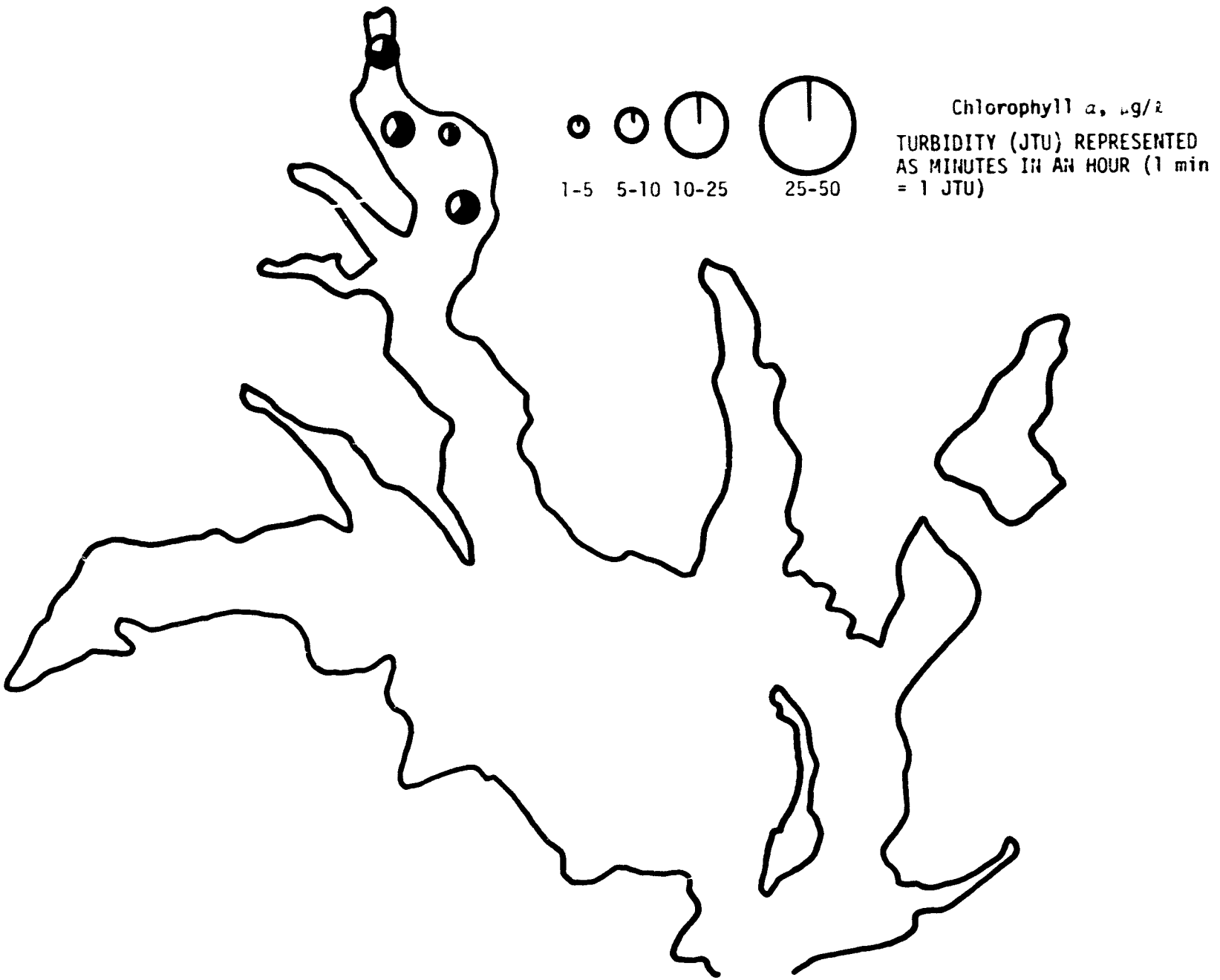

FIGURE 4. SKETCH MAP OF PYRAMID LAKE, 12 JULY 1974

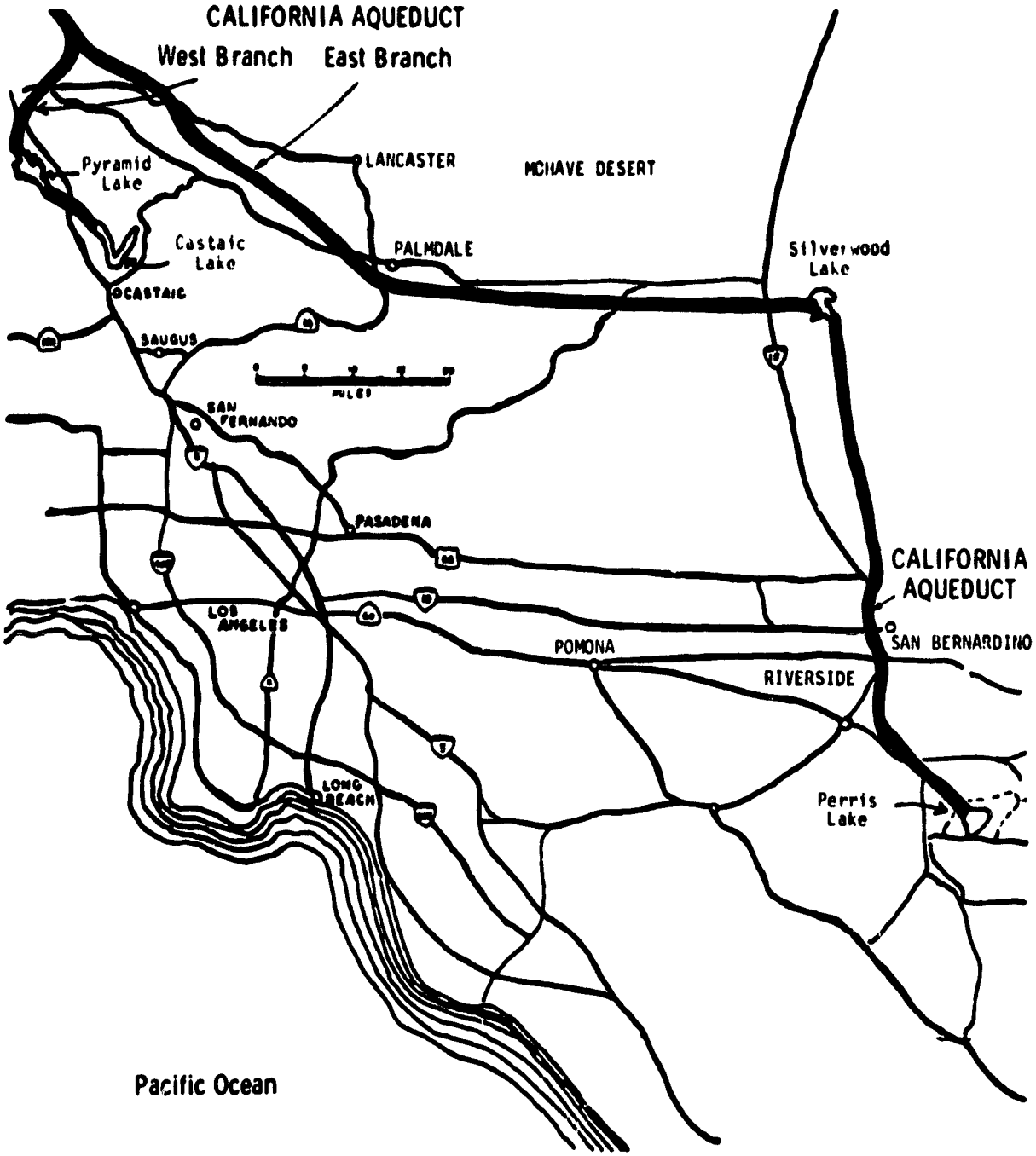

FIGURE 5. LOCATION OF THE SOUTHERN CALIFORNIA RESERVOIRS

TABLE I

PHYSICAL PARAMETERS OF THE SOUTHERN CALIFORNIA RESERVOIRS

Reservoir	Area	Depth		Shoreline	Total Volume
	$\underline{A}$ ha	$\overline{\underline{Z}}$ m	$\overline{\underline{Z}}_m$ m	$\underline{L}$ km	$\underline{V}$ $m^3 \times 10^6$
Castaic	890	45	93	46	400
Perris	931	16.5	35	16	158
Silverwood	394	23.5	--	21	93
Pyramid	550	40.6	--	34	221

TABLE II

PHYSICAL PARAMETERS OF CLEAR LAKE

Basin	Area	Depth		Shore-line	Max Length	Max Width	Total Volume
		Mean	Max				
	$\underline{A}$ ha	$\overline{\underline{Z}}$ m	$\overline{\underline{Z}}_m$ m	$\underline{L}$ km	$\underline{l}$ km	$\underline{b}$ km	$\underline{V}$ $m^3 \times 10^6$
Upper Arm	12,700	7.1	12.2	56	16.4	12.2	904
Lower Arm	3,720	10.3	18.4	39	13.4	4.3	384
Oaks Arm	1,250	11.1	18.4	19	8.5	2.6	138

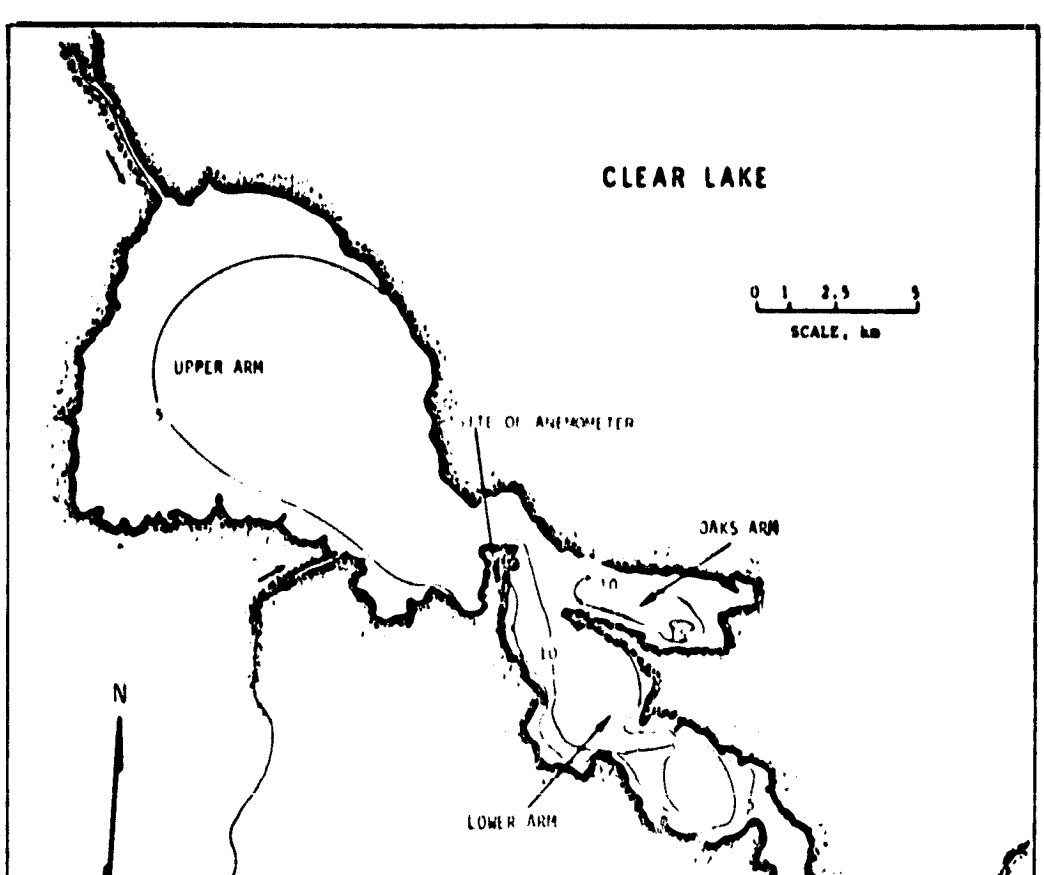

FIGURE 6. SKETCH-MAP OF CLEAR LAKE, CALIFORNIA
(Depths are indicated at 5-m intervals
and hatched areas represent small towns.)

ranges from 56 (valley) to 165 cm (hills), resulting in negligible streamflow after midsummer. Lake temperatures vary from 8-25° C. Thermal stratification persists for only short periods in summer, from a few hours to over a week, with that in Upper Arm being least resistant to breakdown by wind.

Presumably due to the large chemical and biological oxygen demand and high temperatures, the sediment remains anoxic from July until November with the 25 cm of water immediately overlying it also virtually anoxic (0-1.5 mg O_2/ℓ). A major feature of many lakes in northern California including Clear Lake is the high inorganic winter turbidity, mainly from suspended material brought in by the rivers. The vegetation of the watershed is largely foothill woodland with a relatively low, seasonally variable population density of 10-50 humans/km^2.

IV. METHODS

LAKE SAMPLING

Changing meteorlogical, air quality, and on-site water quality conditions controlled the selection of aerial reconnaissance dates. Sampling dates were chosen to give maximum variations in limnological conditions while air quality parameters were favorable (clear skies and moderate sun angle: 35 deg. above horizon). Unfavorable conditions, namely local fog, prevented sampling in August 1974.

During aerial reconnaissance, "water truth" observations of water quality conditions were made. Ten to twenty dip samples were collected per reservoir per flight. These samples were stored in one-liter bottles and kept dark and cool until turbidity could be measured. Water samples were filtered at the reservoir edges. Filtered samples were then stored in ice chests and transported to the laboratory. Such sampling procedure allowed sampling of each reservoir in less than two hours. In turbid or productive lakes, reflectances recorded by remote sensing techniques are influenced largely by particles in the upper part of the water column [15]. Thus the water truth data obtained by the dip sample procedure gives a good approximation of the suspended solid composition which influences spectral responses.

Samples were collected along transects of each reservoir. Transects were laid out so that a representative cross-section of each lake would be encountered. The station location was made to coincide with easily identifiable shore landmarks. On-site measurements of light transmission were taken at several stations (using a Tsurumi-Seiki light meter and a Secchi disk transparency) and field notes were kept of the visual condition of the water.

Sample analysis determined biomass (Chl *a*), algal species, and turbidty. Samples were filtered on GF/C filters, kept basic with $MgCO_3$, and frozen until analysis could take place. Chl *a* was determined by the hot 90% methanol extraction method of Talling and Driver [16]. The analysis of turbidity was carried out using a HACH 2100A nephalometer. Representative samples were preserved with Lugol's solution for phytoplankton identification. Some algal counts were furnished by the Department of Water Resources, Southern California Division, from six stations, using conventional Sedgwick-Rafter cell-counting techniques. Photographic records of algal species, relative numbers, and detritus per living cell ratios were made by SERL for the other stations not covered by the California DWR. A Nikon M.S. inverted microscope with a Nikon A.P.M. camera attachment was used for this purpose. Processing of the film was done by Kodak Corporation according to standard procedures.

REMOTE SENSING

Aerial reconnaissance of the Southern California reservoirs was carried out under the direction of the NASA-Ames Research Center. On three occasions, high altitude aerial photography was performed. Each photographic mission utilized both a Fairchild K-17 camera with a 305 mm focal

length lens and an International Imaging System MK-1 camera with four 100 mm focal length lenses. The K-17 camera used a Wratten 12 filter with Kodak(R) false color infrared film to produce a 225 mm x 225 mm positive with a scale of 1:10,000. The MK-1 camera was designed to record four 100 mm x 100 mm identical images on the same 225 mm x 225 mm area of the negative. Wratten filters 47B, 57A, 25, and 88A along with a special infrared blocking filter were used on respective lenses of the MK-1 camera to allow only one wavelength band through each of its four lenses. Therefore, the MK-1 camera with Kodak multispectral film 2424 or S.O. 289 photographed four identical images in the blue (400-470 nm), green (470-590 nm), red (590-690 nm), and IR (730-950 nm) wavelength bands, respectively. The scale of the MK-1 photographs was 1:30,000. The response of the color infrared film was measured prior to each flight by exposing a portion of the film to a density wedge, and based on this response, color compensating filters were used to insure accurate color reproduction. Calibration is essential if color tone is to be used analytically. (For details of this calibration process, see "Color Balance of Color-IR Film" by O. G. Malan [17].) The response of the four-band film was also measured by exposing a portion of the film to a density step-wedge. In this way four-band film properties could be compared from film exposed on different dates.

On two occasions, a light filtered closed-circuit television camera was used instead of the photographic equipment. Imagery was stored on videotape. A forward camera, shooting at 45 deg. from the horizon, was equipped with a Wratten 25 filter so as to record red and IR light only. The AFT camera was equipped with a Corning visible light filter and pointed directly down from the plane. the advantage of this system is that an indication of chlorophyll along flight tracks can be gained instantaneously.

Imagery analysis involved a twofold approach. Four-band multispectral imagery was analyzed for visual contrast by matching picture scene film density with a standardized wedge calibrated for 15 tonal values. (The wedge contained 21 steps, but it was felt that a maximum of 15 tones could be recognized in the imagery.) To accomplish this, each picture scene which represented backscattered light of a distinct waveband (i.e., blue, green, red, and infrared) was divided into discrete subsections corresponding with sampling stations, and each subsection was assigned a contrast density unit ranging from 1 to 15, with 1 being the lowest possible value, representative of clear lake water. For example, silt laden inflows or algal infested waters contrast strongly with either clear lake water or bottom reflectance.

When wind or water driven currents are active, water masses of varying sestonic composition result, which in turn affect spectral response [7]. Boundaries between clear and particle-rich water masses can often be discerned, and the type of spectral response measured from the particle-rich water mass will be indicative of the particle type (i.e., sediment or biomass). Obviously, a threshold surface particle concentration (which is dependent on the properties of the particle) sufficient to produce visual contrast in the film had to exist. for this reason, analysis was limited to areas where particle concentration was great and visual contrasts could be recognized.

Correlations between waveband spectral response and water-based observations were obtained for a variety of water conditions. Contrast values are valid for relative comparisons only at any one time and represent only generally similar contrasts for different sampling dates. The variations do give a general indication of the nature of the object in view (organic or inorganic) and to some extent its concentration (turbidity or chlorophyll *a*).

Color infrared imagery was analyzed for a second visual contrast unit, that of false color tone. When particle concentration in the water increases, a threshold concentration for the appearance of color tones distinct from shades of grey is approached. The way in which color tones in color IR film develop are indicative of particle type. In lakes supporting water blooms of algae of different groups, certain types appeared to be discernible on the basis of color tone. Also certain types of aquatic weeds and non-living debris could be identified on the basis of their respective color tone.

Spectroradiometric Instrumentation

An ISCO Spectroradiometer was used to measure the reflected light spectra of a known genus and concentration of algae under standard light conditions over a range of wavelengths extending from 350 nm to 1500 nm. The spectroradiometer was equipped with a Simpson recorder which recorded the spectral intensity observed as a function of wavelength ($\mu watt\ cm^{-2}\ m\mu^{-1}$). A one-meter glass fiber optics probe was used to transmit the light from the observation point to the machine's detector. The probe was used without a diffuser, and under these experimental conditions, the field of view could be limited to about a 20-cm diameter. The bandwidth resolution of the ISCO was approximately 15 μm.

Experiments were carried out under artificial illumination consisting of two 30-watt cool-white fluorescent lights, two 30-watt daylight fluorescent lights, and two 300-watt tungsten reflector flood lamps. These were arranged in a manner so as to give a spectral curve similar, though not identical, in shape to incident sun and skylight when the sun was approximately 30 deg. from the horizon on a cloudless Northern California day (Figure 7). A shallow (10 cm) flat-bottomed container lined with aluminum foil and painted black at the bottom sufficed as an approximate lake basin [18]. The light source was measured for both downwelling spectral irradiance and upwelling reflected light from a glossy surface before, during, and after such an experiment. The light source was arranged so as to be at the zenith angle from the tank (Figure 8).

The spectroradiometer recorded slightly different values on the two scales used (visible 350-750 μm, IR 750-1500 μm) but no attempt was made to relate the two scales as only relative spectral signatures were considered. No corrections for non-linearity of the sensor were made either, for the same reason. All measurements were taken at a fixed location relative to the tank and light array. Artificial lighting was utilized in preference to natural sunlight for two reasons. First, the laboratory study was made during the winter when sunlight conditions were poor. Second, artificial lighting kept a near constant illumination in comparison to sunlight which fluctuates widely with sun angle. Only the reflectance values recorded between 400 μm and 1050 μm are presented in this report.

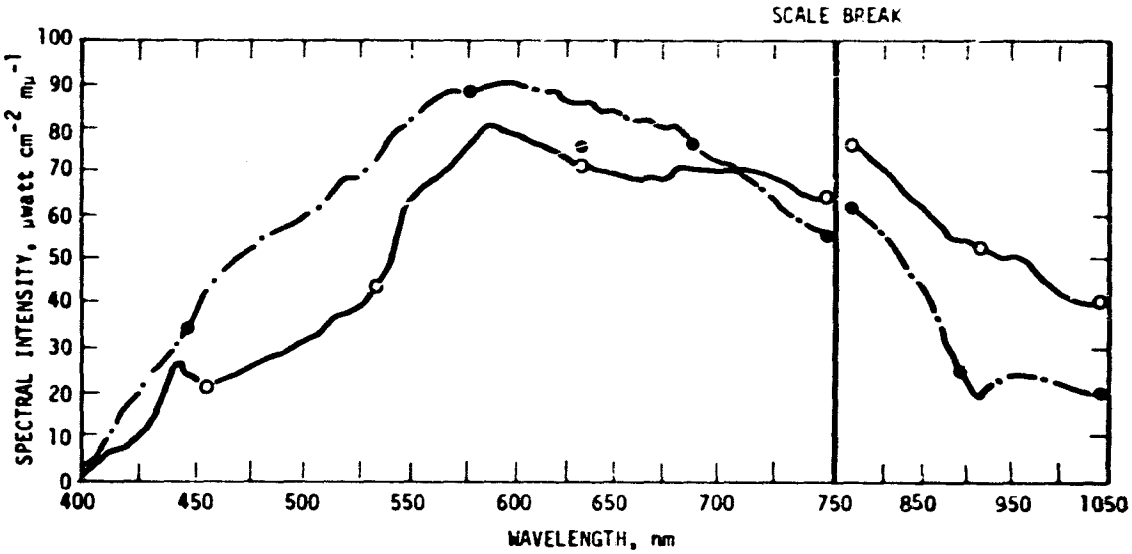

Note: No substantial changes were noted in the spectrum of the artificial light bank during the course of the experiments. All the spectral signatures presented in the experimental section should be considered relative to the above artificial light bank spectrum. Both curves were recorded by the spectroradiometer, the daylight spectrum was recorded with a diffuser which reduced the light intensity; the artificial spectrum was not. All spectra given in this report are relative, not absolute energy values.

FIGURE 7. COMPARISON OF TYPICAL DAYLIGHT AND ARTIFICIAL SPECTRA EXPERIMENTS AS MEASURED BY AN ISCO SPECTRORADIOMETER

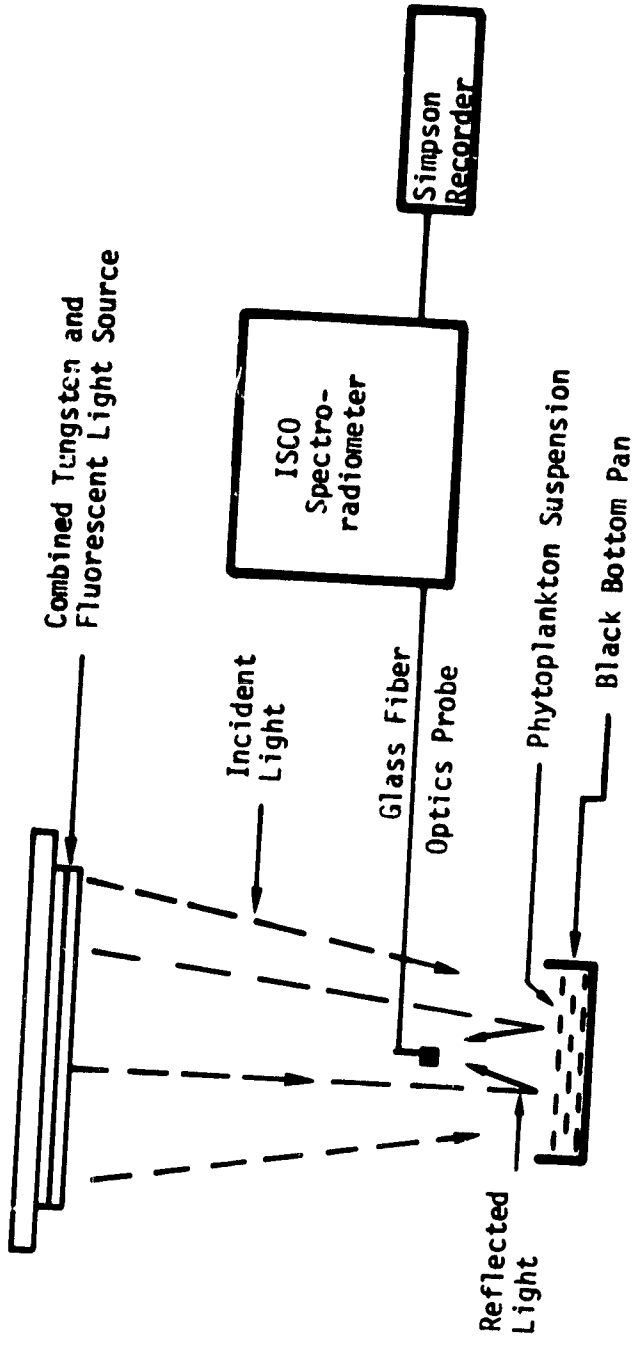

FIGURE 8. LABORATORY SETUP FOR SPECTRAL REFLECTANCE MEASUREMENTS

Observations were limited to this range for two reasons. First, the sensitivity to the instrument falls off rapidly in the ultraviolet and far infrared. Second, remote sensing imagery used in the aerial reconnaissance was sensitive to roughly the same region of the electromagnetic spectrum. Results are illustrated both as the raw spectra recorded by the ISCO spectroradiometer and as a percentage of incident light. Percentage reflectance values have been computed only for critical wavelengths, but all portions of the spectra presented are relative to the artificial illumination curve in Figure 7.

Specimen Collection and Preparation for Spectral Analysis in the Laboratory

Specimens representative of the major aquatic phenomena, normally found in reservoirs, were collected for spectral analysis. The samples included: *Aphanizomenon flos-aquae* (*Cyanophyta*), *Chlamydomonas*, *Chlorella* and *Phagus* (*Chlorophyta* and *Euglenophyta*), *Spirogyra* and *Ulothrix* (*Chlorophyta*), the common filamentous diatoms–*Cymbella*, *Tabellaria*, *Nitzchia*, duckweed (*Lemna* sp.) and debris (dust, dry grasses, twigs, bark, wood chips, etc.). The living samples were collected from ponds and lakes which exhibited large, healthy growths. *Spirogyra* and *Ulothrix* along with the planktonic *Aphanizomenon flos-aquae* and floating macrophyte *Lemna L.* were easily obtainable in a near monoculture. *Aphanizomenon* dominated the late fall and winter phytoplankton in Clear Lake, California [19, 20], and were present in amounts similar to nuisance blooms in reservoirs [3]. Hence both the *Cyanophyta* and attached growth samples were easily harvested. For both the samples representative of flagellated green algae and diatoms, a near monoculture could not be obtained, but samples with a predominance of one species could be collected. *Phagus* and *Chlamydomonas* were the main algae present in the flagellated green algae sample, each constituting some 40% of the sample crop. The diatoms were for the most part common filamentous forms found in ponds with *Cymbella* and *Nitzchia* being the dominant species. In both these samples, however, numerous bacteria were evident, which was not the case with the other samples. For convenience, these samples will be referred to as *Phagus* and *Cymbella*.

Massive suspensions of natural phytoplankton containing groups with major structural differences were collected, either decaying naturally or in a healthy state, and exposed to high light intensities which caused cell breakdown and lysis. For an assay of a time-dependent change in reflected light signature, thick suspensions of *Aphanizomenon flos-aquae*, *Spirogyra*, and a mixture of *Phagus* and *Chlamydomonas* were used. For the *Aphanizomenon* suspension, a healthy mat of algae was placed in the simulated lake basin, intensely illuminated, and scanned with the spectroradiometric instrumentation at time intervals corresponding to changes in the appearance of the suspension. For the *Spyrogyra* suspension, a healthy mat of algae and a mat of equal volume of the same algae showing definite signs of decay were used. The decayed sample was a spongy, surface mat showing obvious signs of cell lysis. Also a mat of equal volume of the same algae showing signs of an organism attached to the *Spirogyra* was collected. These states represent three obvious health states for attached algal growth. A mixed unicellular green algal suspension was collected from the top centimeter of a local sewage pond possessing a surface film of flagellated algae. Since it was unavoidable that a mixture of healthy and unhealthy algae were collected, this sample was

intensely illuminated for 4 hours. At this time, a large surface film of algae covered the simulated lake. Microscopic examination of the algae in this surface film determined that these normally motile algae were dormant and appeared lifeless, apparently stunned or killed by the intense radiation. Those still present underneath the film exhibited normal activity. A distinct color tone difference (dark green) was observed by eye in the dormant surface film compared to the active algae (light green).

In the experiments dealing with altered physiological states, gas vacuolated suspensions of *Aphanizomenon flos-aquae* were subjected to pressures generated in an overlying gas phase using an apparatus similar to that described by Walsby. In order to accommodate the massive amounts of algae used however, a 5-liter pressure resistant receptacle (a domestic pressure cooker) was substituted for the 10 ml colorometer tube suggested by Walsby. Gas from a cylinder was admitted via a diaphragm regulator and needle valve to the required pressure, monitored on a test gauge. Pressure was increased in 0.5 atmosphere steps, and when the desired pressure was reached it was maintained for 30 seconds to assure completion of gas-vacuole destruction. Samples were first equilibrated with air by gentle shaking so that the gas vacuoles came to ambient pressure. All measures given herein are pressure over the ambient pressure (1 atm.). After the desired pressure was obtained, held, and released, the suspension was returned to the black-bottom pan where reflectance was measured over the visible and infrared wavelengths.

Since the algae with collapsed gas vacuoles sank to the bottom of the pan, a layer of water formed over the algae despite the intense concentration. In order to compare the spectrum obtained from the algae after gas vacuole collapse to the buoyant gas vacuolated sample, the suspension was filtered through a fine nylon mesh (35 μ) to remove water which formed over the algae. The suspension at that point was returned to the tank where spectral measurements could be made.

Rapid Scanning Spectrometer (RSS) Instrumentation

Because of the relatively slow scanning speed of the ISCO spectroradiometer (approximately 2 min.), observations are often difficult to make *in situ* where spectral signatures change continuously with wind and wave action. For use under grant NSG-2003, a rapid scanning Tectronix spectrometer has recently been acquired for this purpose. Although the instrument was not available for use at the Southern California reservoirs, the authors have recorded some preliminary data at Clear Lake, California, which will be referred to whenever the Clear Lake data relate to the Southern California study. A description of the experimental technique is therefore in order.

The Tectronix spectrometer was used to measure the spectral reflectance curve of algal/water mixtures *in situ* under daylight illumination. The spectrometer (J-20/7J20 RSS) contains a Czerny-Turner monochrometer, two interchangeable gratings, silicon-vidicon target, and electronic circuitry. Light dispersed by the monochrometer is focused on the vidicon target which simultaneously gathers spectral information at all wavelengths within the wavelength span of the gratings. The spectral information is

then electronically scanned from the target and the resultant signal, after processing, is displayed on a Tectronix 7313 series oscilloscope (Figure 9). The oscilloscope was equipped with a Tectronix C-5 oscilloscope camera so that the spectral signature of the object in view could be recorded from the oscilloscope screen. Only the grating with the 400 nm wavelength span was used in this study and only the information from a span of 400 to 800 nm was recorded for this study. The amount of light impinging on the vidicon can be regulated by a slit width. For this investigation a 100-μ slit width was chosen. The spectral reflectance curve of a water body under daylight illumination was measured from a boat. A 20-millisecond scanning time gave the best results. Instrumentation was battery powered for this purpose.

Observations were made with the spectrometer pointed at a 45 deg. angle down at the water and at a right angle from the sun (Figure 10). In this way, sun glint was avoided. Changes in illumination were observed by placing a highly reflective styrofoam pad parallel to the water and in line with the viewing slit. Thus, solar and skylight irradiance reflected from this surface could be used as a measure of total irradiance. Results show total irradiance at the approximate time the spectral signature was taken. At certain wavelengths a percent reflectance value was computed in order to make general correlations between laboratory and field work.

Microphotographic Instrumentation

A Nikon inverted M.S. microscope equipped with a Nikon A.P.M. camera attachment and a 35 mm camera was used to photograph both reflected and transmitted light received from an algal specimen. For reflectance exposures, the light from a tungsten source was transmitted through a field diaphragm and objective into an illuminator mounted on the microscope. A beam splitter directed the light through the objective toward the specimen. The light reflected by the specimen was transmitted by the objective and proceeded through the tube to the camera attachment. For transmitted light, the order the light path followed was the normal one: source, illuminator, objective, camera. Different objective (X 10, X 20, X 40, and X 100) were used in the study.

The film used to record images of algal cells was Kodak (1E-135-20) false color infrared film. This choice was made for several reasons. First, the film was chosen for its sensitivity in the green and red wavelengths as well as the infrared. Since resolution in the light microscope is greater at shorter wavelengths, the inclusion of shorter wavelengths within the photo would enhance resolution of fine algal details within the algae [21]. Second, since the eye is more sensitive to color tones than shades of grey [22], cellular constituents with a proportionately greater waveband response might be more easily identified. Third, multiband film with sensitivity in the visible as well as the infrared wavelength bands can be used to illustrate how the cells adapt to light of a normal daylight condition. The mechanism [10] which promotes

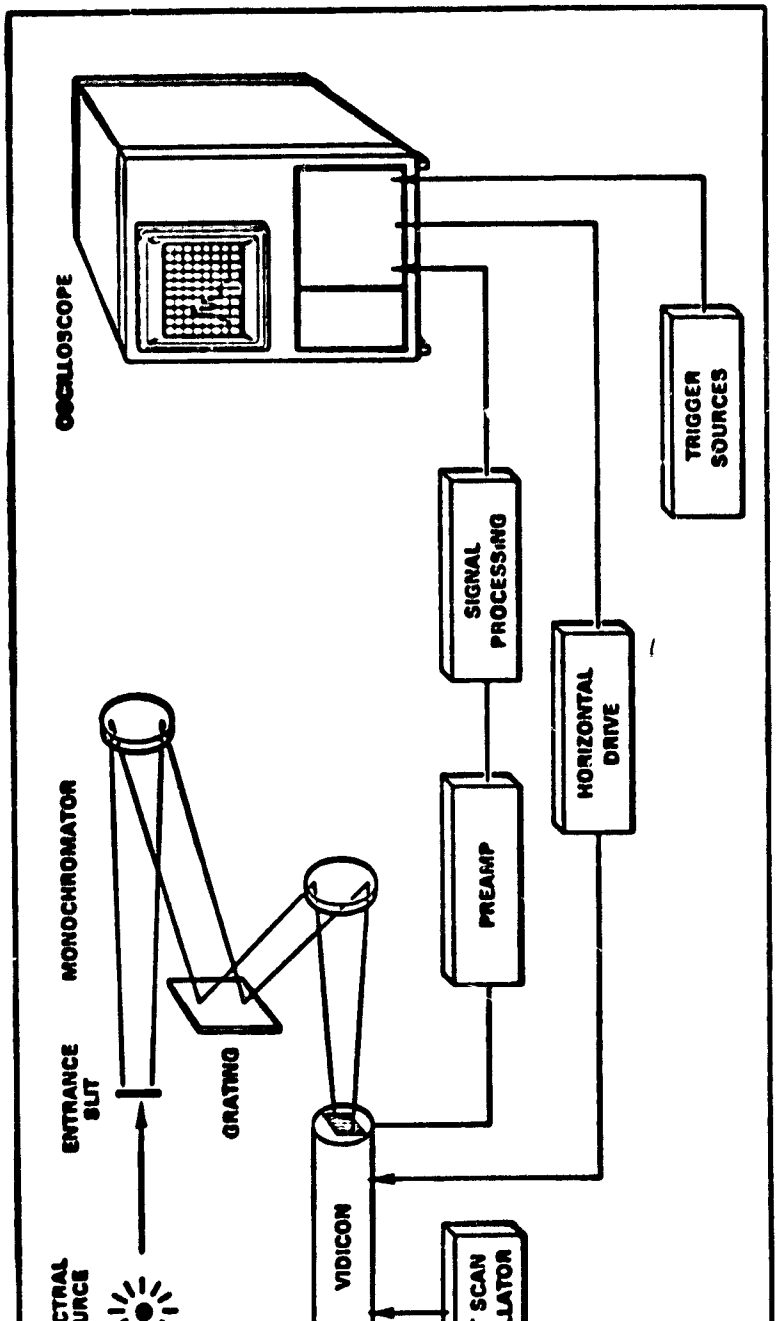

FIGURE 9. SPECTROMETER UNIT

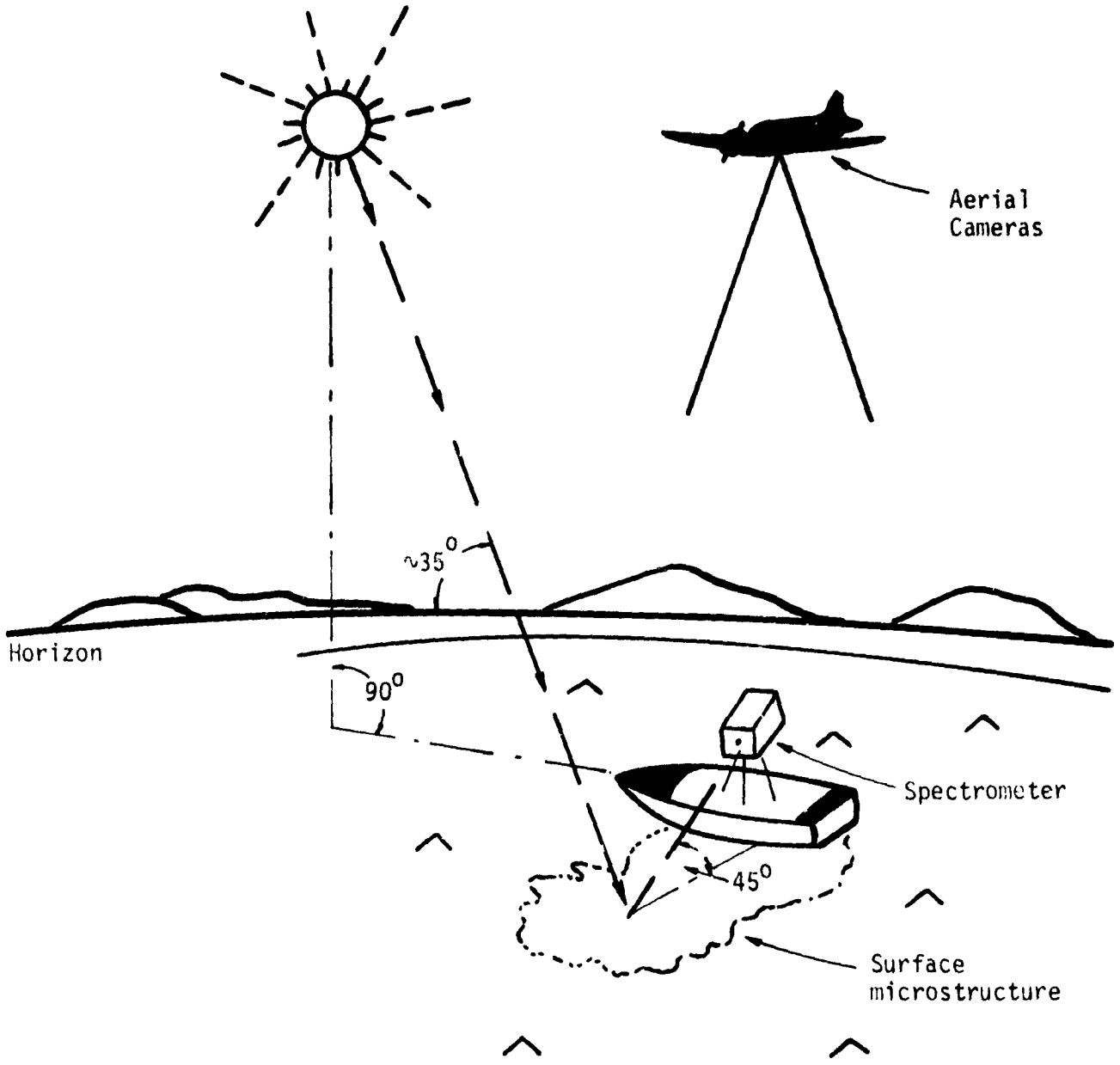

FIGURE 10. SCHEMATIC OF CLEAR LAKE REFLECTANCE MEASUREMENTS WITH TECTRONIX RSS SPECTROMETER

infrared response by algae is in dispute (fluorescence or particle backscattering). Thus wavelengths were measured which use either fluorescense or backscattering, to discern which component was most significant on the basis of the cellular constituents. Also, since color infrared film is sensitive in the far red (685 nm) where fluorescence is greatest, as well as in the infrared (700-900 nm), a color tone difference might distinguish one phenomenon from the other.

For use with color infrared film, the light emitted by the tungsten source was filtrated to a spectrum similar to daylight. The light source was first measured with the Spectroradiometer; then Wratten filters 12, 30B, 50C, and 50C-2 were used to block blue light and color compensate the remaining spectrum (Figure 11). Since color infrared film has no standard ASA rating, several trial exposures were made on each batch of film before selecting the proper exposure time. Exposure was then regulated by the camera attachment.

To determine whether or not *in vivo* chlorophyll fluorescence played a large part in the IR response, the microscopic instrumentation was equipped with a Corning glass filter CS-5-60 as a screen so that only light from the blue end of the light spectrum would impinge on the specimen. It has been shown that light from the blue end of the spectrum has the maximum efficiency in promoting fluorescence. A Kodak #29 filter was fitted over the camera lens so that only light from the 680 nm to 900 nm wavelength range could be recorded. This setup is nearly identical to the type used in fluorimeters to record *in vitro* and *in vivo* chlorophyll fluorescence. The major difference was in the light source as the tungsten illumination produced light intensities impinging on the specimen similar to those used to capture light scattered by the algae.

Specimen Preparation

Specimens representative of several major algal groups—*Cyanophyta*, *Chlorophyta*, *Chrysophyta*, *Cryptophyta*, and *Euglenophyta*— were collected from their natural environment and photographed within the same day. Specimens were also photographed within minutes of slide preparation to avoid possible cellular stresses. The sequence of the steps from the glass slide on which the algae were mounted was: algae, lake water, No. 1 cover slip, and oil immersion when the 100 X objective was used. Photographs were taken in a dark room to exclude diffuse light.

To define the role of gas vacuoles in producing light scattering effects, blue-green algae (*Cyanophyta*) were subject to a further treatment. The algae were first photographed with gas vacuoles intact and then after destruction of gas vacuoles accomplished by the classical hammer, cork, and bottle experiment [23].

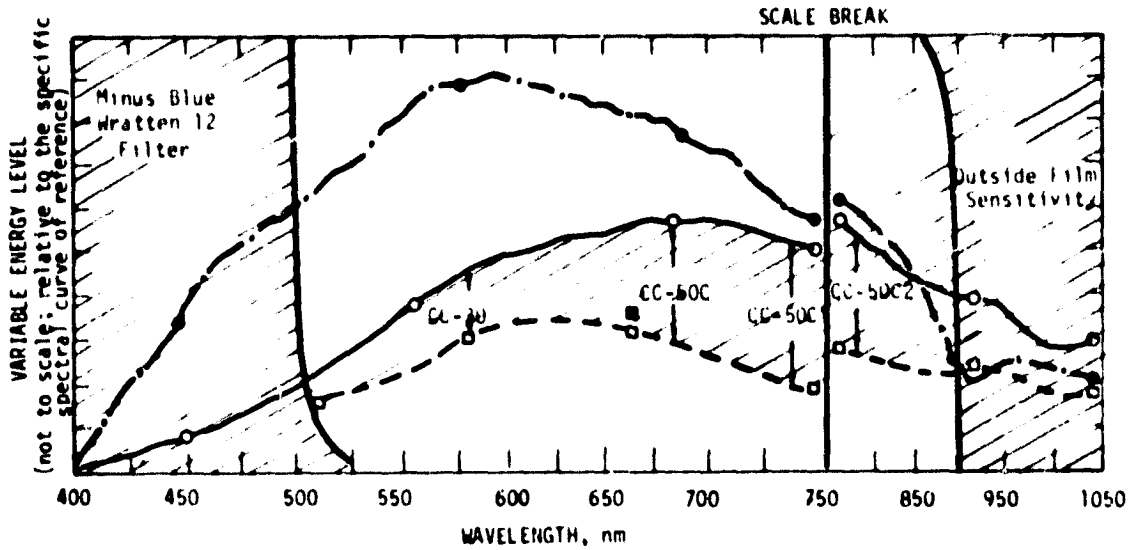

Typical solar and skylight irradiance

Tungsten source irradiance

Tungsten source irradiance with color compensation filters

Note: Shaded areas represent light excluded from microphotographic cameras.

FIGURE 11. COMPARISON OF THE SHAPE OF A TYPICAL DAYLIGHT SPECTRAL SIGNATURE AND THE SHAPE OF A TUNGSTEN SOURCE SPECTRAL SIGNATURE ALTERED FOR MICROPHOTOGRAPHIC STUDIES

V. THEORY

GENERAL

The concentration of phytoplankton, sediment, and other suspended solids found in lakes or reservoirs implies a level of productivity and is often a measure of water quality [13, 33, 14]. Multispectral sensors can be used to measure the spectral reflectance of water bodies containing suspended solids, and in turn, spectral reflectance can itself be a measure of suspended solids concentration or trophic state. But when a body of water subject to electromagnetic radiation is viewed by a sensor, the device receives reflected radiation not only from the water body with suspended solids but also from the air/water interface, particles in the air, dissolved organic material, and from the lake bottom if the lake is shallow. Also, the electromagnetic radiation must pass through two media, air and water, each of which may alter the incident radiation in a variety of ways.

Therefore, when remote sensing techniques are used to characterize water quality, four important parameters must be considered:

1. The spectral character of the radiation source I_λ;
2. The attenuation of radiant energy by the medium through which it travels, τ_λ;
3. The characteristic spectral reflectance of the water body at any trophic state, P_λ (suspended solids and water);
4. Background reflectance either from the lake bottom or redirected light from nearby obstruction [24].

The spectral reflectant I_{W_λ} of water bodies gathered by a sensing device can be thought of as:

$$I_{W_\lambda} \propto P_\lambda(\text{suspended solids and water})\tau_\lambda I_\lambda \tag{1}$$

Since the sun provides a convenient source of radiation it was the natural choice for this study. The radiation of the sun may be regarded as that of an incandescent black body [22]. The radiation received at the surface of a measuring instrument on earth obeys the ordinary law of transmission [25]

$$I = I_c e^{-n_a M} \tag{2}$$

where n_a is the extinction coefficient of the air referred to one standard atmosphere and M the length of the path of the radiation in atmospheres. The quantity I_c is called the "solar constant" and represents the rate at which solar radiation must be delivered on a unit area normal to the incident rays, at the outside atmosphere, to account for terrestrial observation. The radiation actually received at any point on the earth's surface depends on the time of day, season, latitude, and transparency of the

atmosphere [25]. The extinction coefficient of the air multiplied by the pathlength traveled can be redefined as τ_λ, attenuation by the atmosphere.

Radiation (I) received can further be defined as having a certain distribution of radiant energy, which is:

$$I' = I_\lambda' = \text{spectral character as a function of wavelength} \quad (3)$$

The description of radiant energy from the sun as presented accounts only for direct illumination. Indirect solar radiation, skylight or reradiated light from the earth also accounts for a varying proportion of the light impinging on a water body. It too has a spectral character (I_λ") and has a unique attenuation (τ_λ") factor. Skylight adds to direct solar radiation (sunlight and skylight) to form a unique spectral character:

$$I_\lambda' + I_\lambda'' = I_\lambda = I_c e^{-\tau_\lambda' \tau_\lambda''} = I_c e^{-n_a M} \quad (4)$$

If certain rules are observed during aerial reconnaissance, the spectral character of the radiant source can be maintained as a constant. That is, if the layer of atmosphere intervening between the source, object, and sensing device is constant, and clouds, dust, and photochemical haze are minimal, the attenuation effect will be nearly constant and sun and skylight illumination will be nearly uniform from one reconnaissance to any other [22]. To meet these conditions, it is conventional to plan reconnaissance flights to coincide with a unique solar elevation and defined air quality conditions. For aquatic studies, the solar elevation acceptable for photographic missions is 35±5 deg. on the horizon. By choosing this angle, unwanted solar glare from the air/water interface can be avoided [22]. Obviously, perfect air quality conditions cannot always coincide with flight dates, hence an acceptable compromise will have to be made under most circumstances. Such a compromise should be based on the type of imagery desired. For remote sensing of vegetation, the green, red, and near infrared wavebands often contain the most useful information for photointerpretation. If sensitivity to these wavebands is desired, image quality will be high despite the presence of smog, since photochemical haze absorbs little light, but does promote Rayleigh scattering. Figure 12 shows that the primary effect of smog is in the shorter wavelengths—green, blue, and ultraviolet. Moisture in the presence of fog or clouds strongly absorbs infrared wavebands and scatters visible and infrared light. This reduces the use of imagery for interpretation of water quality. More complete treatment of problems related to atmospheric attenuation is given in "Imaging with Photographic Sensors" [22].

With atmospheric attenuation (τ_λ) a near constant, the spectral character of the radiant source (I_λ) is a near constant, and the spectral reflectant (I_{W_λ}) measured from a water body will be a direct measure of the trophic state of a water body (P_λ suspended solids and water) if the air/water interface reflectance is minimal (no solar glare) and if the lake is large (>2/3 ha) and physically (or at least optically) deep (no background reflectance). Simply stated:

$$I_W \propto K_{(I_\lambda \tau_\lambda)} (P_\lambda \text{ suspended solids and water}) \quad (5)$$

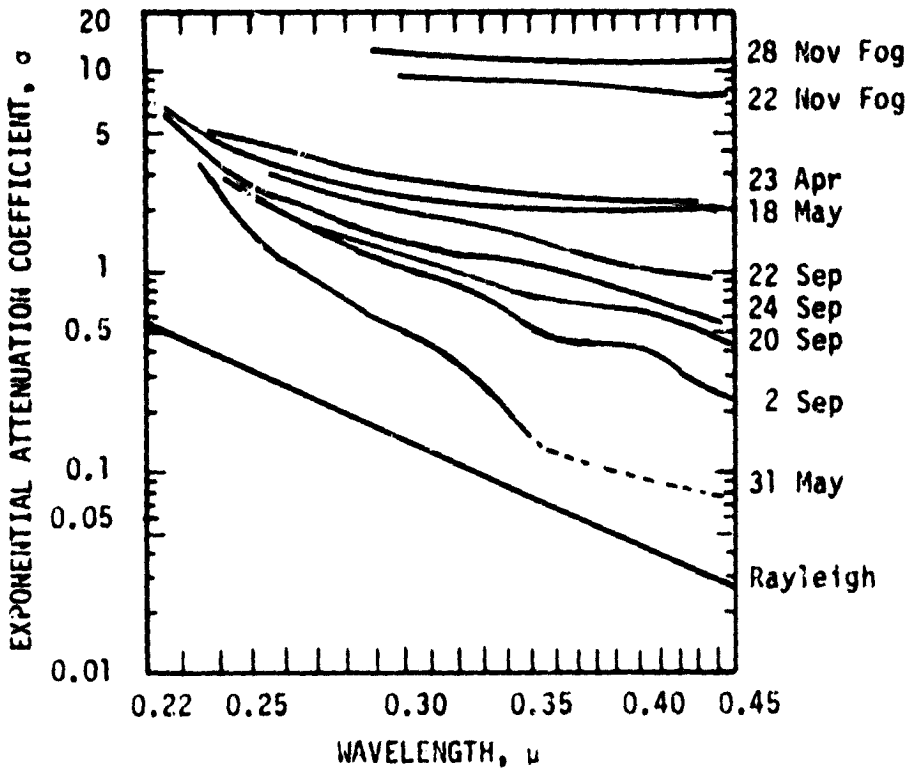

Typical attenuation curves illustrating the full range of atmospheric conditions, Pasadena, California, 1949.

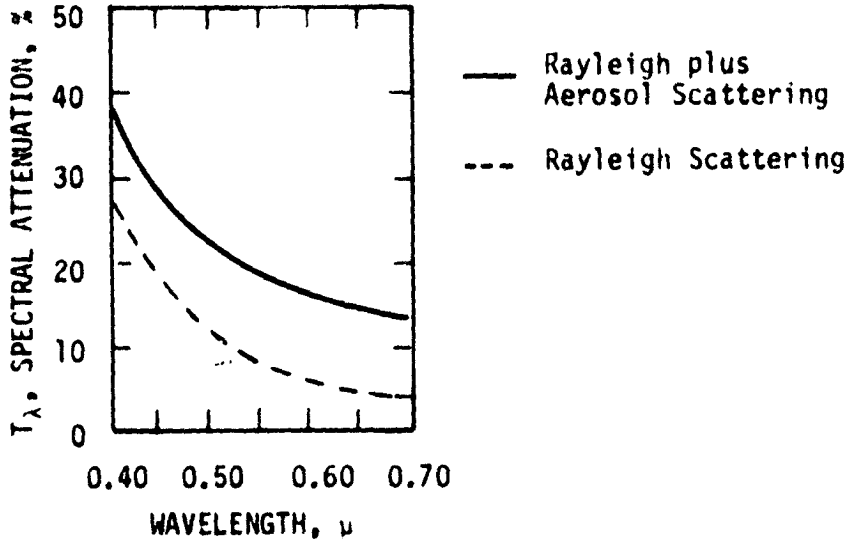

Plot showing percentage of attenuation due to Rayleigh plus aerosol scattering and Rayleigh scattering alone.

FIGURE 12. EFFECT OF ATMOSPHERIC CONDITIONS ON SPECTRAL ATTENUATION [22]

If the characteristic spectral reflectance of a water body can be related to known suspended solid concentrations and defined attenuation values,

$$P_{\lambda}(\text{solids and water}) = \frac{I_{w_{\lambda}}}{K(I_{\lambda}\tau_{\lambda})} \tag{6}$$

water quality can be determined solely from the spectral reflectance gathered.

The characteristic reflectance of a water body (P_{λ} solids and water) is determined by the fate of incident light. Incident light striking the surface of a water body can suffer four fates: absorbtion, reflection, transmission, or scattering [25]. The absorbtion, transmission, or reflective characteristics of a water body are of concern only insofar as they represent light which will not be detected by a sensing device. That light which is scattered in an upward direction from a water body will affect a detector, and light scattering by water bodies as set out by Whitney [26] can be thought of as follows.

If an inverted, flat ring sensing device (internal radius r, external radius r + dr, thickness dz) is placed in a horizontal plane at depth 0 of a lake (Figure 13), the device will detect light scattered toward the device within an element of volume,

$$dV = \frac{2\pi z^2 \sin \psi_w}{\cos^3 \psi_w} d\psi_w dz \tag{7}$$

where

$$dr = \frac{z}{\cos^2 \psi_w} d\psi_w \tag{8}$$

Incident light on a horizontal plane within this volume and at any depth z is equal to

$$I_{z_{\lambda}} = I_{0_{\lambda}} e^{-\eta' t bz} \tag{9}$$

where

η'_t = mean extinction coefficient

= $\eta_w + \eta_{pc}$ where η_w is due to water, η_p to suspended particles, and η_c to dissolved material

bz = mean optical depth

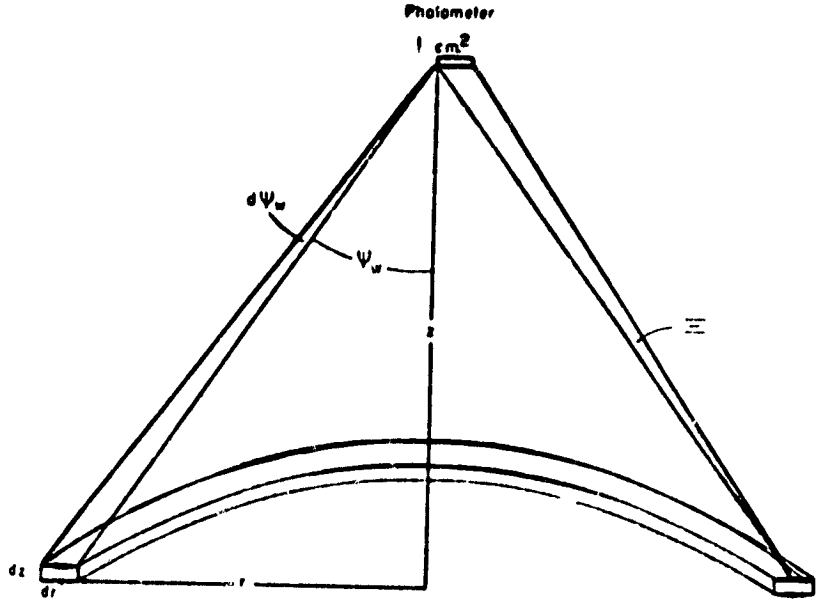

FIGURE 13. GEOMETRY OF WHITNEY'S SCATTERING THEORY [25]

Energy, I_{z_λ}, will be absorbed or scattered within any volume element according to equation [25]. Differentiating,

$$dI_{z_\lambda} = -\eta' t b I_{0_\lambda} e^{-\eta' t b z} dz \tag{10}$$

or for an area at depth z,

$$dI_{z_\lambda} = -\eta' t b I_{0_\lambda} e^{-\eta' t b z} dV \quad . \tag{11}$$

Energy scattered in any direction by any element of volume dV will be

$$S_s b I_{z_\lambda} dV = S_s b I_{0_\lambda} e^{-\eta' t b z} dV \quad , \tag{12}$$

where

S_s = distance traveled by a quantum of light
b = mean optical path.

If the solid angle subtended by the instrument is Ξ, the energy scattered toward the instrument will be

$$\frac{\Xi}{4\pi} S_s b I_{0_\lambda} e^{-\eta' t b z} dV \quad , \tag{13}$$

where

$$\Xi = \frac{\cos^3 \psi_w}{z^2} \quad , \tag{14}$$

and the sensor is at depth 0_m.

From equations (7) and (14)

$$\frac{\Xi}{4\pi} S_s b I_{0_\lambda} e^{-\eta' t b z} dV = \frac{S_s b I_{0_\lambda}}{4\pi} \frac{2\pi z^2 \sin \psi_w \, d\psi_w \, dz}{\cos^3 \psi_w} \frac{\cos^3 \psi_w}{z^2} e^{-\eta' t b z}$$

$$= \frac{S_s b}{2} I_{0_\lambda} e^{-\eta' t b z} \sin \psi_w d\psi_w dz \quad . \tag{15}$$

In traveling to the sensor, the energy must cross a path which has a distance of $z/\cos \psi_w$; where scattering or absorbtion can take place. Therefore the quantum of energy, dI_{w_λ}, actually received by the instrument from

any element of volume dV is

$$dI_{w_\lambda} = \left(\frac{S_s b I_{0_\lambda}}{2} e^{-\eta' t bz} \sin \psi_w \, d\psi_w \, dz\right) \exp\left(\frac{-\eta' t z}{\cos \psi_w}\right)$$

$$= \frac{S_s b I_{0_\lambda}}{2} \exp\left[-\eta' t z\left(\frac{1 + b \cos \psi_w}{\cos \psi_w}\right)\right] \sin \psi_w \, d\psi_w \, dz \, . \quad (16)$$

If ψ_w varies from 0 to $\pi/2$, and z from 0 to ∞, the quantum of energy striking the sensing device will be

$$I_{w_\lambda} = S_s b I_{0_\lambda} \int_0^{\pi/2} \int_0^{\infty} \exp\left[-\eta' t z\left(\frac{1 + b \cos \psi_w}{\cos \psi_w}\right)\right] \sin \psi_w \, d\psi_w \, dz. \quad (17)$$

Solving,

$$I_{w_\lambda} = \frac{S_s I_{0_\lambda}}{2\eta'}\left[\frac{b - \ln(1 + b)}{b}\right] \quad (18)$$

$$R_p = \frac{I_{w_\lambda}}{I_{0_\lambda}} = \frac{S_s}{2\eta'}\left[\frac{b - \ln(1 + b)}{b}\right] \quad (19)$$

where R_p is the ratio of incident light striking the detector as it faces away from the water to that which is scattered by the water body and strikes the detector as it faces down into the water. Only light which is backscattered toward the receiver can be measured, however. Therefore the total extinction coefficient η'_t will be

$$\eta'_t = \eta'_w + \eta'_{pc} + \frac{S_s}{2} \quad (20)$$

If

$$S_s = F_s(b)\, \eta'_t \, R_p \quad (21)$$

where

$$F_s(b) = \frac{2b}{b - \ln(1 + b)} \quad (22)$$

it is found that $F_s(b)$ varies relatively slowly with b (mean optical path - $1/\cos \psi_r$)

b (mean optical path), meters	1.0	1.1	1.2	1.3	1.4	1.5
$F_s(b)$	6.52	6.14	5.83	5.57	5.35	5.15

For most purposes, a mean value of 5.9 for $F_s(b)$ is sufficiently accurate [25]. Therefore:

$$S_s = 5.9n'_t R_p \tag{23}$$

and can be conventionally expressed as a percentage

$$P_s = 100 \frac{S_s}{n'_t + \frac{S_s}{2} - n'_w}$$

In lakes or reservoirs, a wide range of spectral signatures is normally found, as the concentration of suspended solids and dissolved color varies. For lakes which have concentrations of phytoplankton which assume nuisance proportions, certain spectral signatures are all too familiar. The dull yellow-green produced by a blue-green algal bloom is typical of the spectral signatures which dishearten the agencies in charge of water quality control.

Although such phenomena have been observed for hundreds of years, understanding of the spectral signature of water blooms has for the most part been confined to areas of visible light spectrum (400 nm to 700 nm) [15]. Recent advances in both photographic and spectroradiometric design have made available sensing devices which have a sensitivity throughout the electromagnetic spectrum [22]. Such devices held close or away (remote) from the object of view can detect incident light backscattered from water bodies both within the visible light spectrum and encompassing the ultraviolet (200-390 nm), near infrared (700-900 nm) and the infrared (900-3000 nm). These wavelength bands along with the equally important visible light band may be used to characterize water quality. The spectral signature of water bodies is dependent on concentration of suspended solids and their composition. Thus remote sensing devices with sensitivity to more than one waveband are needed to provide information useful in identifying trophic states and categorizing aquatic phenomena. For example, when the concentration of suspended biomass increases, the area of greatest spectral response shifts from the blue, as in Lake Tahoe, to the green, as in many mesotrophic lakes, and at times to the infrared in eutrophic lakes like Clear Lake. Lakes which are either very turbid or high in dissolved color (e.g. Gelbstoff in dystrophic lakes) may reflect well in the red.

To this end, multispectral color infrared film and four-band multispectral film are both broad band films, sensitive to both visible and the IR wavelength bands of the electromagnetic spectrum (Figure 14). Color infrared film has three dye layers which are coupled to three wavelength bands—near infrared (700-900 nm), red (600-700 nm), and green (500-600 nm). (See Figure 15.) The dye responses are inversely proportional to the exposure from their respective wavelengths. For example, objects reflecting well in the infrared wavelength band but poorly in the red and green bands will cause the cyan dye coupled to infrared response to be diminished while the magenta and yellow dyes are enhanced. In this way, wavelengths outside the visible light spectrum can be assigned a certain false color tone from the visible light range. The color coding of Kodak color infrared film used in this study is: green appears blue; red appears green; infrared appears red. Each band of the four-band film used in the study

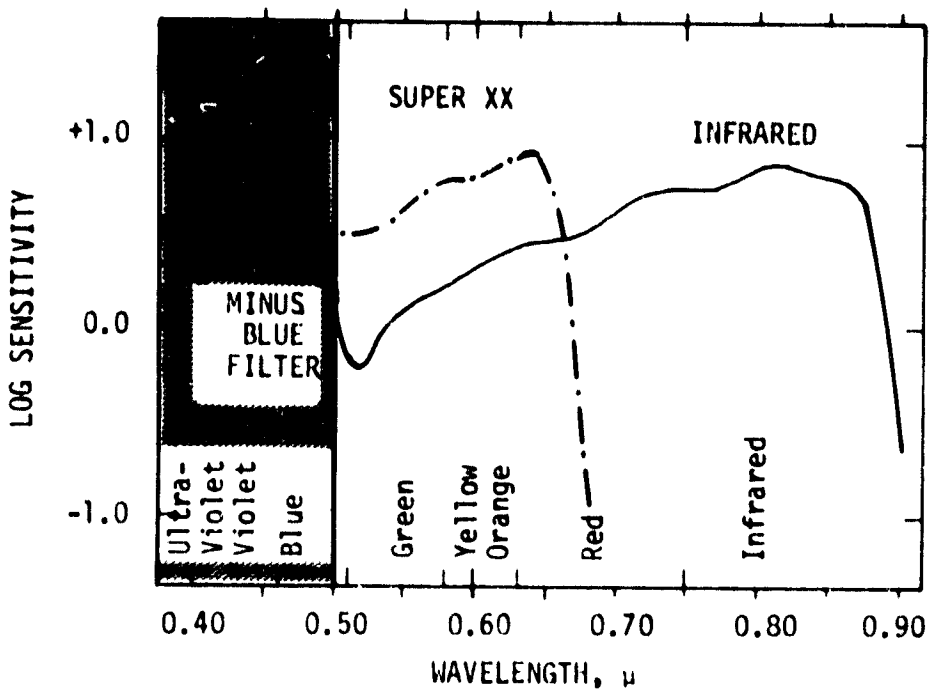

Note the effect of the minus blue filter and the cutoff wavelengths for both films.

FIGURE 14. SPECTRAL SENSITIVITY OF KODAK INFRARED AEROGRAPHIC FILM (TYPE 5424) AND COMPARISON WITH KODAK SUPER XX AEROGRAPHIC FILM (TYPE 5425) AT VARIOUS WAVELENGTHS [22]

is directly proportional to the intensity of the wavelength band to which it is exposed. Both visible and infrared radiation screening filters must be used to allow exposure of only one waveband in a particular picture frame. The closed-circuit television camera used in the study also functions in direct proportion to wavelength bands, hence it is filtered in a similar fashion.

Both color infrared film and four-band multispectral film have advantages and disadvantages. Since both films cover the same useful area of the electromagnetic spectrum, the disadvantages are not inherent to the wavelength range capabilities of the film, rather problems of photointerpretation exist for both films. Exposure of wavebands in four-band imagery can be analyzed by measuring film density in stepwise fashion, with either a density wedge or a densitometer. Since exposures are registered in black and white, only a limited number of film density values (approximately 20 with the naked eye [22]) can be established using a density wedge and visual comparisons. Although a densitometer theoretically could be more useful in assigning numerical values to film densities, cost is prohibitive and turnover time is great. Technical difficulties arising from lens fall-off effects also complicate the use

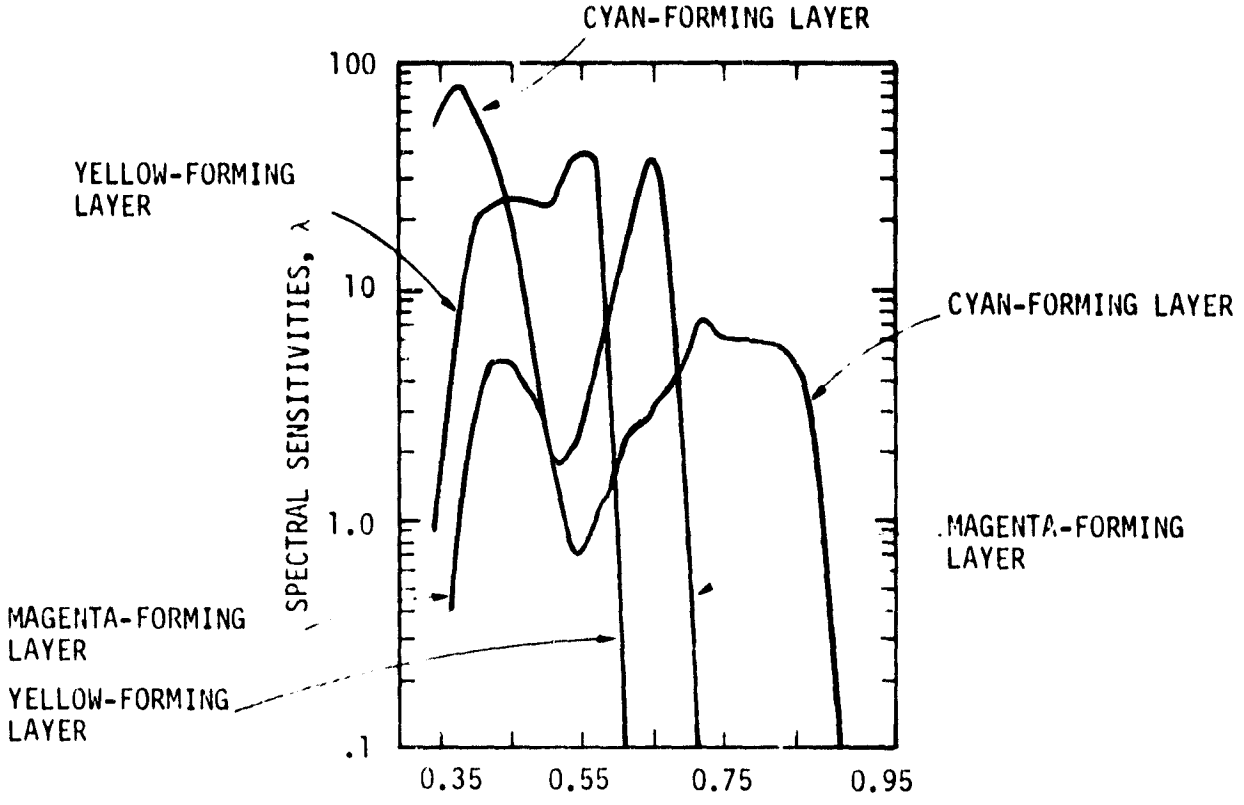

FIGURE 15. SPECTRAL SENSITIVITY OF KODAK COLOR INFRARED AEROGRAPHIC FILM DYES [22]

of densitometry. Color infrared film offers two advantages. First, exposures in each waveband are combined by a chemical process rather than a physical one used in the four-band. Recent advances in the emulsion sensitivity and color-coupling dyes have improved the fidelity of this process [22]. A chemical process offers a more sensitive method for measuring band intensities when compared to measuring film densities by eye. Second, since the image is recorded in color and the human eye is more sensitive to color tone than to shades of grey, subtle changes in spectral response are more easily recognized. There is some dispute over the sensitivity and usefulness of false color infrared films [27]. However, as Malan [17] notes, "doubts about the utility of color IR film are probably due to the fact that the photographic technique employed did not exploit the full capabilities of the medium." For analytical use of color IR film optimum color balance is essential. Inherent disadvantages in the film lie in the fact that the different wavebands are inseparable. Since the absorption and scattering properties of water vary in their effects on wavelength bands, a wide variety of spectral signatures may be recorded as physical and biological factors change. Since wavebands cannot be separated, it is more difficult to attribute changes in spectral signature to a physical or a biological process. A possible solution to the problems may be found in the use of narrow band multispectral scanners or spectroradiometers. Here, water quality is measured by an electronic pulse rather than a conventional imaging device. Such techniques are still in an experimental phase and the cost is prohibitive. The use of (color infrared and four-band)

multispectral photography currently offers a more economical means of obtaining useful remote sensing data [28]. Low cost multispectral systems are available commercially [2, 29].

PHYTOPLANKTON REFLECTANCE

Reflectance by chlorophyll-containing plants varies as a function of wavelength. A floating higher aquatic plant (e.g. the duckweed *Lemna*, Figure 16) has a spectral signature with a major peak in the near infrared and a minor peak in the green [30]. Since the human eye is unable to detect infrared light, chlorophyll-containing plants appear green in sunlight [11]. The reflectance properties of lower plants such as phytoplanktonic algae are much less understood because they are highly modified by the spectral properties of the aquatic ecosystem.

To understand why the spectral response of phytoplankton solution may vary as a phenomenon dependent on both wavelength and concentration, the events which promote a spectral signature should be understood. The first, probably main, event which contributes light to the reflected light spectra of water bodies is simple mechanical scatter from suspended particles with a different refractive index. As with atmospheric scattering, particle size may have an important effect. The second events contributing light to the spectral signature are photochemical: fluorescence and phosphorescence. Studies to date on the mechanism of light reflectance by phytoplankton have not clearly discerned the prominence of these two events in contributing light to the infrared region [10]. Absorbtion either by chlorophyll *a*, *b* or *c*, or by accessory pigments removes light from the spectrum, and Yentch [31] has shown that the primary effect in commonly encountered concentrations of phytoplankton is in the 400-500 nm and 660-680 nm regions.

Using the above considerations, several workers have proposed models for measuring the chlorophyll content of water bodies. Clark *et al.* [13] have shown that changes in the percentage of light backscattered in the blue and green ranges of the spectrum can be related to changes in chlorophyll *a* concentration (Figure 17). In this case, increased reflectance in the green would result from greater particle scattering while depressions in the blue would result from the presence of more chlorophyll *a*. Other investigators have constructed models based solely on the 670-700 nm region or on the 420-480 and 620-700 nm bands [12, 14, 32-34] (Figure 16). These workers, however, have for the most part been dealing with oligotrophic water bodies where phytoplankton concentrations were several magnitudes less than those commonly found in water in which we worked. For use in these eutrophic systems, such models may prove of little benefit since the rate of change in these spectral regions due to increases in chlorophyll *a* will be minimal at modest concentrations. From the data of Clarke *et al.* (Figure 17) it can be seen that when chlorophyll *a* concentration exceeds 4 µg/ℓ, reflectance in the blue drops to below 2% of incident light. Wezernak notes that significant problems arise in using selected wavebands which have normally low reflectance [14].

Secondly, although the reflectance peaks and depressions in the visible wavelengths provide some useful information about the presence of chlorophyll *a*, in water bodies with a mixture of algal species,

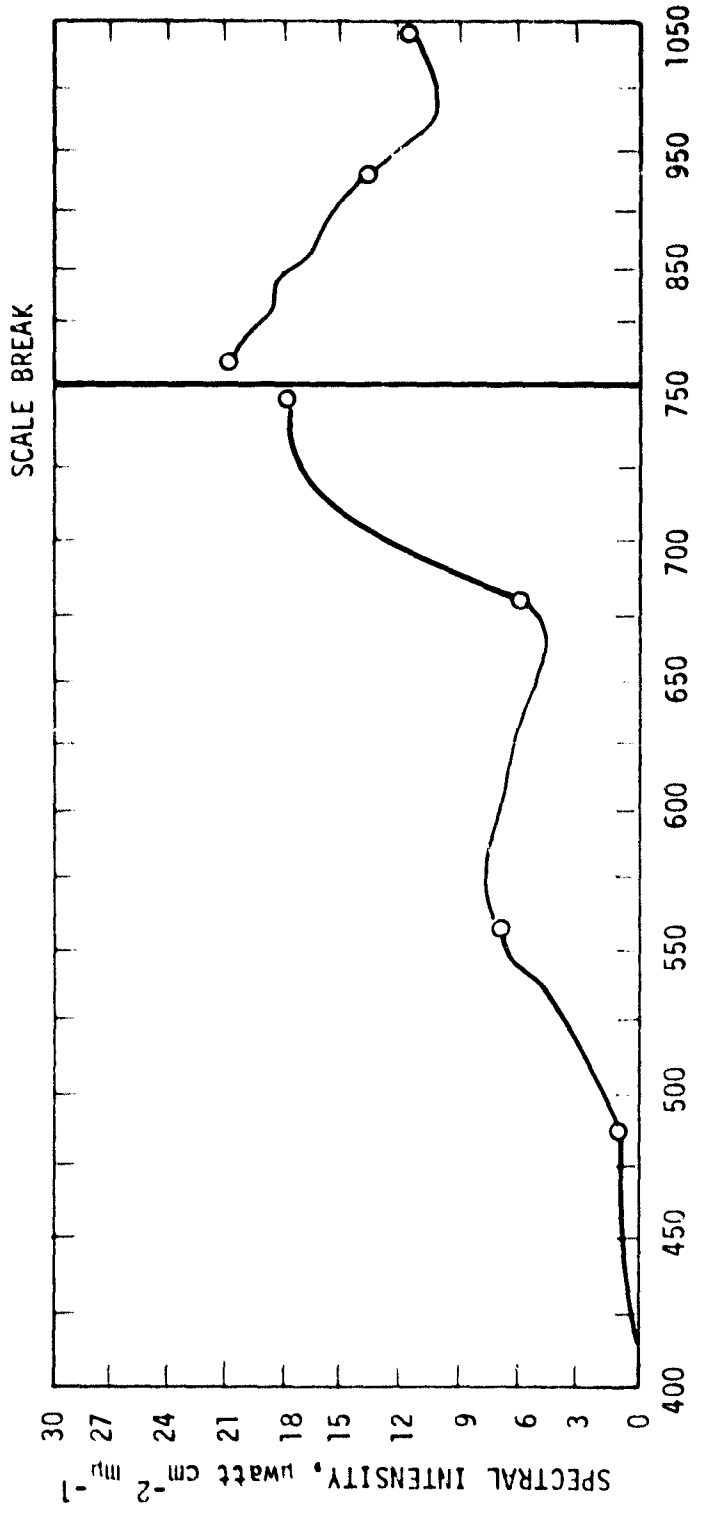

(Note: The reflectance signature was recorded by the spectroradiometer under artificial illumination, simulating daylight.)

FIGURE 16. SPECTRAL REFLECTANCE SIGNATURE OF A FLOATING, AQUATIC HIGHER PLANT: *Lemna*

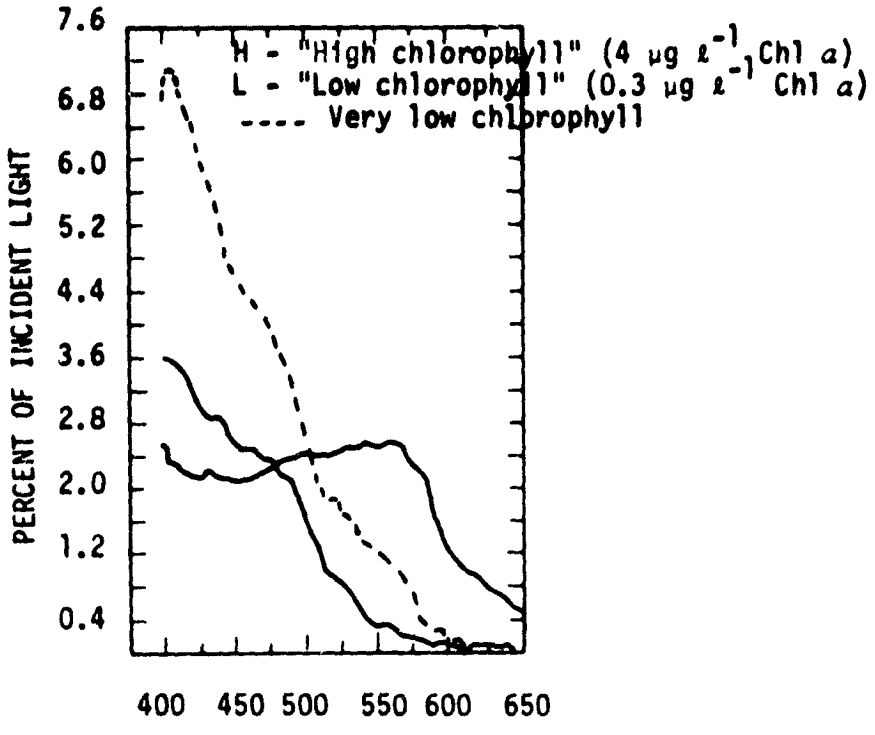

FIGURE 17. REFLECTANCE OF VARIOUS OCEANIC CHLOROPHYLL CONCENTRATIONS

Various accessory chlorophylls and accessory pigments (phycocyanin *c*, fucoxanthin, etc.) may overlap regions of normally high reflectance. Wezernak *et al.* have made a point that no one simple modular approach to the problems of assessing trophic state by spectral analysis is suitable in all cases [14].

Gramms and Boyle have constructed one model for differentiating blue-green algae from green algae based upon such accessory pigments (Figure 19). Here, differences in reflectance at 625 and 650 nm may be due to the presence of phycocyanin *c* [35]. The model accounts for two components, blue-green and green algae; but in many lakes a third component, that of accessory pigments from diatoms and dinoflagellates may also contribute to the spectral signature in a way not yet predictable. Such a model also faces the same constructions as previous ones in that the changes which can be observed in this region are small, which would make rapid identification by aerial photographic reconnaissance difficult. Separation of components from complex spectral signatures made up from different algal species, inorganic sediment and dissolved color based upon observations in the visible region alone where all these components react uniquely, is undoubtedly a difficult if not impossible task. Over the past 12 years the Principal Investigator has made many absorbance curves of mixed, suspended populations of blue-geen and other algae. Without exception no distinguishable pattern was produced when more than one type of algae was present. Natural populations are usually mixed and such visible spectra seem inadequate.

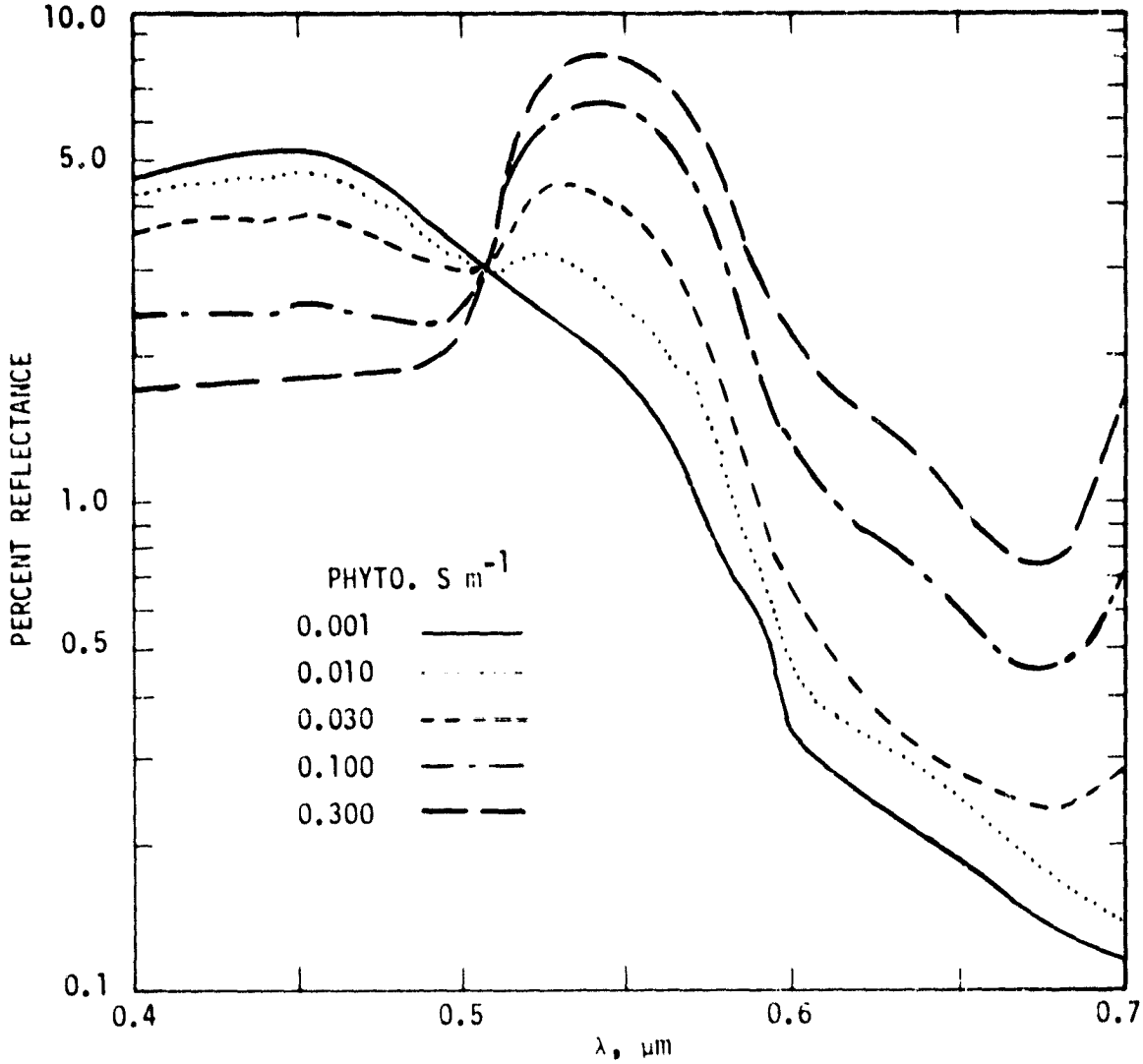

FIGURE 18. CALCULATED CHANGE IN REFLECTANCE OF WATER WITH INCREASING CONCENTRATION OF PHYTOPLANKTON (AFTER G. SUITS) [12]

Studies undertaken at Clear Lake, California, have indicated that a potential exists for using the near infrared band in a chlorophyll model [5, 6, 18]. *In situ* studies on Clear Lake have established that buoyant masses of blue-green algae found in the upper 10 cm of surface water promote a strong infrared response, similar in magnitude to that of higher plants [5, 6, 18, 36]. If the spectral response of these objectional algal scums is similar to the spectral signature of a forest, several conclusions can be made.

1. First, at some point, natural populations of phytoplankton are great enough to form a near optically opaque surface, similar to that of leaves.

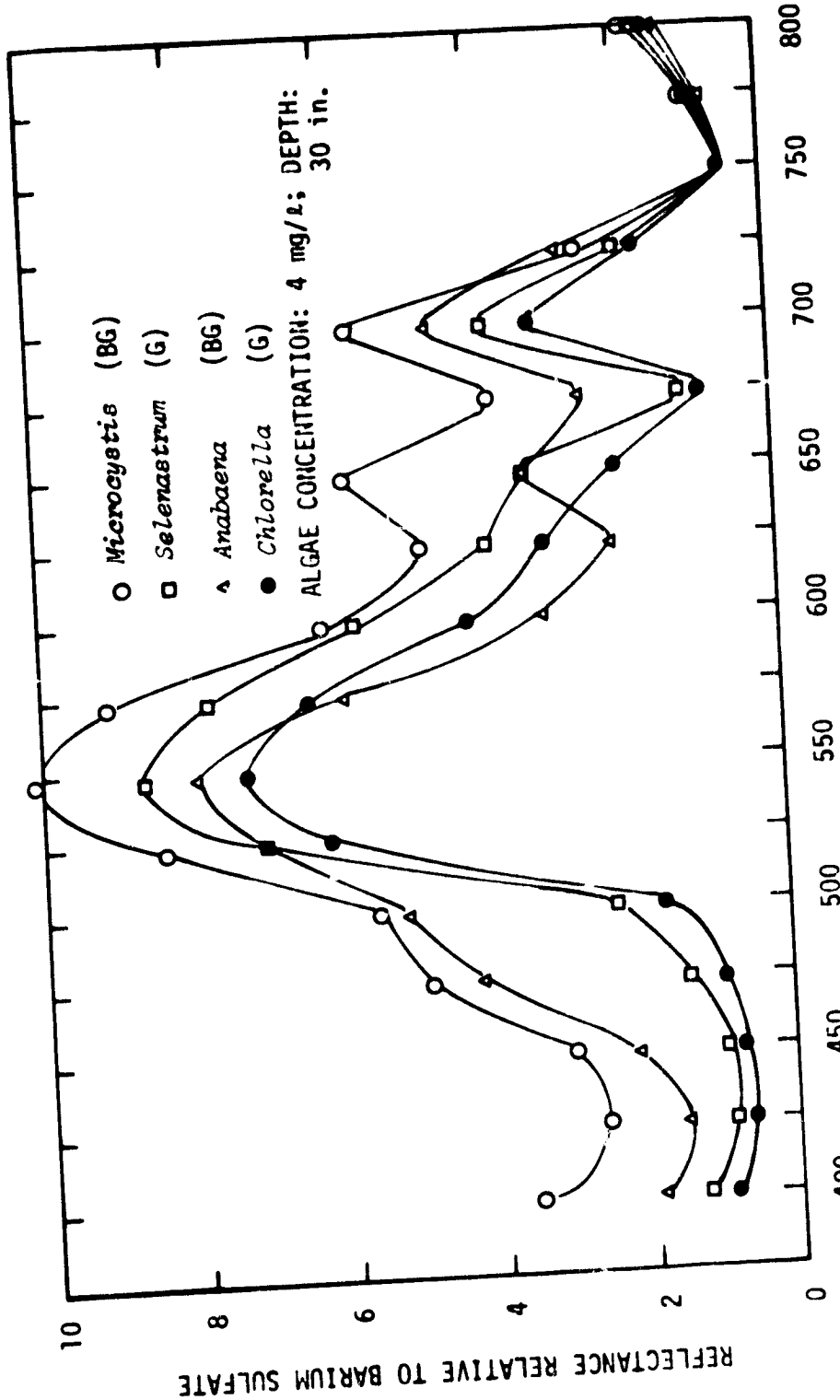

FIGURE 19. RELATIVE SPECTRAL REFLECTANCE CURVES—TWO GREEN AND TWO BLUE-GREEN ALGAE [35]

2. Studies by Gausman and others have established that the infrared response of leaves is primarily due to changes in refractive index between hydrated cell walls and intracellular air spaces [37]. Clearly, if the response of intense surface concentrations of blue-green algae is equal in magnitude to that of leaves, the physical laws which govern the mechanism should apply.

3. Near the lake surface and at these high concentrations, the effect of water on the spectral signature is small and the suspension can be thought of as a solid.

4. By studying the surface properties of such near solids, knowledge of how phytoplankton reflect light can be gained and any spectral anomalies due to phytoplankton should be applicable to more dilute suspensions.

5. The infrared band has potential for monitoring the presence of nuisance algal scums in lakes or reservoirs.

At the same time, several questions arise:

First, to what extent do all phytoplankton share this property which has been ascribed to blue-green algae?

Secondly, since physiological stress in plants has been shown to have a measurable effect [37] on spectral response of higher terrestrial plants (Figure 20), how to phytoplankton respond to physiological stress?

Thirdly, at what concentration does an algal suspension form a near optically opaque surface?

Based on the preliminary observations of the Clear Lake study, it seems surprising that the infrared band has not received more attention in the study of chlorophyll models, and especially as a means of differentiating nuisance blue-green algae from other possibly more desirable algae. If distinctive features of phytoplankton reflectance are to be found in the infrared zone, it may be possible to determine phytoplankton type as well as concentration. Different reflected light spectra of algae have long been known to algal taxonomists, since when algae are viewed under a light microscope variations in the visible light spectrum are apparent and in part form the basis of their classification. Many of these variations in spectral signature within the visible region can be attributed to complicated effects of carotenoid pigments [38]. But as yet, remote sensing techniques have not been able to discern what color differences due to phytoplankton can be recognized by multispectral imagery. This is not surprising as aerial photographs taken at thousands of meters altitude cover areas of 2-5 square kilometers while an individual alga covers only 5-10 square microns in that area. The characteristic response of a very high concentration of five species was examined which represent three algal types found in lakes and reservoirs of the semi-arid zone—green algae, blue-green algae, and diatoms. The concentration of natural populations used in laboratory study were chosen to ensure that the response of the suspension would be most like that of an optically opaque

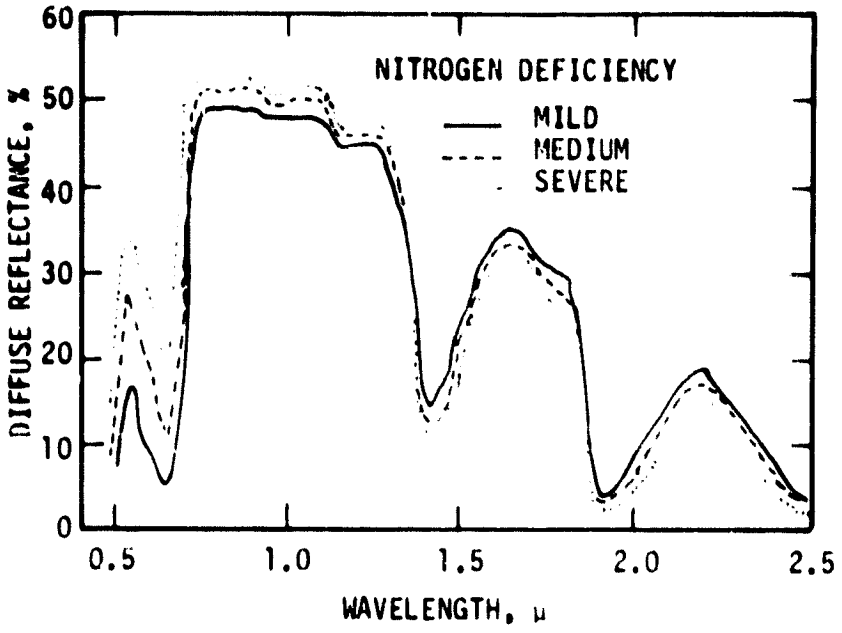

Effect of nitrogen deficiency on the diffuse reflectance of sweet pepper [30].

Spectral reflectance in the long-wavelength ultraviolet of bark and leaves of an apple tree. Data for both moisture-stressed and healthy materials are shown [22].

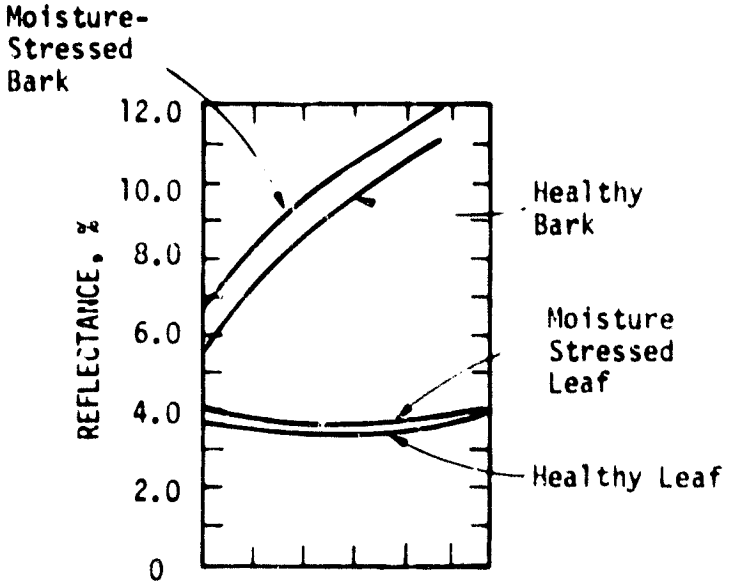

FIGURE 20. EFFECT OF ENVIRONMENTAL AND NUTRIENT STRESSES ON SPECTRAL REFLECTANCE OF HIGHER PLANTS

surface, while still retaining the natural form. (This would not be true if the algae were dried.) We have assumed that such a surface would promote the largest infrared response possible. The results of this study determine the feasibility of differentiating nuisance blue-green algae from the other types.

SEDIMENT REFLECTANCE

Spectral signatures received from the backscattering of light by inorganic sediment in lakes and reservoirs vary as a function of wavelength, particle composition, concentration, and size [7]. The spectral signatures of inorganic suspended solids are often readily distinguishable from those of phytoplankton. Generally speaking, sediment appears to reflect well at visible wavelengths, particularly in red, and IR reflectance is usually low. A commonly observed response from sediment shows a spectrum much like that of normal daylight with a shift to the yellow or orange region (Figure 21). This is a crude approach to the analysis of sediment reflectance patterns. (For further details see ref. 14. This relative spectral signature was recorded on 21 February 1975 (1233 hr.) at Clear Lake, California. A sampling crew was stationed in a boat near the mouth of the lake's major inflow, Rodman Slough, just after a major winter storm. The signature was recorded under natural daylight conditions, and the fiber optics probe was directed down toward the water from 10 cm elevation. Turbidity was measured at 55 JTU. Chlorophyll a was found to be less than 1.0 $\mu g/\ell$.

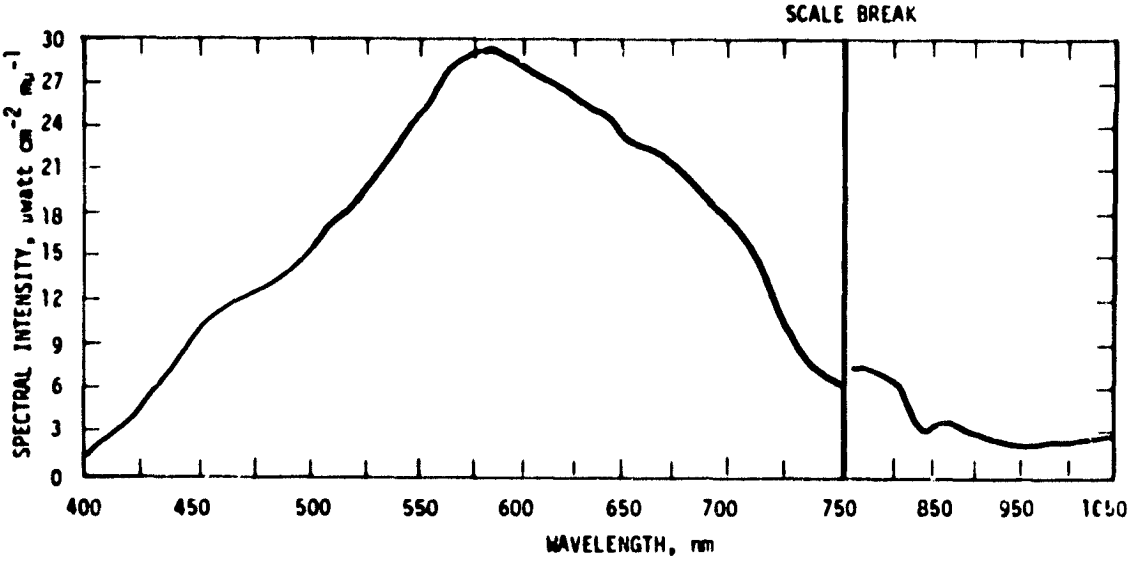

FIGURE 21. A TYPICAL SPECTRAL SIGNATURE FROM WATER WITH A LARGE AMOUNT OF SUSPENDED INORGANIC SEDIMENT MEASURED WITH AN ISCO SPECTROPHOTOMETER

VI. RESULTS

LABORATORY STUDIES (MAINLY QUALITATIVE) ON REFLECTANCE OF NATURAL POPULATIONS OF NUISANCE ALGAE AND HIGHER PLANTS

Plant Taxonomic Groups and Their Characteristic Reflectance Signatures

A comparison of the spectral signatures resulting when taxonomically different phytoplankton constitute the suspended solids in the test tank was made (Figures 22-25). Figure 22 shows the spectral properties of a concentrated suspension with representative green algae, diatoms, and blue-green algae on the same energy scale, and Figure 23 shows the reflectance spectrum of green algae and diatoms on an expanded energy scale. Figure 24 compares the shape of the spectral signature of *Lemna* to green algae, neglecting the disparity of energy reflected, and Figure 25 presents a similar comparison of the signatures of green algae, blue-green algae, and diatoms neglecting energy inequalities. The results of the study can be summarized as follows:

Blue-green algae and the macrophyte *Lemna* reflect much more light than either green algae or diatoms. Reflectance in the infrared band is 3 to 4 times greater for these two aquatic organisms in comparison to an equal concentration of either the green algae or diatoms (Figure 22 and Table III).

Despite the similarity in quantity of light reflected, a basic dissimilarity exists in the general shape of the spectral curves of the blue-green algae and *Lemna*. Green algae and *Lemna* exhibit a greater similarity of reflectance, since any two waveband ratios are nearly identical for the two organisms (Figure 24 and Table V).

Another dissimilarity exists between algae of different groups. Diatoms behave in a unique optical fashion when compared to either blue-green or green algae. Discounting the disparity of energy, it is apparent that diatoms reflect a proportionately greater amount of light from the red waveband than either blue-green or green algae and that the peak in the green has shifted 25 nm to the red (Figure 25 and Table III).

Minor discrepancies exist in the spectral signature of individual Chlorophytes. The filamentous green alga, *Spirogyra*, is shown to reflect slightly more light in the infrared band than a mixed population of unicellular green algae or the filamentous *Ulothrix* (Figure 23).

The broad band of reflectance noted in the infrared range of all samples (Figures 22-25) suggests that particle scattering of light rather than a photochemical event is the primary event affecting the spectral signature in this region. Fluorescence would produce sharp distinct peaks.

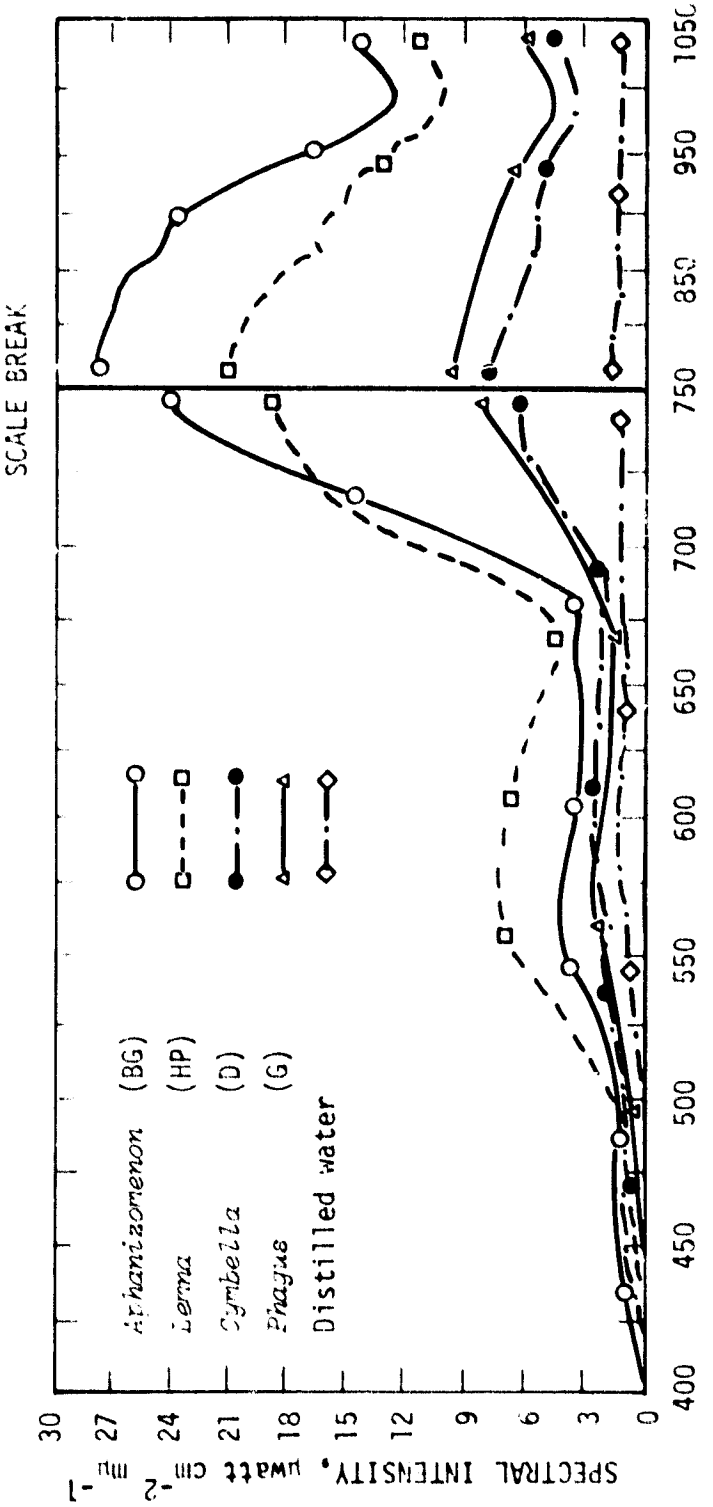

(BG) = BLUE-GREEN ALGA (HP) = HIGHER PLANT (D) = DIATOM (G) = GREEN PLANT

FIGURE 22. SPECTRAL REFLECTANCE CURVES OF FOUR AQUATIC PLANTS (Chl a CONCENTRATION: 200 mg/L)

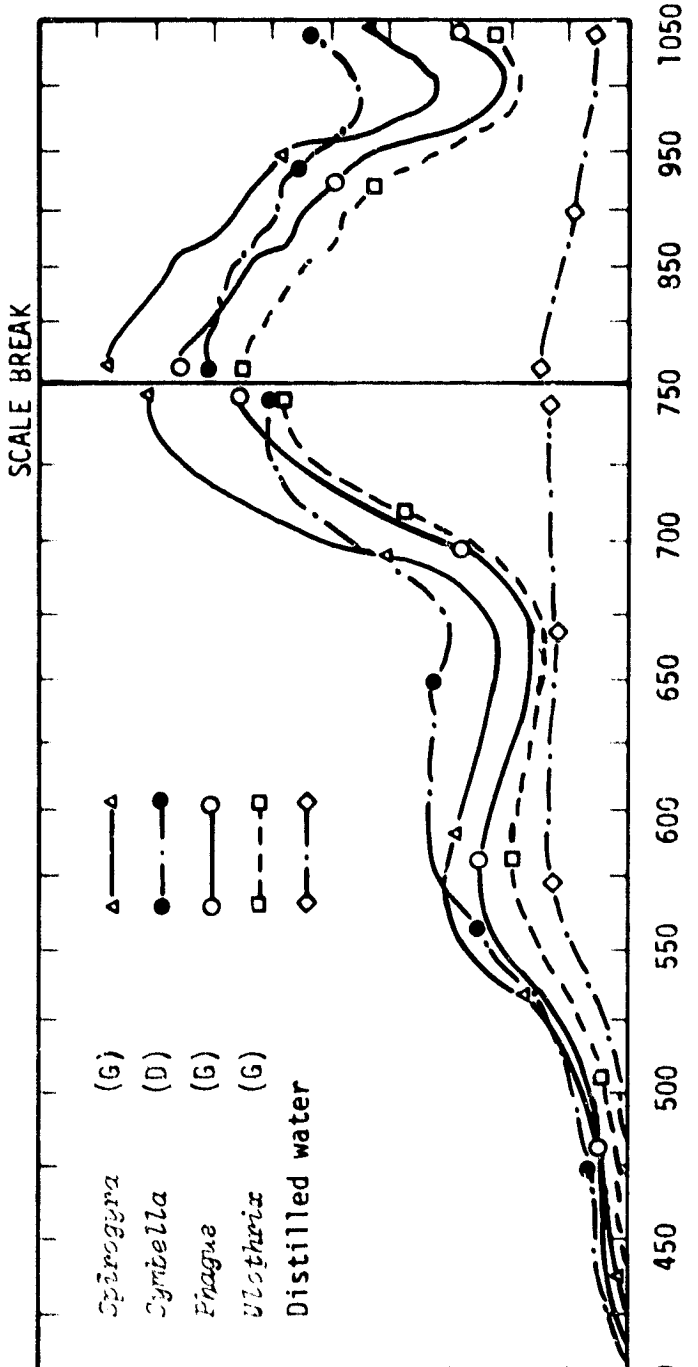

(G) = GREEN ALGA (D) = DIATOM

FIGURE 23. SPECTRAL REFLECTANCE CURVES OF GREEN ALGAE AND DIATOMS ON AN EXPANDED ENERGY SCALE (Chl a CONCENTRATION: 200 mg/ℓ)

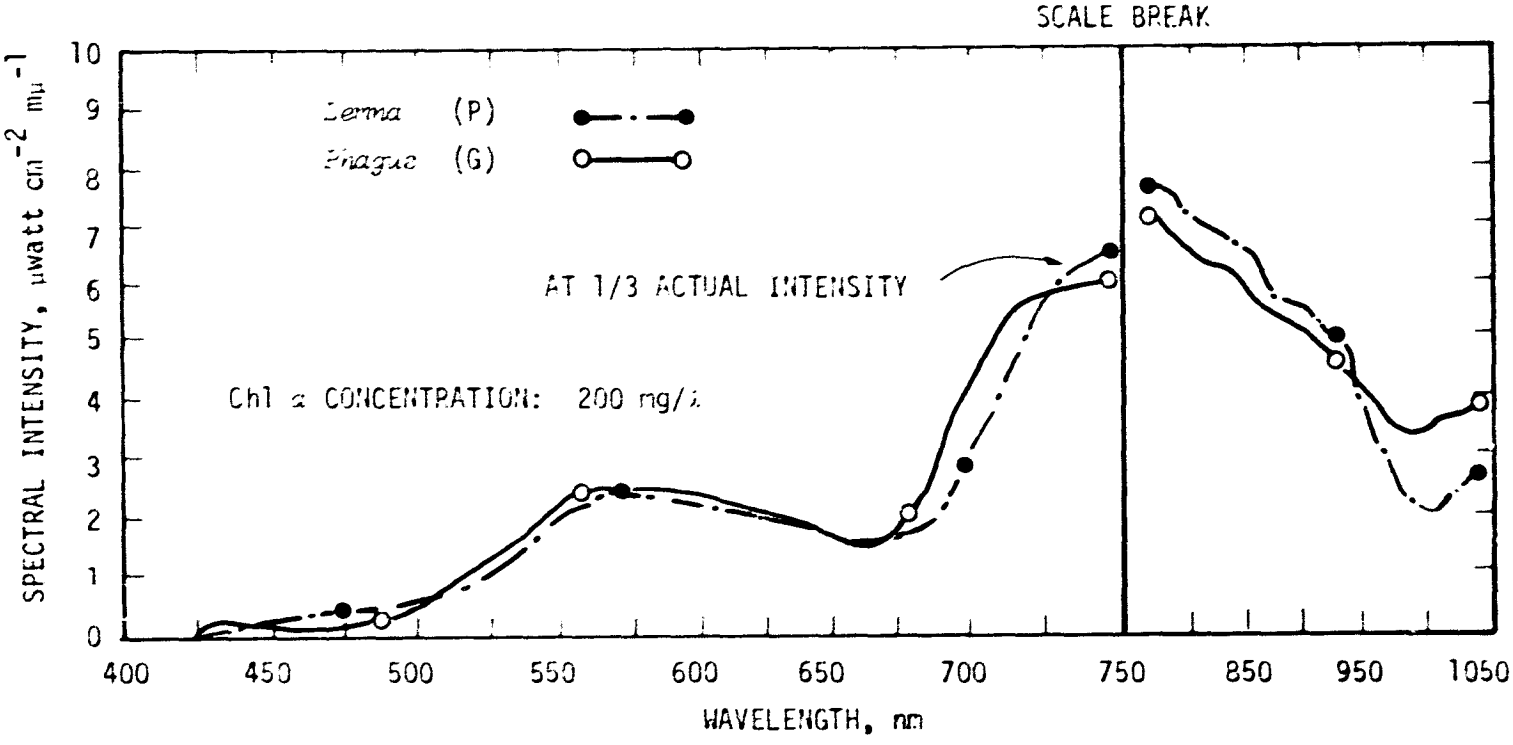

FIGURE 24. COMPARISON OF THE SHAPE OF THE SPECTRAL REFLECTANCE CURVES OF A GREEN PLANT AND A GREEN ALGA

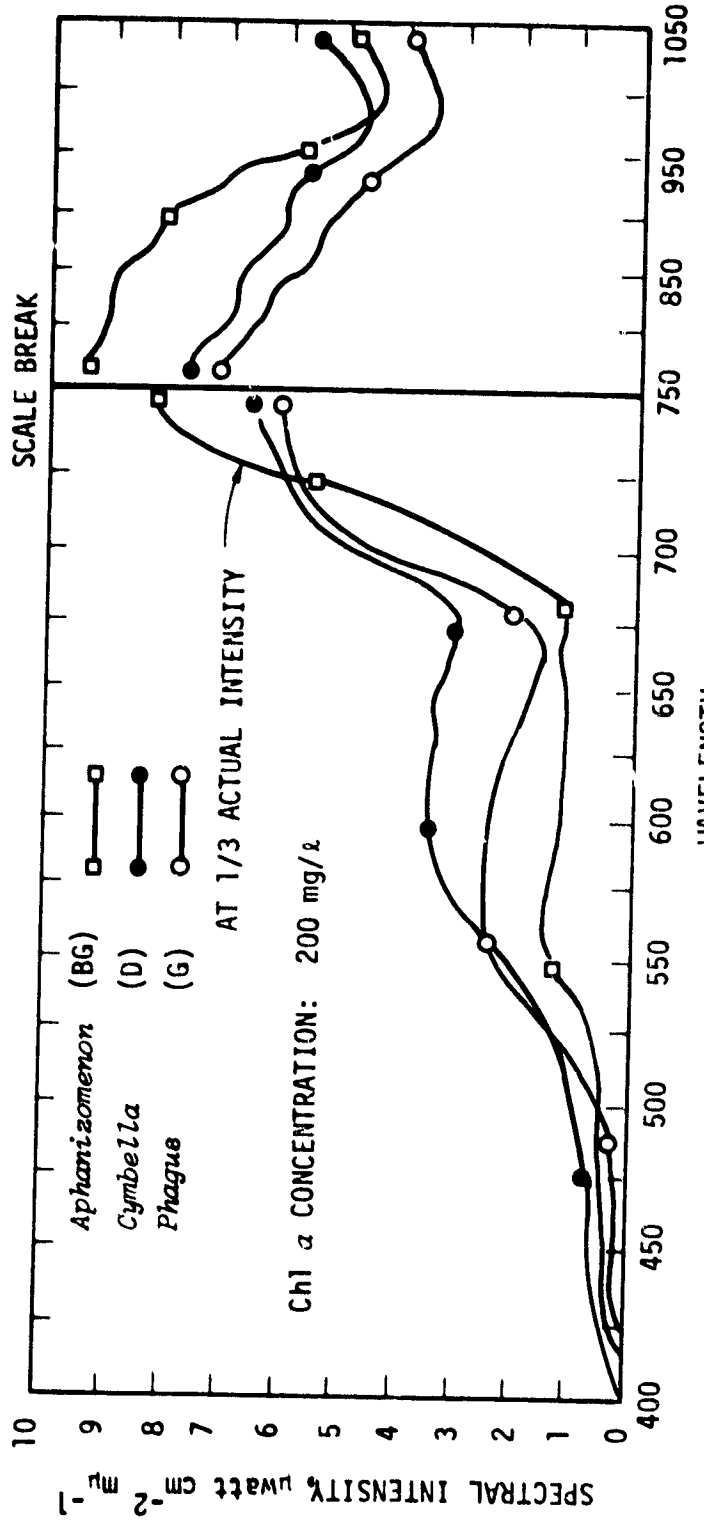

(BG) = BLUE-GREEN ALGA (D) = DIATOM (G) = GREEN ALGA

FIGURE 25. COMPARISON OF THE SHAPE OF THE SPECTRAL REFLECTANCE CURVES OF THREE ALGAL TYPES

TABLE III

REFLECTANCE VALUES AS A PERCENTAGE OF INCIDENT LIGHT FOR EQUAL QUANTITIES OF DIATOMS, BLUE-GREEN ALGAE, GREEN ALGAE AND *Lemna*

Specimen (200 mg/ℓ Chl *a*)	Reflectance as a % of Incident Light				
	440 nm	565 nm	625 nm	650 nm	730 nm
Aphanizomenon (BG)	4.1	6.0	4.5	5.1	40
Lemna (HP)	4.1	10.7	9.6	7.1	31
Spirogyra (G)	2.1	4.0	3.6	3.1	13
Phagus and *Chlamydomonas* (FG)	2.1	3.3	3.0	2.4	10
Ulothrix (G)	1.9	2.7	2.5	2.3	9
Cymbella and *Nitzchia* (D)	2.1	3.7	4.8	5.0	10

(BG) Blue-green alga
(HP) Higher plant
(G) Filamentous green alga
(FG) Flagellated green alga
(D) Diatom

TABLE IV

REFLECTANCE VALUES OF SPECIMENS AS A PERCENTAGE OF *Aphanizomenon flos-aquae* REFLECTANCE FOR EQUAL QUANTITIES OF EACH GROUP

Specimen (200 mg/ℓ Chl *a*)	Reflectance as a % of Blue-Green Algal Reflectance				
	440 nm	565 nm	625 nm	650 nm	730 nm
Aphanizomenon (BG)	100	100	100	100	100
Lemna (HP)	100	178	213	140	78
Spirogyra (G)	51	67	80	61	33
Phagus and *Chlamydomonas* (FG)	51	55	67	47	25
Ulothrix (G)	46	45	55	45	23
Cymbella and *Nitzchia* (D)	51	62	107	98	25

(BG) Blue-green alga
(HP) Higher plant
(G) Filamentous green alga
(FG) Flagellated green alga
(D) Diatom

TABLE V

VALUES FOR THE REFLECTANCE RATIOS (565/730, 625/730, 650/730) FOR DIATOMS, BLUE-GREEN ALGAE, GREEN ALGAE, AND *Lemna*

Specimen (200 mg/ℓ Chl *a*)	Reflectance Ratios		
	565/720 nm	625/730 nm	650/730 nm
Aphanizomenon (BG)	0.1625	0.125	0.145
Cyclotella and *Nitzschia* (D)	0.42	0.50	0.55
Spirogyra (G)	0.5	0.42	0.33
Ulothrix (G)	0.40	0.34	0.30
Phacus and *Chlamydomonas* (FG)	0.42	0.34	0.30
Lemna (HP)	0.42	0.34	0.30

(BG) Blue-green alga

(D) Diatom

(G) Filamentous green alga

(FG) Flagellated green alga

(HP) Higher plant

Effect of Cellular Architecture on Spectral Signatures—Variations in the Reflectance of *Aphanizomenon flos-aquae* as a Function of Gas Vacuolation and Other Cellular Components

Based on the hypothesis that gas vacuoles present in *Aphanizomenon flos-aquae* promote increased light scattering, changes in spectral composition due to the gas vacuoles were determined.

A comparison of the resultant spectral signatures obtained when the algae were subject to discrete pressures is presented in Figure 26. The spectral signature taken when the algae were subject to 6.8 atmospheres pressure is shown on Figure 27 at an expanded energy scale. The results of the study can be summarized as follows:

Gas-vacuolated blue-green algae subject to gas-vacuole collapse by pressure show a stepwise decrease in light reflected over the entire spectrum measured with a stepwise increase in pressure. The relative shape of the curve remains more or less unchanged before, during, and after gas vacuole collapse by pressure (Table VI).

When gas vacuoles of *Aphanizomenon flos-aquae* are subject to 6.8 atm pressure, a two-thirds reduction in the intensity of light backscattered is observed. At this point, the intensity of light reflected in the infrared band is near that of green algae, while in the visible range the values drop below that of the green algae (Figure 28).

Role of Cellular Constituents (Other than Gas Vacuoles) in Promoting Light Scattering

Although the intensity of light reflected by *Aphanizomenon flos-aquae* was reduced when gas vacuoles were collapsed, the essential shape of the spectral signature remained virtually unchanged (Figure 27). The obvious conclusion is that the mechanism of light reflectance is primarily a function of cell constituents of varying refractive index, and for this reason gas vacuoles, chloroplasts, cell walls, storage vacuoles, membranes, chromatophores, and pyrenoids found in algae may all help scatter incident light. Photographic records of light transmitted and reflected by representative algal species were also made. Figure 38E-F illustrates color reproductions of false color infrared photos of the blue-green alga *Anabaena flos-aquae* using transmitted light. Figure 39 illustrates a reflected light photo of the same. Figure 38E represents algae with gas vacuoles present, with the exception that the cells in the lower middle row of Figure 38E (marker B) have lost their gas vacuoles. The algae were cultured with ample nutrients and illumination until the gas vacuoles collapsed due to the production of photosynthetic products which increase turgor pressure [39]. The gas vacuoles appear as crystal-like objects near the periphery of the protoplast and their ability to reflect or transmit infrared light is demonstrated in Figure 38E by the strong red tone indicative of infrared response. Figure 38F shows the same algae after gas vacuoles were crushed by the classic cork, hammer, and bottle experiment (Van Klebahn, 1898) [23]. All pictures were taken at the same magnification of 600 x.

Gas vacuoles appear to act like fragments of glass lodged in the cell, reflecting or transmitting light depending on their orientation

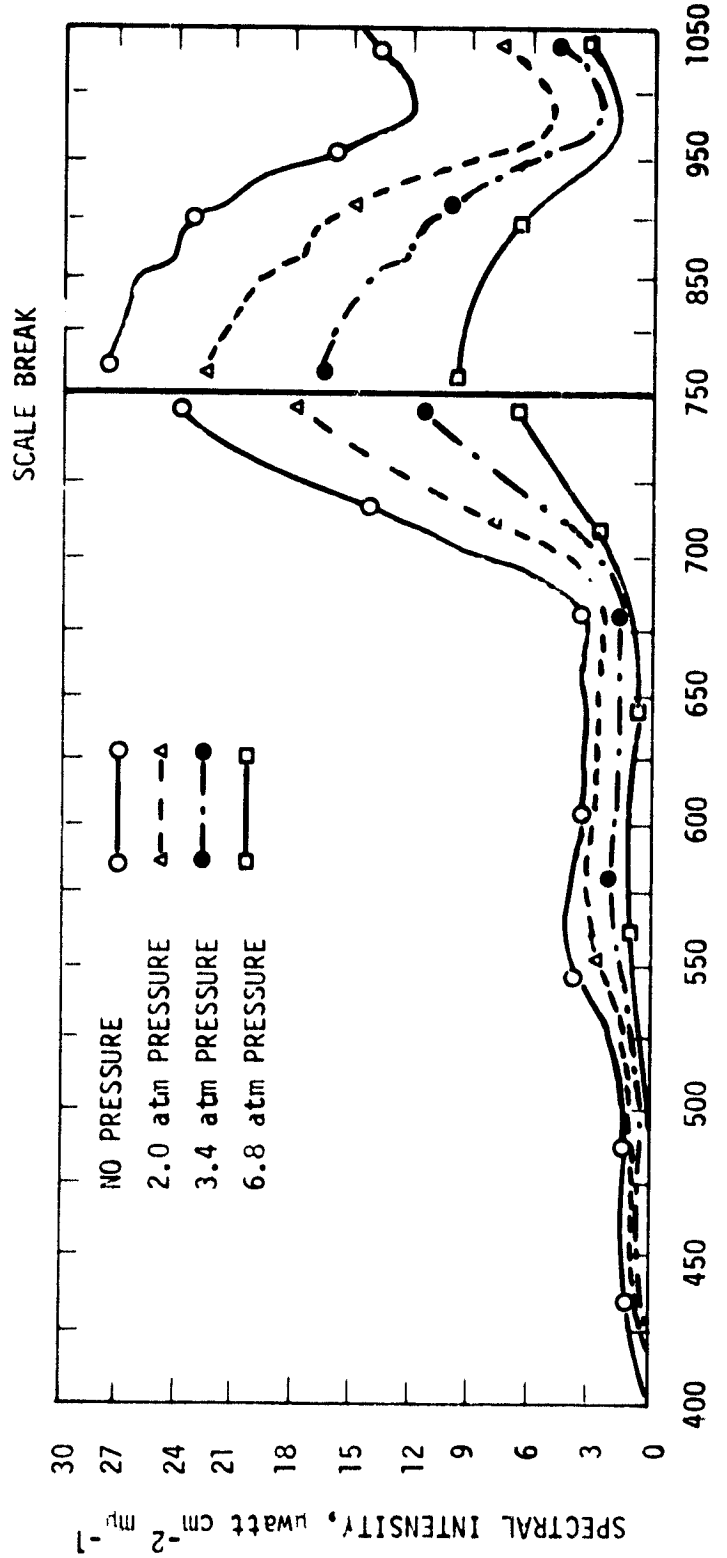

FIGURE 26. VARIATION IN SPECTRAL REFLECTANCE OF *Aphanizomenon flos-aquae* AS A FUNCTION OF GAS VACUOLE COLLAPSE UNDER PRESSURE (Chl *a* CONCENTRATION—200 mg/ℓ)

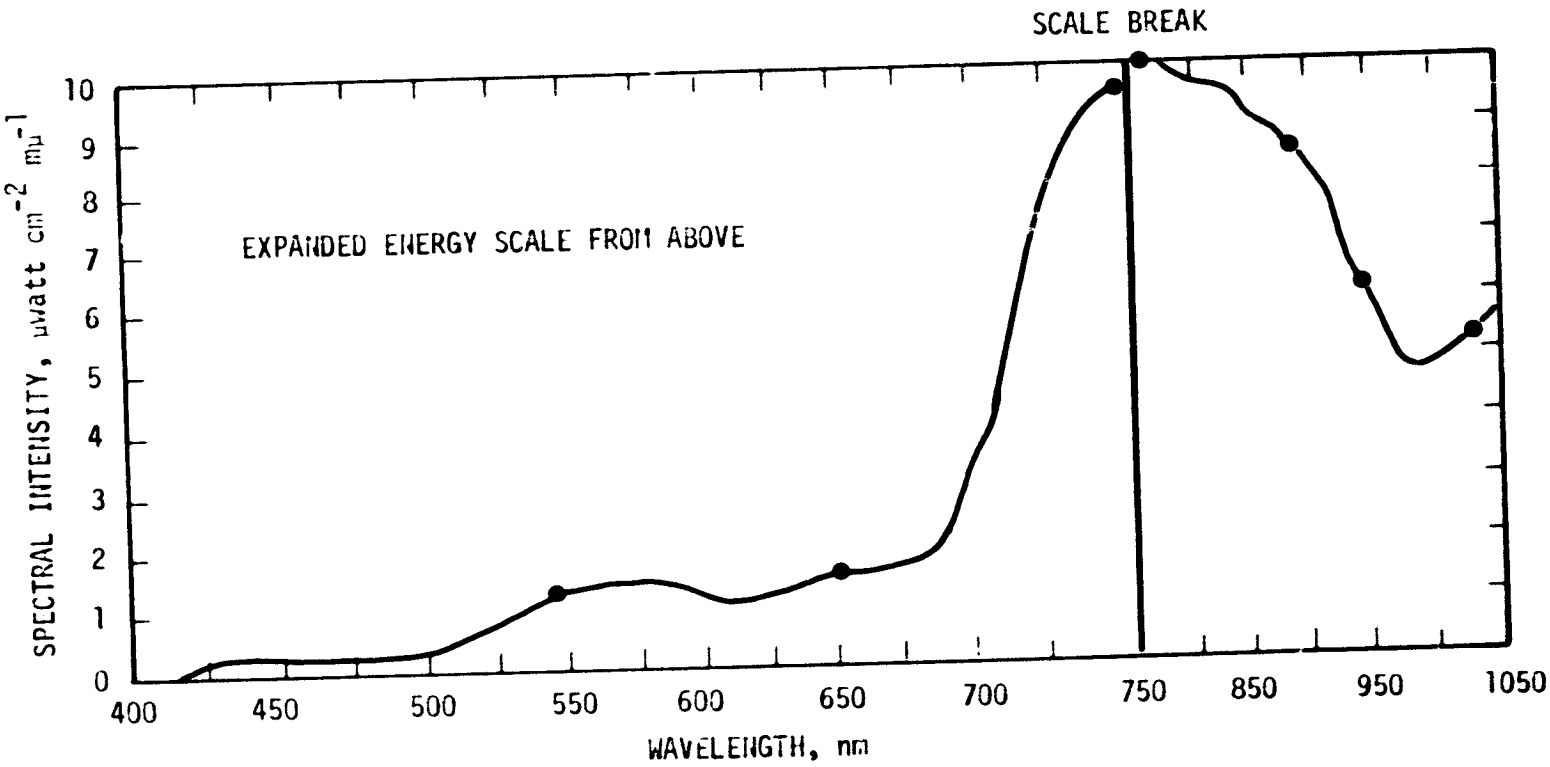

FIGURE 27. SPECTRAL REFLECTANCE CURVE OF *Aphanizomenon flos-aquae* WITH GAS VACUOLES COLLAPSED BY 6.8 atm. PRESSURE

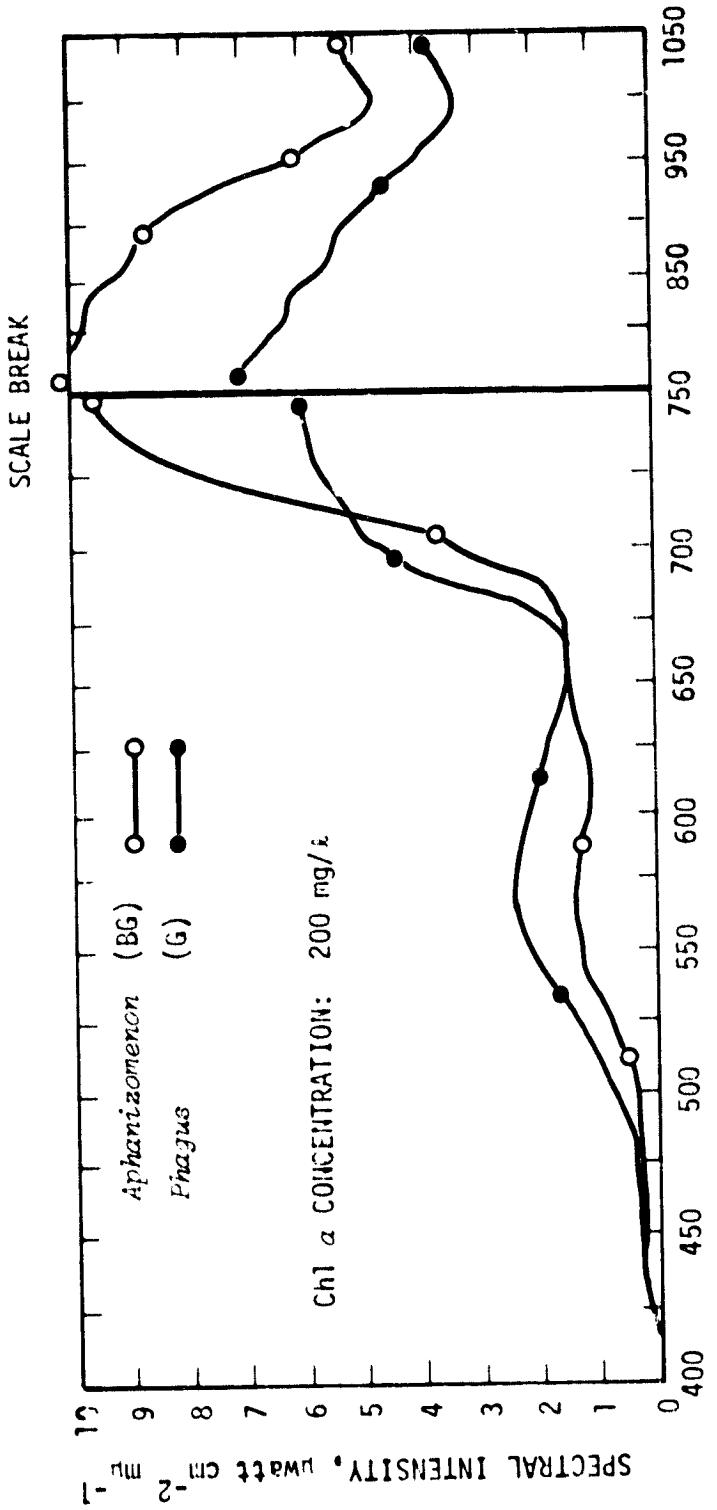

(BG) = BLUE-GREEN ALGA (G) = GREEN ALGA

FIGURE 28. COMPARISON OF THE SPECTRAL REFLECTANCE CURVES OF *Aphanizomenon flos-aquae* WITH GAS VACUOLES COLLAPSED BY 6.8 atm PRESSURE AND *Phagus*

TABLE VI

VALUES FOR THE REFLECTANCE RATIOS FOR BLUE-GREEN ALGAE BEFORE AND AFTER GAS VACUOLE COLLAPSE
Aphanizomenon flos-aquae, 200 mg/ℓ Chl *a*

Reflectance Ratio	With Gas Vacuoles	Without Gas Vacuoles
565/730 nm	0.1625	0.161
625/730 nm	0.125	0.133
650/730 nm	0.145	0.160

to incoming light (Figure 38E, F). The change in the index of refraction encountered at the gas vesicle membrane appears to cause Fresnal reflection. Consider the geometric relationships involved in taking this photo. Radiant energy from the light source passed through a ground glass diffuser and was then focused on the specimen. If the plane of reference is the plane in which light is travelling (the plane perpendicular to the glass slide), light impinges on the slide with most of the radiant energy approaching from an angle of incidence of 0 deg. The glass slide in this instance constitutes a single transparent plane and from Figure 29 it can be seen that the main portion of light striking the slide should be transmitted. Hence, in the transmitted light photos the areas adjacent to the algal cells appear slightly blue on false color film (indicative of green, the predominant light component of the spectrum striking the slide). In the reflected light photos, the areas adjacent to the cells appear black, indicating that very little light is reflected. However, if the object in the reflective plane is a semi-transparent algal cell with gas vacuoles randomly oriented within the cell, incident light will strike the vacuoles from a variety of angles varying from 0 deg. to 90 deg. and the percentage of light transmitted will vary in a predictable but complicated fashion dependent upon each vacuole's orientation to incident light. If the angle is sufficiently large, light will be critically reflected.

The variability of response from gas vacuoles in the photos illustrates that orientation of gas vacuoles within the cell plays a large role in determining the magnitude of light transmitted or reflected. Resolution is generally poor in the reflected light photos and the response is variable from cell to cell, apparently due to random gas vacuole orientation. It seems, however, that the predominant infrared reflection originates from the

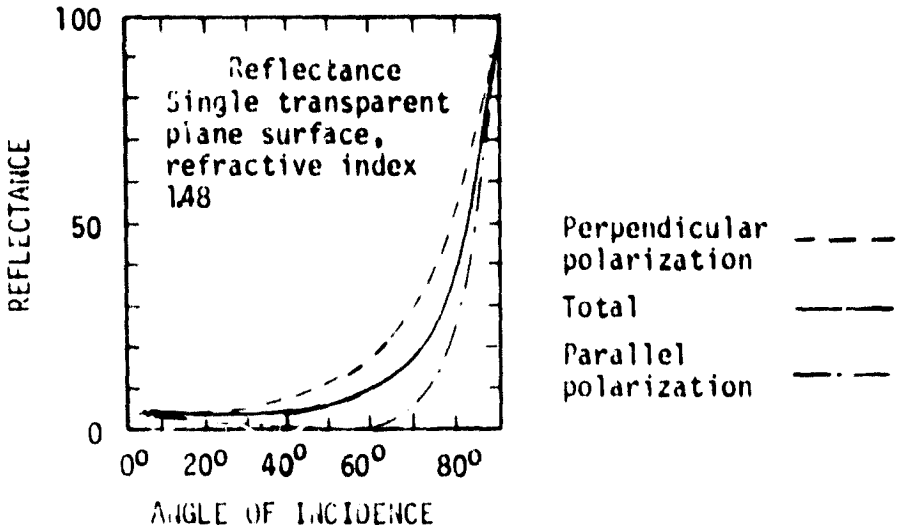

Note: Theoretical reflectance from a single transparent plane surface having a refractive index of 1.48, in air, computed from the Fresnel formulas. The three curves are for light polarized with the electric vector perpendicular to the test plane, light polarized with the electric vector parallel to the test plane, and (TOTAL) unpolarized light. The test plane is the plane perpendicular to the reflecting surface and containing the incoming ray of light [37].

FIGURE 29. THEORETICAL REFLECTANCE OF A SINGLE, TRANSPARENT PLANE SURFACE

peripheral area where gas vacuoles are present. This also appears as a halo effect surrounding the entire cell. Qualitatively, Figure 38E appears similar with the exception that the infrared halo effect is greatly diminished in the transmitted light photo. Interestingly, since the magnitude of infrared response from the gas vacuole region in either the transmitted or reflected light photos is similar, the indication is that gas vacuoles are oriented more in the plane of incident light. Hence, critical reflectance occurs more often than would be anticipated if the vacuoles were in the perpendicular plane. In a sense, gas vacuoles appear from the photos to be oriented so as to shield the cell from high light intensity. The infrared halo also appears to confirm this, although work by Walsby (personal communication) casts doubt on the shielding hypothesis.

Figure 39E-F illustrates the lack of infrared response by algae without gas vacuoles. Numerous other species of green algae, diatoms, and flagellated algae were photographed in a similar fashion, but again the infrared response was largely absent by comparison with the blue-green algae. Figure 39E-F also shows the dramatic effect of removing gas vacuoles.

A certain amount of infrared response can be detected as coming apparently from tannin in vacuoles of *Spirogyra* (Figure 39E), as a halo effect surrounding cell walls (Figure 39E-F), and as a halo effect surrounding pyrenoids (Figure 39E). No attempt was made to quantify the

nature of this response; rather it was intended just to show how the production of certain cellular components might possibly affect spectral response.

To determine whether or not *in vivo* chlorophyll fluorescence played a large part in the NIR response, color IR microphotographs were employed using a Corning glass filter CS-560 as a screen so that only blue light would excite chlorophyll and a Kodak #29 filter over the camera lens so that only light from the 680 nm to 900 nm wavelength range would be recorded. This array is nearly identical to that used in fluorimeters to record chlorophyll fluorescence. NIR light was captured on the film, but the exposure time was in the order of hours as compared to the ∿0.1-sec exposure needed to record NIR light originating from the reflected light array. Although the filters required a compensation factor of 2-4 (due to less light irradiance in the blue region by the source), the contribution of fluorescence to the reflected light spectra of healthy algae seems minor.

Effect of Decay on Reflectance Signatures

In real lake systems algae exhibit a variety of physiological states which presumably effect the reflected light signature (c.f. Figure 20 and the effect of N on reflectance of sweet pepper leaves).

The results of the study can be summarized as follows:

For gas vacuolated blue-green algae, the reflected light response as a function of temporal decay produced a drop in infrared reflectance. Visible light reflectance increased as the suspension of healthy algae died and lysis occurred (Figure 30). Since the response in the infrared region is quite similar to that observed when gas vacuoles are caused to collapse under pressure, gas vacuoles may play a large part in the signature change. Increased reflectance in the visible wavelengths may be due to the uncoupling of the photosynthetic apparatus, or to pigment decomposition.

For filamentous green algae, the reflected light response as a function of decay increased reflectance in the infrared range as gas bubbles formed and thus promoted increased light reflectance (Figure 31). As the photosynthetic apparatus reacted to more favorable light conditions, CO_2 and O_2 evolution also increased. In dense populations of filamentous algae, gas was sometimes trapped among the filaments [40]. Reflectance in the visible range was little changed, perhaps indicating that not only greater light penetration and reflection but also preferential absorbtion of desirable wavelengths occurred. The gas bubble in this sample may have served a useful light shielding function. As more favorable conditions for algal growth were created, the filamentous forms became favorable host substrates for other algal types. Attached filamentous algal growths often supported large growths of attached diatoms. If the diatom growth is successful in such an environment, the reflected light signature begins to indicate diatom presence, reflectance in the infrared range drops as gas bubbles are lost, and the spectral curve for the visible range comes to represent that of a typical diatom suspension.

For unicellular green algae (Figure 32), a reflected light signature change similar to that of attached green algae was observed.

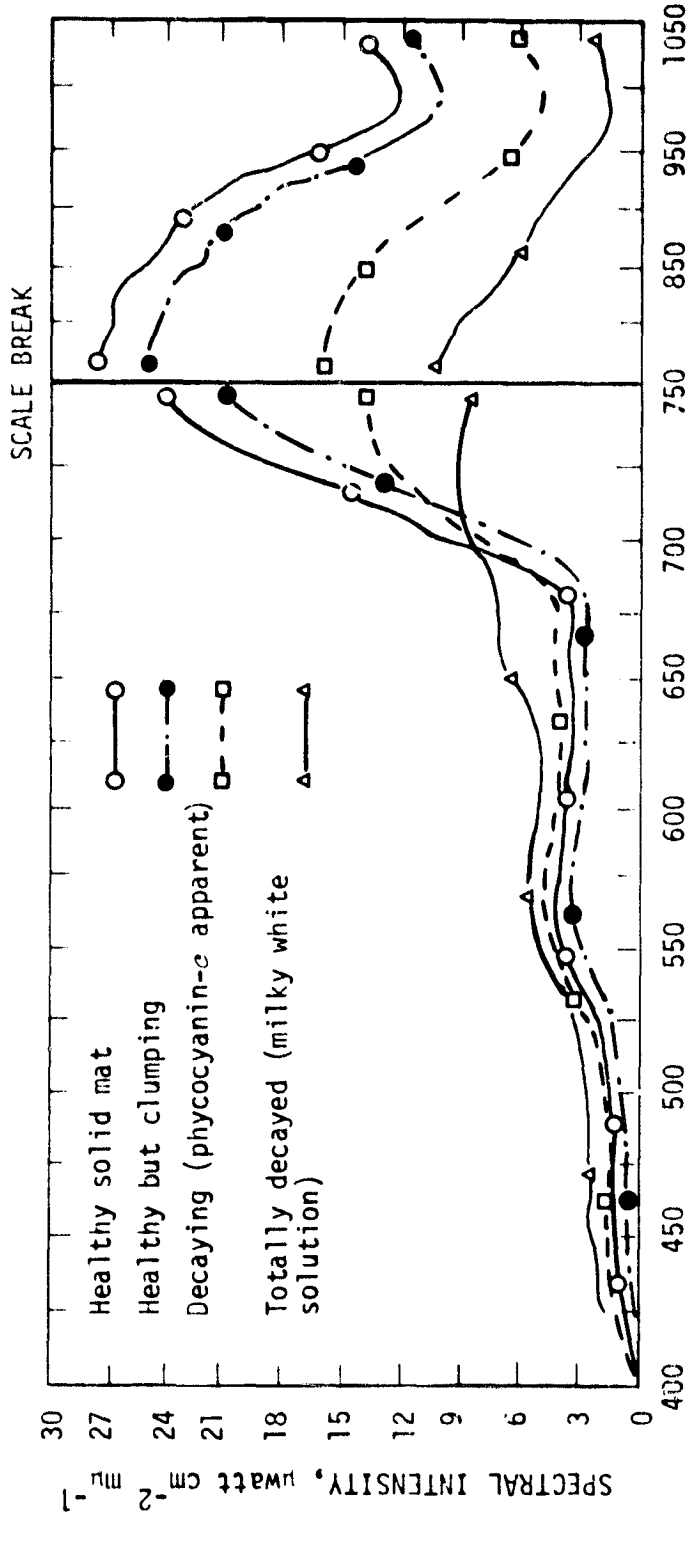

FIGURE 30. VARIATIONS IN SPECTRAL REFLECTANCE OF BLUE-GREEN ALGAE AS A FUNCTION OF CELL ACTIVITY DISRUPTION AND EVENTUAL DEATH. (ORIGINAL Chl *a* CONCENTRATION: 200 mg/ℓ)

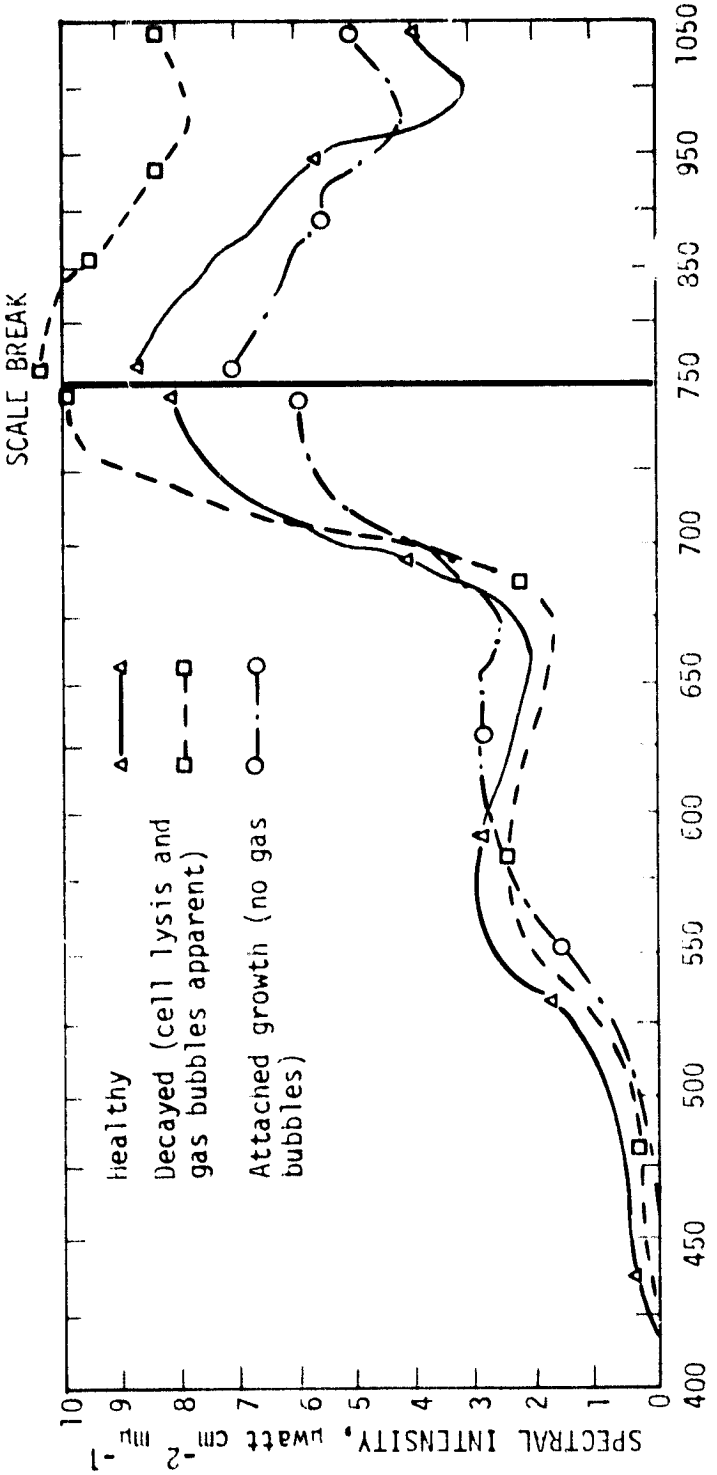

FIGURE 31. VARIATIONS IN SPECTRAL REFLECTANCE OF GREEN ALGAE AS A FUNCTION OF CELL ACTIVITY DISRUPTION AND DEATH (ORIGINAL Chl *a* CONCENTRATION: 200 mg/m^3; SUBJECT: *Scenedesmus*)

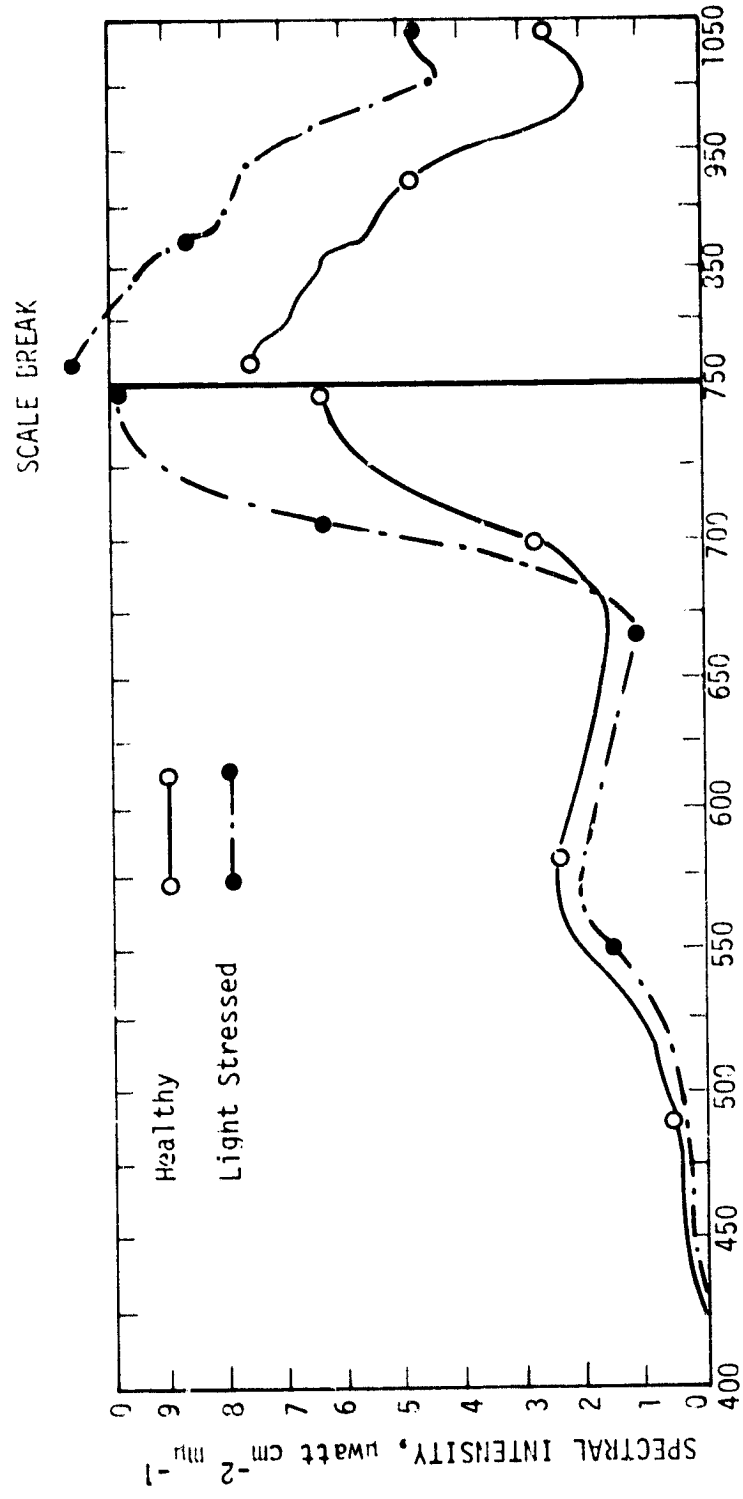

FIGURE 32. VARIATIONS IN SPECTRAL REFLECTANCE OF GREEN ALGAE AS A FUNCTION OF CELL ACTIVITY DISRUPTION AND DEATH (SUBJECT: *Enagus*–Chl *a* CONCENTRATION - 200 mg/ℓ)

Flagellated green algae responded to more favorable light conditions by migration. When light conditions changed rapidly, some algae were trapped on the surface in unfavorable conditions. The incident light striking water with a thick surface algal film passed through a plane of abnormally high refractive index. Since the diffuse incident light must pass a highly irregular layer of neustonic algal cell walls before water contact is made, light scattering increased. A differential response to infrared light could be observed. However, no explanation is readily apparent. Changes in pigment structure may be partially responsible.

Intracellular and intercellular air spaces in concentrated phytoplankton suspensions thus have a large influence on reflected infrared light response. An experiment to measure the spectral response of plant material suspensions largely lacking photosynthetic apparatus but having intracellular air spaces was performed (Figures 23 and 24) to estimate the importance of refractive index discontinuities of cellular constituents. This can be compared to the importance of photochemical events such as fluorescence in contributing light to the infrared region. As can be seen in Figure 33, a suspension of cellulose matter (twigs, bark, wood chips, etc. called debris) has reflectance value in the infrared range quite similar to that of green algae. A substantial deviation in the red band of the visible light spectrum is apparent and indicative of the lack of photosynthetic pigments [30]. A suspension of diatoms, by comparison, can be seen to reflect light over a visible region in a similar way to debris because it possesses fucoxanthin which absorbs in the green [41].

The similarities in shape (broad bands) and intensity of infrared reflectance by debris and phytoplankton suggest that fluorescence is indeed only a minor component of infrared light registered as reflectance. Of course, the debris used in this experiment may have a variable infrared response dependent upon the degree of porosity and hence buoyancy. Generally, however, the experiment indicates that particle scattering, not photochemical events, contribute by far the greatest proportion of light in the infrared wavelength bands.

Discussion of Laboratory Data

The results of the laboratory study serve as a basis for a number of conclusions which may be useful in remote sensing of water bodies.

Reflectance of Aquatic Phenomena. The reflected light spectral signatures from the algal or plant suspensions at concentrations used show an inverse relationship to known absorbance spectra of photosynthetic pigments. Table VII and Figure 35 illustrate the distribution of photosynthetic pigments and their absorbtion spectra in algae [41]. The composition of pigments in duckweed perhaps most resembles that found in green algae. Blue-green algae which are known to contain chl *a* (reflectance peak 435. 670-680 nm) and phycocyanin-*c* (absorbance peak 618 nm) as the predominant photosynthetic pigments have reflectance peaks at approximately 565 nm, 650 nm and 720 nm. The presence of phycocyanin-*c* can be seen in the depression from 575 nm to 630 nm and a minor peak at 650 nm. Comparison of *Aphanizomenon* with either duckweed or green algae (Figures 22 and 25) illustrates that green algae reflect more light from 575-630 nm while *Aphanizomenon* absorbs here. Green algae which contain Chl *a*

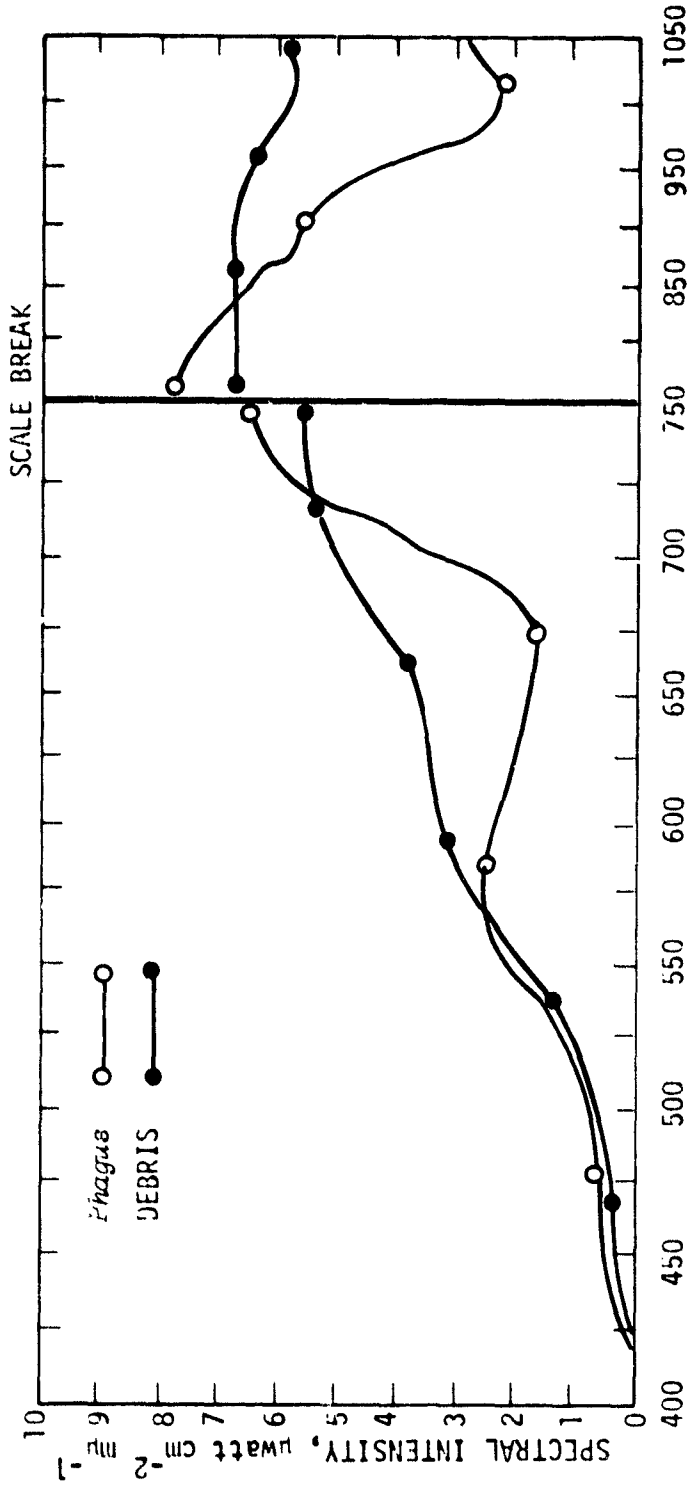

FIGURE 33. COMPARISON OF THE SPECTRAL REFLECTANCE CURVE OF DEBRIS AND GREEN ALGAE (*Phagus* Chl *a* CONCENTRATION: 200 mg/ℓ; DEBRIS CONCENTRATION: 120 g/ℓ WET WEIGHT)

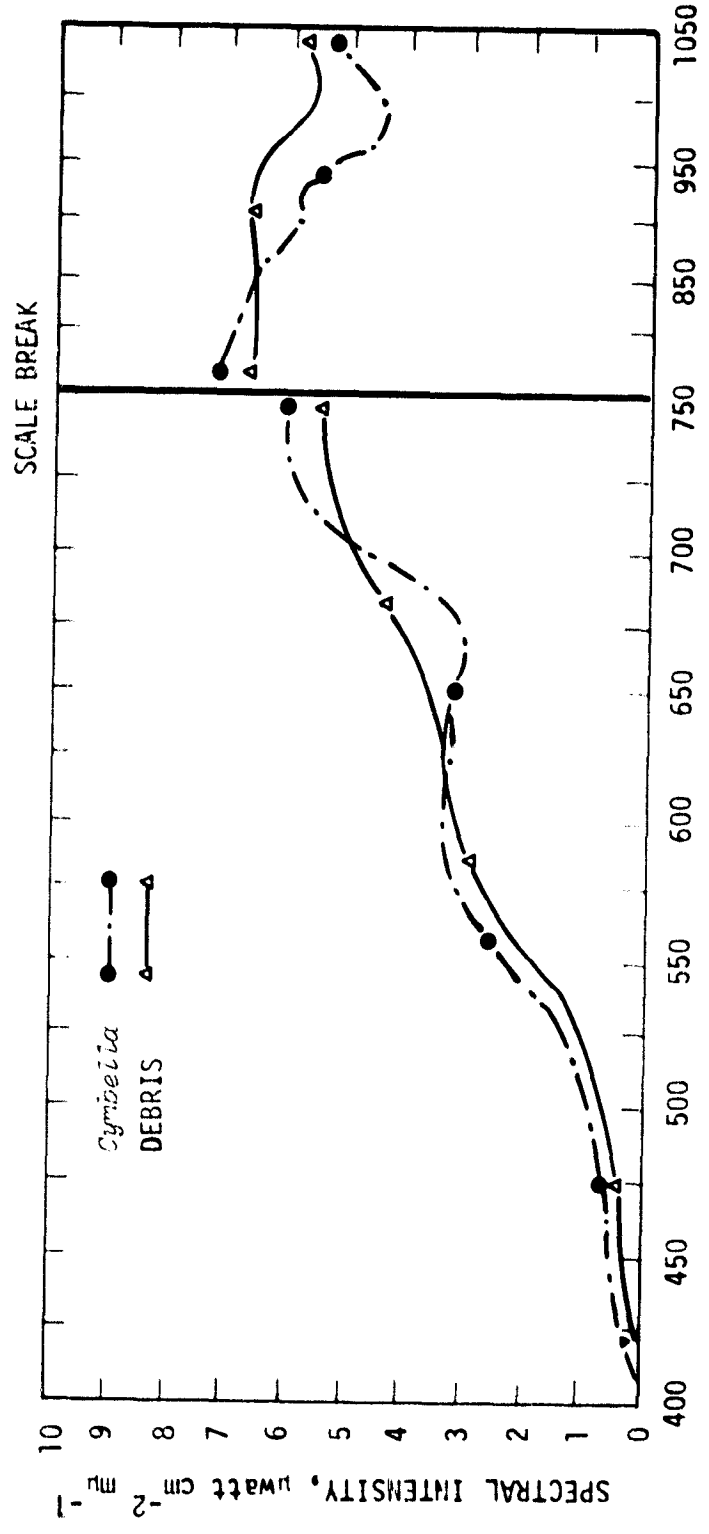

FIGURE 34. COMPARISON OF THE SPECTRAL REFLECTANCE OF DEBRIS AND DIATOMS (*Cymbella* Chl *a* CONCENTRATION: 200 mg/ℓ; DEBRIS CONCENTRATION: 120 g/ℓ WET WEIGHT)

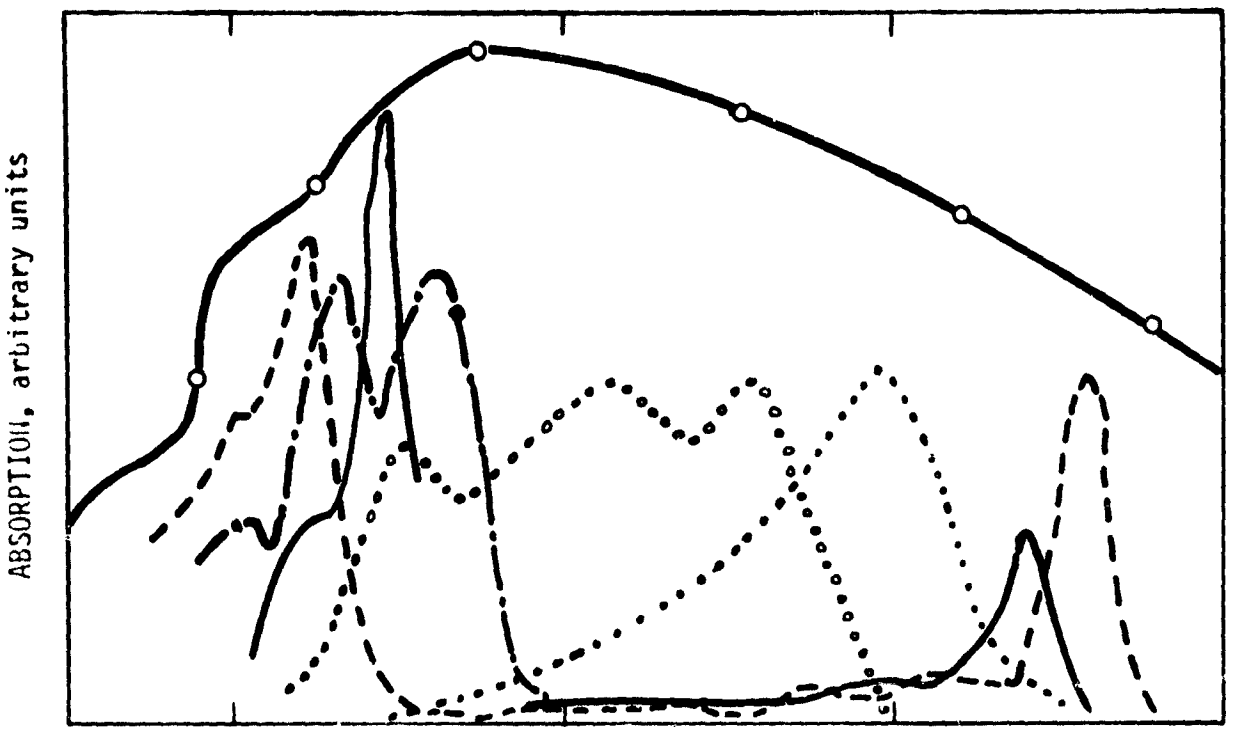

Chlorophyll ----

Chlorophyll ——

Carotenoids —·—

Phycoerythrin -.-.-

Phycocyanin .....

Solar spectrum —··—

ABSORPTION SPECTRA of the photosynthetic pigments measures the amount of light they absorb at various wavelengths. The chlorophylls have two absorption bands, one in the blue and one in the red. They are green because they transmit the intermediate wavelengths. The carotenoids absorb shorter wavelengths and appear yellow or red. Phycoerythrin, which absorbs blue through yellow light, is red and phycocyanin, absorbing long waves, appears blue. Together the pigments absorb most of the light in the solar spectrum [43].

Note: These spectra have been recorded from pigments extracted in organic solvents not *in vivo*. *In vivo*, the spectra would change slightly.

FIGURE 35. ABSORPTION SPECTRA OF PHOTOSYNTHETIC PIGMENTS

TABLE VII
THE PHOTOSYNTHETIC PIGMENTS [41]

A. The Chlorophylls			
Type of Chlorophyll	Characteristic Absorption Peaks		
	In Organic Solvents, nm	In Cells, nm	Occurrence
Chl *a*	420,662	435, 670-680 (several forms)	All algae
Chl *b*	455,644	480, 650 (two forms?)	Green algae
Chl *c*	444,626	Red band at 645	Diatoms and brown algae
Chl *d*	450,690	Red band at 740	Reported in some red algae (?)

B. The Carotenoids		
Types of Carotenoids	Characteristic Absorption Peaks, nm	Occurrence
I. Carotenes		
α-carotene	In hexane, at 420, 440, 470	In red algae and in siphonaceous green algae it is the major carotene
β-carotene	In hexane, at 425, 450, 480 (the 480 nm band may be shifted to 500 nm *in vivo*)	Main carotene of all other algae
II. The Xanthophylls		
Lutein	In ethanol, at 425, 445, 475	Major carotenoid of green algae and red algae
Fucoxanthin	In hexane, at 425, 450, 475 (*in vivo*, absorption extends to 580 nm)	Major carotenoid of diatoms and brown algae

C. The Phycobilins		
Types of Phycobilins	Absorption Peaks	Occurrence
Phycoerythrins	In water and *in vivo*: 490, 546, and 576 nm	Main phycobilin in red algae; also found in some blue-green algae
Phycocyanins	At 618 nm, in water and *in vivo*	Main phycobilin of blue-green algae; also found in red algae
Allophycocyanin	At 654 nm, in phosphate buffer (at pH 6.5) and *in vivo*	Found in blue-green and red algae

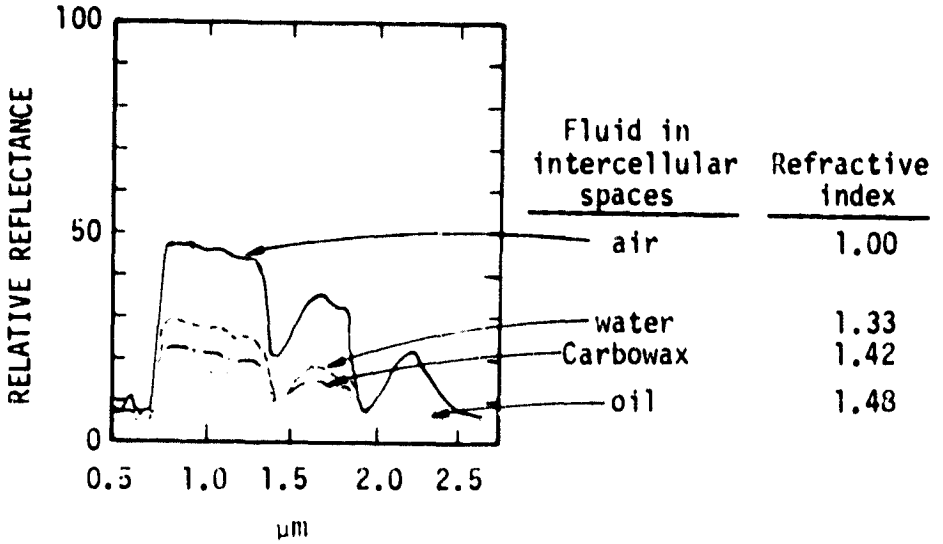

The most obvious refractive index discontinuities in a leaf are the interfaces between the intercellular air and the wet cell walls, but other diffusing elements are present. The contribution of air-wall interfaces to the leaf reflection can be estimated by eliminating these interfaces; that is, by replacing the air with a medium of higher refractive index. Figure 36 shows the effects of such replacement. Various liquids, mostly oil mixtures, having refractive indices between 1.42 and 1.52, were vacuum-infiltrated into leaves. Minimal reflectance for a soybean leaf was obtained with a medium having a refractive index of 1.47 or 1.48, which must have been the best approximation to the average refractive index of the wet mesophyll cell walls. Figure 36 shows that internal discontinuities other than the air-cell interfaces are responsible for a significant part of the light reflection by a leaf [37].

FIGURE 36. ROLE OF AIR-CELL INTERFACES IN LEAF REFLECTANCE

(absorbance peak 435, 670-680 nm), Chl *b* (absorbance peak 480, 650 nm), *B*-carotene (absorbance peak 425, 450, 500 nm) and lutein (absorbance peak 425, 445 and 475 nm) as the predominant photosynthetic pigment have only two reflectance peaks, one at 565 nm and one at approximately 720 nm. Diatoms which contain Chl *a*, Chl *c* (absorbance peak 444, weak absorbance peak 645), *B*-carotene and fucoxanthin (absorbance peak 425, 450, 475, 550 nm) as major photosynthetic pigments have a reflectance curve slightly different from either blue-green or green algae. The normal peak in the green has been displaced to 600nm. The peak of reflectance in the infrared again occurs at approximately 720 nm, a peak in the red appears at 650 nm, and the magnitude of response in the whole infrared range is similar to that of green algae. Since the genera used are only broadly representative of a particular group and pigment quantities vary from species to species, it is also supposed that reflected light spectral curves from other members of the group will behave only in a generally similar fashion. A most interesting feature is that both blue-green algae and diatoms (which lack Chl *b*) have minor reflectance peaks in the red region at 650 nm. Both green algae and the higher plant *Lemna* (which contain Chl *b*) have no distinct reflectance peak in this region. The peaks and depressions in reflectance from this area are not very distinct, possibly because of overlapping weak absorption shoulders. These exist beyond known maximum absorption peaks for chlorophylls and carotenoids found in these algae. The presence of such a high concentration apparently induces nearly complete absorption of light within the visible range.

Gramms and Boyle [35](as mentioned in Chapter III) noticed a more pronounced variation between species around the 620-650 nm range when dealing with lower concentrations, and as a consequence proposed that the differences in reflectance at 625 and 650 might serve as a basis for differentiating the two (Figure 19). Two objections to this model can readily be seen from our study. First, since these workers were dealing with laboratory cultures grown under ideal light conditions, the populations in all probability lacked or had very few gas vacuoles. Hence, the much more obvious distinctive feature of the blue-green algae, i.e., the fourfold increase in reflectivity in the infrared with gas vacuoles, went unnoticed (Table IV). It should be noted that their instrumentation may not have been adequately sensitive in the infrared band (personal communication with S. Klooster). Second, in noting that diatoms have a reflectance peak at 650 nm, the same as blue-green algae, it is possible that mixtures of green algae and diatoms would, under some circumstances, have a composite spectral signature in the 600-700 nm region similar to blue-green algae. In many cases, diatoms and green algae are present at the same time, and diatoms reflect well at 650 nm while green algae absorb moderately well at 625 nm. Differentiating this signal from the typical blue-green algal signal <u>in real lakes</u> may be difficult if only the ratio 620/650 nm is used.

This study showed that all phytoplankton solutions investigated reflected light well into the infrared, but *Aphanizomenon flos-aquae* infrared specific reflectance was four times greater than representatives of other algal groups. Reflectance was greater than in the visible portion of the spectrum where the increase was only 50% (Table IV). Since equal concentrations of duckweed and *Aphanizomenon* reflected light with similar intensity in the infrared band, it is suspected that a structural element present in both duckweed and *Aphanizomenon* but absent in algae from other groups was the cause. Since duckweed is a higher plant with intracellular

air spaces of a low refractive index found in the spongy mesophyll and *Aphanizomenon* is a typical gas vacuolated blue-green alga, it is probable that gas vacuoles were the element responsible.

The absorbance and scattering properties of the various phytoplankton solutions have several distinctions which may be used to characterize their presence in lakes or reservoirs. Blue-green algae can first of all be characterized as strong light reflectors. A second distinction is their unique ratio of light scattered in the infrared compared to the visible light (Table V). At the concentration of natural population used, the ratio of peak reflectance in the visible (550 nm) to peak reflectance in the infrared (720 nm) was approximately 0.16 (for algae of other groups the ratio was closer to 0.5). This figure represents a peak attainable for a very high concentration of natural lake phytoplankton. This ratio may not hold for the same algae subject to other environmental stresses and most certainly will not hold if the concentration is below the "bloom" threshold. Nevertheless, even at lower concentrations this distinctive higher reflectivity should identify blue-green algae. Diatoms and green algae, in contrast, can be characterized as weak light reflectors with light reflected in the peak of the infrared band exceeding that of the peak reflectance of the visible band by only a little more than 2:1. Diatoms alone might be distinguished from green algae on the basis of their increased reflectance in the 600-650 region, relative to the IR (720 nm).

Effect of Cellular Architecture. When gas vacuoles collapse under pressure reflected light decreases. Thus the gas vacuole is the structural component responsible for the high reflectivity of natural populations of blue-green algae. However, it is not clear whether or not the intensity of light lost by the collapse at the high pressure of 6.8 atm is the maximum loss. Three reasons might be responsible for a further decrease:

First, hydration of the cell may result as gas vacuoles collapse under pressure. Gas vacuoles represent about 10% of cell volume at maximum gas vacuolation. When replaced by water, refractive index discontinuities could be abnormally high. Wolley [37] has shown that for leaves, replacing the intracellular air spaces with media of varying refractive indices, a variety of reflectance values will be obtained (Figure 36). Water has a midway reflectance value in this experiment.

Secondly, the phytoplanktonic algae used were quite resistant to sinking even after exposure to 6.8 atm pressure. Walsby [40] has suggested that colonies of blue-green algae may trap escaping gas as the vacuoles collapse if the colonies are massive. Such gas pockets might still promote light scattering. Our suspensions were held for 10 minutes after pressurization before spectral measurement. During this time a second, distinct color change was observed. Whether or not this color change was due to the release of gas and whether or not all gas was released at that time is not clear.

Thirdly, lack of sufficient pressure for total gas vacuole collapse may have been responsible for higher reflectivity. The instruments were capable of reaching and sustaining a maximum of only 6.8 atm. Walsby [42] has shown that for a natural population of *Oscillatoria agardhii*

var. *isothrix*, total collapse did not occur until nearly 8 atm pressure had been exerted. A few gas vacuoles may have promoted a disproportionate amount of light scattering dependent upon their relation to incident light.

Since gas vacuoles are known to collapse naturally as osmotic pressure in the cell increases due to photosynthesis of sugars [39], it is reasonable to suspect that natural changes in reflectance signatures may occur depending on the time of day or season at which the signatures are recorded. Our natural populations were collected during winter months and in the early morning and hence represent perhaps a maximum state of gas vacuolation [3, 17]. High sunlight during summer may result in a loss of gas vacuoles [17, 39, 44] and hence a weaker spectral reflectance. Since the shape of the spectral curve is relatively unchanged before, during, and after gas vacuole collapse, it appears that gas vacuoles, not individual gas vesicles, are the component which alters light. Gas vacuoles would reflect light, whereas individual gas vesicles scatter light because of their particle size [39]. If light were scattered instead of reflected, changes in the shape of the spectral curve would be anticipated, especially in the blue.

Gausman [45] has shown on studies of higher plants that refractive index discontinuities other than those due to cell wall-air space interfaces appear to contribute little light to the IR. For example, Figure 37 illustrates the scattering of light by cell walls and cytoplasm for the common plant *Heliconia humile*. In this case, the cell walls and cytoplasm scatter light in a fashion which would be expected from plant material, but no statistical difference between scattering by cell walls and internal areas was found.

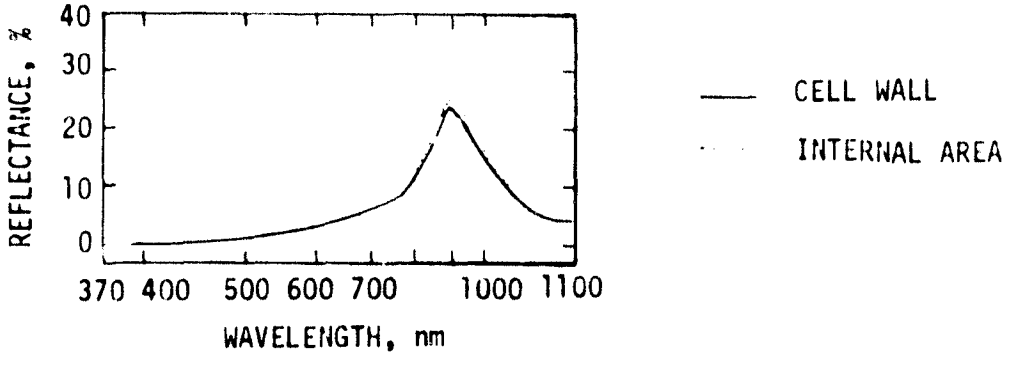

FIGURE 37. ROLE OF CELL WALL ON SPECTRAL REFLECTANCE IN *Heliconia humile*

This study has shown that such a case is not true ror certain algae. In the case of blue-green algae which contain internal gas vacuoles, both reflected and transmitted light photos identify the light scattering role of gas vacuoles. Also, the slight halo of infrared light (translated red) surrounding both gas vacuolated and non-gas vacuolated samples tends to indicate that for algae there may be a cell-wall effect. The scattering properties of the cell wall appear unique from internalized areas for a number of reasons. First, the cell walls of algae are often geometrically more complex than those of higher plants (i.e., diatoms). Second, many algae have flagella, mucilage, etc. associated with the cell wall area. In both cases, protruding non-plane, rough surfaces would affect incident light so as to increase scattering [45]. Also, it appears from the photos that some organelles of the algae may enhance scattering. The reddish tone of tannin vacuoles observed in *Spirogyra* may in fact account for the slight increase in reflected light observed on a macroscopic scale. Studies of other cell constituents such as polyphosphate storage granules, cell vacuoles, lipid storage vacuoles, etc. would be useful.

Just as the nature of the spectral distribution of incident light striking an algal cell depends upon the scattering and absorption coefficients of the water through which it must pass, so the nature of the spectral distribution striking the internal organelles of the algal cell depends upon the scattering and absorption coefficients of the cell material through which it must pass before encountering the organelle. The reflectance of *Anabaena flos-aquae* (Figure 38E, F) illustrates how the spectral distribution of incident light changes as the light crosses the cell wall surface, the gas vacuoles, and finally the internal cell area. The figure, together with other unpublished work, suggests that infrared light is bent away from internal areas, for these often appear blue in false-color film (meaning more green reflectance). In this instance, it may be significant to consider the arragement of cell organelles and the distance that incident light must travel before encountering them. In the case of *Anabaena flos-aquae*, gas vacuoles are arranged at the periphery of the protoplast. Other blue-green algae such as *Aphanizomenon flos-aquae* or *Microcystis aeruginosa* have gas vacuoles embedded randomly throughout the protoplast. It is easy to conjecture that cell organization affects the scattering properties of algae. The apparent differing response of the peripheral area of the cell to infrared wavelengths suggests that wavelength dependent reflectance and absorption characteristics exist in these areas. Since isolated gas vacuoles contain no pigmentation and appear as milky white in solution [40], gas vacuoles cannot be responsible for this wavelength-dependent observation. It was shown that when gas vacuoles were caused to collapse, no proportional changes occurred between wavebands, indicating that gas vacuoles do not scatter light according to wavelength. Hence the interaction of light with cellular constituents in this zone alters the incident spectrum so as to make infrared wavelengths the largest component striking the gas vacuole. Highly reflective gas vacuoles then redirect this altered spectrum. Figure 37, part of Gausman's work, seems to support this conclusion as cell walls and internal areas of plant cells are shown to reflect more infrared than visible light [45].

REMOTE SENSING MEASUREMENTS ON RESERVOIRS AND LAKES

Introduction

In the preceding section an indentifying characteristic of blue-green algae, namely a strong infrared response, was measured and characterized as to how the physiological state of the algae alters this response. For these results to be of use to water resource agencies, the ease of recognition of the unique infrared response must be determined for aerial photographs. I.e., at what concentration does a particular phytoplankton suspension produce a distinguishable signature in an aerial photograph? Will this be of use in identifying nuisance algae before they present a problem?

The definition of an unacceptable concentration of nuisance algae in a lake cannot be quantitatively answered in a simple way. A serious water quality problem in a drinking water reservoir may be considered only a minor nuisance in a recreational lake used for surface activities. Hence, a method must be developed for determining the presence of nuisance aquatic phenomena in the water over a wide range of concentrations. Given the limitation that at present only low-cost conventional aerial imaging devices (i.e., aerial photography or closed-circuit television) can satisfy the cost and turnover time restrictions for monitoring water quality in typical size lakes or reservoirs of the semi-arid zone, it was necessary to to pose two more questions.

1. How do nuisance scums of aquatic plants which have known spectral signatures (e.g. Figures 22-28, 30-34, 38-39) appear in aerial photography?

2. How do the spectral signatures of both nuisance and desirable aquatic phenomena change with algal and sediment concentration?

A characteristic feature of most nuisance plants is their uneven distribution. They are "weed species" able to exploit rapidly a newly disturbed environment. Planktonic blue-green algal populations show such patchiness (spatial and temporal heterogeneity) both vertically and horizontally. Such patchiness is highly influenced by the wind, which concentrates horizontally, and by light, which affects vertical concentration. Blue-green plankton all possess gas vacuoles which are formed under low-light conditions and caused to collapse by photosynthetically produced sugars under higher illumination (Horne [3] and Walsby [39]). The net result is often a series of algal patches very near the surface, ranging in size from 2-5 cm up to km. Small-scale variations in algal concentrations over a few meters are called microstructure (Wrigley and Horne, [6]) and are distinct from macrostructure where patches are in the km range (Powell *et al.* [46]). The distinction is important, since it is likely that microstructure is dominated by physical processes (turbulence, buoyancy) while macrostructure is biologically or chemically dominated (plant growth, nutrient recycling).

The patchiness and patterning of blue-green alga populations can distinguish nuisance blue-green algae from desirable phytoplankton. Changes in the spectral signatures of nuisance blue-green algae with

A

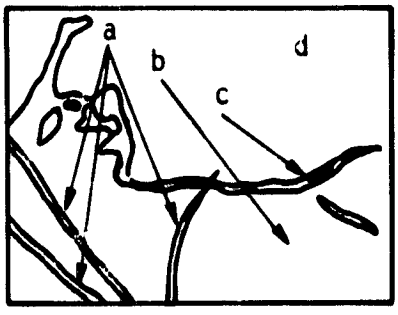

Summer patchiness of a bloom of *Aphanizomenon flos-aquae*, Clear Lake, Ca.–Oaks Arm, 9 July 1973 (ref. Horne [3], Horne and Wrigley, in prep. [47])
a. Boat tracks
b. Approximate position of sampling station, Chl *a* = 600 µg/ℓ.
c. Decayed algae
d. Open water

B

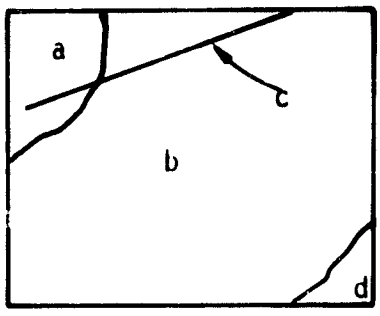

Surface macrostructure of *Aphanizomenon flos-aquae*, Clear Lake, Ca.–Oaks Arm, 2 March 1973 (ref. Horne and Wrigley, in prep. [47])
a. Chl *a* = 30 µg/ℓ.
b. Chl *a* = 15 µg/ℓ
c. Boat wake
d. Shoreline trees

C

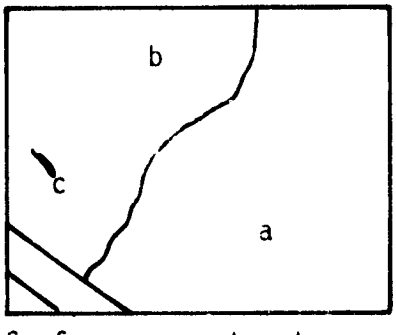

Surface macrostructure resulting from *Anabaena flos-aquae*, Perris Reservoir, 12 September 1974
a. Chl *a* ∿ 10 µg/ℓ (Sta. 3)
b. Chl *a* ∿ 4 µg/ℓ
c. Boat

D

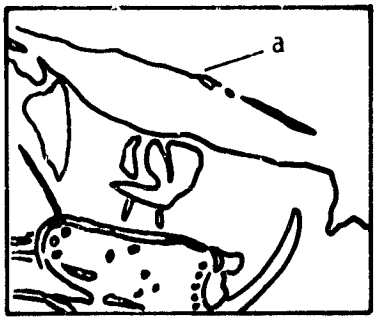

Surface microstructure due to grass, dust and wood debris on Castaic Reservoir, 12 July 1974
a. Sampling–Sta. 6
Chl *a* = 32 µg/ℓ

E*

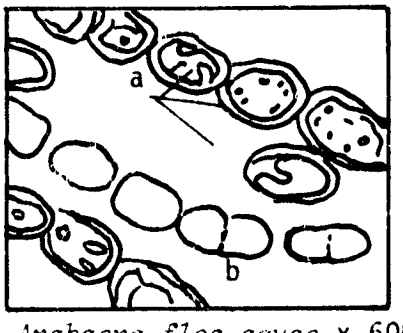

Anabaena flos-aquae x 600
a. With gas vacuoles
b. Without gas vacuoles

* Transmitted light photo

F

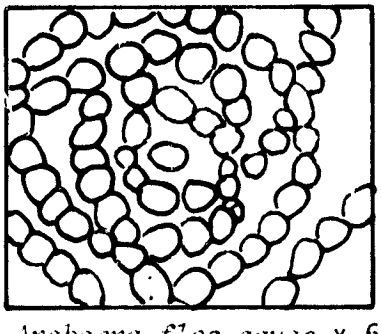

Anabaena flos-aquae x 600 after collapse of gas vacuoles under pressure

FIGURE 38. KEY

FIGURE 38. COLOR TONE OF VARIOUS RESERVOIR NUISANCE PHENOMENA AND DETAILS OF THE CELLULAR CAUSES

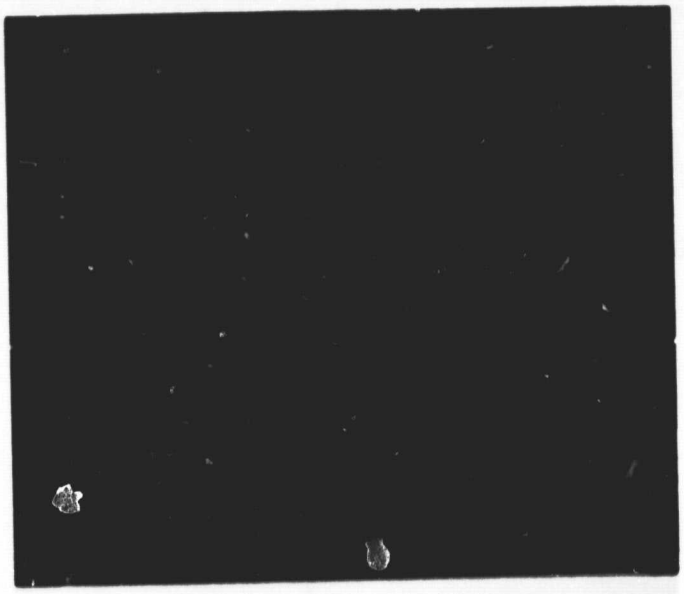

concentrations may be rephrased as: At what concentration can the patchiness of blue-green algae be recognized, and as concentration changes can blue-green patterning still be distinguished from that of other aquatic phenomena? Fewer examples of nuisance algal blooms were evident in Southern California during the test period than in eutrophic Clear Lake. As a consequence, a great deal of the data gathered by remote sensing techniques in Southern California was not as easily interpreted. In many cases, suspended solids (algae, debris, sediments) were below the threshold level for recognition by photographic or television imagery. In order to determine whether or not the laboratory observations with a spectroradiometer could be confirmed by aerial photographic measurements, a comparison was made with the known aerial spectral signatures from a lake with more blue-green algae. Such a lake is Clear Lake, California, and some preliminary spectral signatures are given of nuisance blooms of blue-green algae [5, 6, 36].

Spectral Signature Variations as a Function of Particle Type and Concentration

The two color plates (Figures 38 and 39) are reproductions of original false color infrared photos gathered by aerial reconnaissance of the Southern California reservoirs and Clear Lake, California. Each figure has within it a section where surface algal, macrophyte, or debris concentration is great enough to form a nearly opaque surface. Spectral variations evident as distinct false color tones are apparent when the figures are compared. These spectral variations correlate with a change in algal or plant type, not in concentration. Represented in these figures are blue-green algae (predominantly *Aphanizomenon flos-aquae*, Figure 38A and B), attached green algae (mainly *Spirogyra*, Figure 39B), attached green algae that are mainly *Cladophora* (Figure 39C), an aquatic macrophyte (*Lemna*, Figure 39D), and debris (Figure 38D). Figures 38B-C and 39A are similar color infrared photos where surface water algal concentrations are less than those of the other figures. Color tone variations correlate with a change in particle concentration in these instances. Those figures which represent living plant material observed during aerial reconnaissance possessed apparently healthy intact, living cells, An exception is shown in Figure 38A. The white area corresponds to a mass of algal cells where cell breakdown and lysis were observed.

The following section deals with field observations showing that:

1. Algal species could be differentiated by remote sensing techniques and,

2. Surface algal concentration could be approximated by remote sensing techniques based on infrared response in photographs.

Algal Spectral Signatures—Blue-Green Algae. Figure 38A is a reproduction of a false color infrared photo taken over Clear Lake, California. The fiery red portion of the photograph represents a portion of the lake with a dense patch of the blue-green alga *Aphanizomenon flos-aquae* [3, 47]. Samples gathered within the fiery red zone were found to contain ~0.6 mg/ℓ Chl *a*. Samples outside contained 20 µg/ℓ.

The fiery red tone in the false color pictures of *Aphanizomenon flos-aquae* has been known to occur frequently in aerial photographs of this lake [47].

A

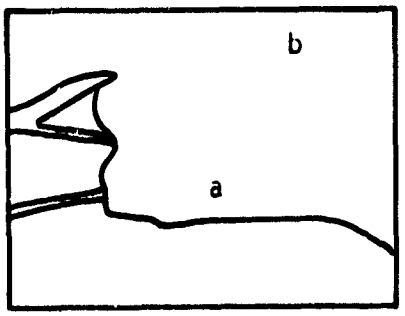

Shoreline, Perris Reservoir
12 July 1974
a. Shallow water
b. Deeper water

B

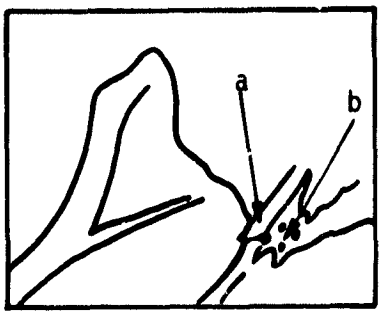

Shoreline, Perris Reservoir
12 September 1974
a. Darker area indicative of attached growth below surface
b. Attached Periphyton (mainly *Spirogyra*) Chl *a* = ∿50 mg/ℓ

C

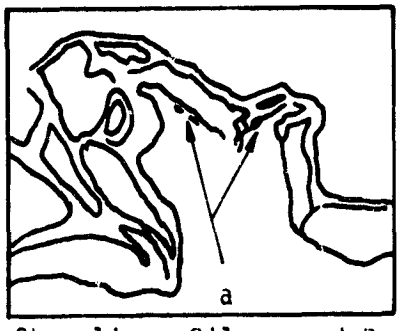

Shoreline, Silverwood Reservoir
12 September 1974
a. Attached Periphyton (mainly *Cladophora*) Chl *a* est. ∿ 50 mg/ℓ

D

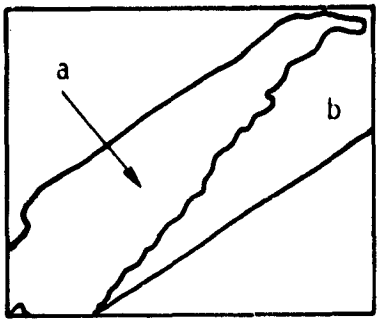

Sewage pond near Clear Lake, Ca.
20 February 1975
a. *Lemna* - Chl *a* ∿200 mg/ℓ
b. Open water

E*

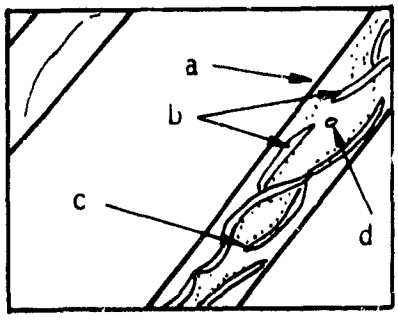

Green alga - *Spirogyra* x 150
a. Cellulose cell wall
b. Spiral chloroplasts
c. Tannin vacuoles (?)
d. Oil, starch reserve bodies

F*

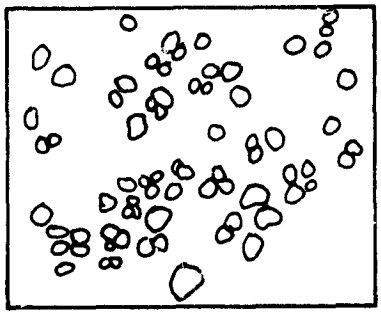

Coccoid green alga x 300

* transmitted light photo

FIGURE 39. KEY

FIGURE 39. COLOR TONE OF VARIOUS RESERVOIR NUISANCE PHENOMENA AND DETAILS OF THE CELLULAR CAUSES

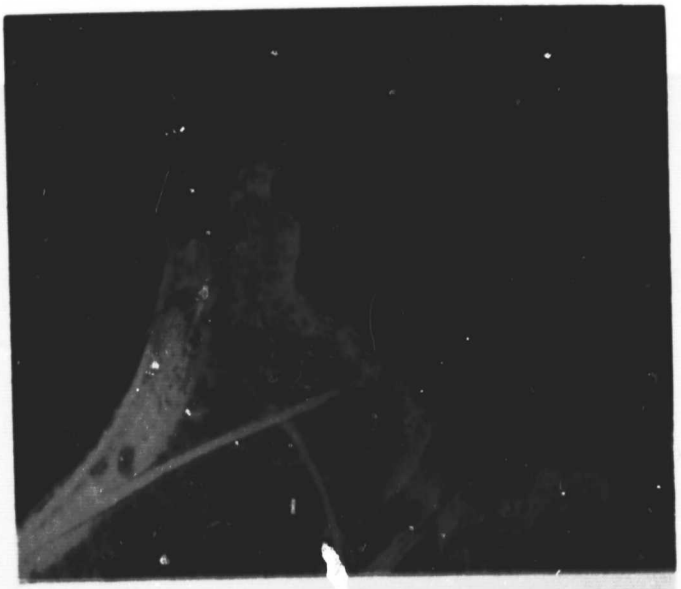

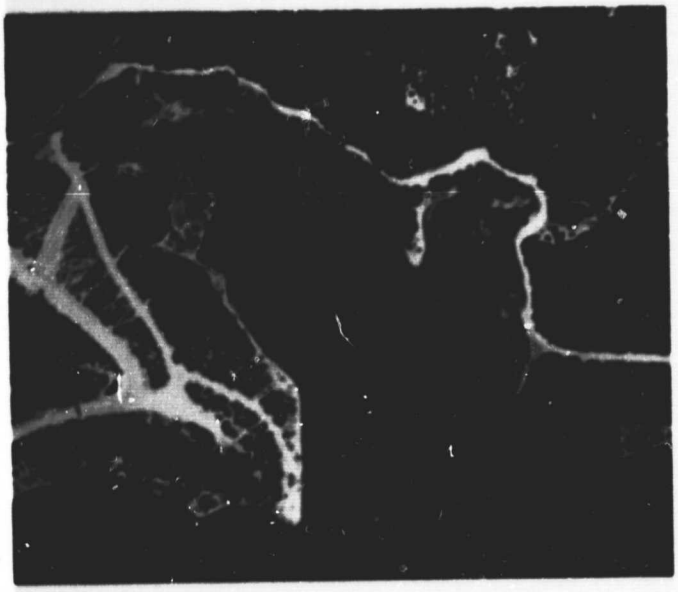

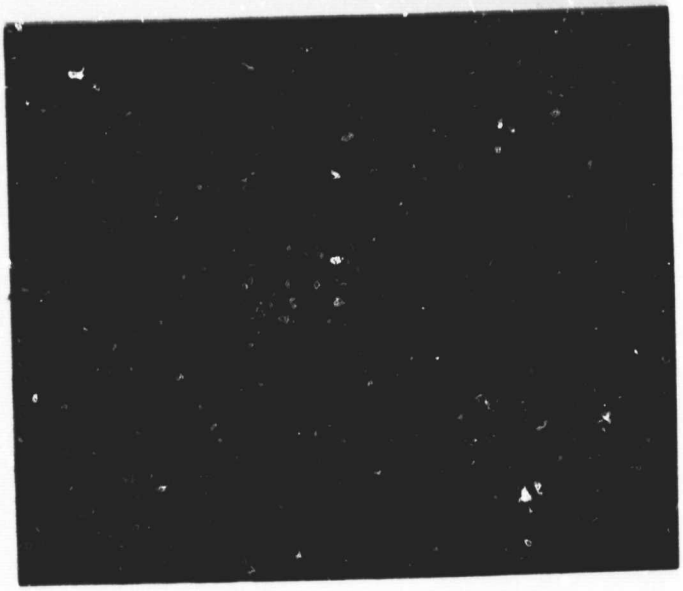

This photograph was chosen as an excellent example of a massive algal suspension with sharp boundaries and no visible signs of decay. Reflectance in this figure is due to intact living cells like those used in the laboratory study. And although the concentrations measured in the field and those used in the laboratory are not equal, the algal patch presents a near opaque surface. The algal mass extended down some 50 cm into the water column.

Although the intensity of this signal varies at several points within the photo, the color tone does not appear to change. In other words, though the intensity of the signal appears to change, the shape of the spectral curve (reflectance ratios) appears to be relatively constant. This is not to say that other color tones have not been observed on Clear Lake, but when other color tones have been recorded, they have been associated with die-off scums. Obviously when mixtures of healthy gas-vacuolated blue-green algae with a deep red tone are mixed with decaying, lysing cells with a white tone as noted in Figure 38A, a range of false color tones will be observed.

Historically, therefore, the typical spectral signature of a healthy, massive concentration of blue-green algae has been associated with the fiery red tone. Recently, however, with the acquisition of the rapid scanning Tectronix spectrometer this has been documented better. Figure 40 illustrates the spectral signatures of a natural population of *Aphanizomenon* measured *in situ* on Clear Lake. In the midst of a massive algal patch, concentrations were found to vary substantially within a few meters. However, even though concentrations were found to vary from 0.97 mg/ℓ to nearly 8 mg/ℓ Chl *a*, the shape of the spectral curve changes only slightly. Reflectance ratios remain approximately the same (Table VIII). Aerial photographic coverage was provided when these spectral signatures were recorded and the area where sampling crews were stationed appeared a deep red tone similar to Figure 38A. At the present time, however, there is no explanation why the spectral signatures recorded *in situ* from algal masses promoted a stronger infrared response than did those studied under laboratory conditions; this despite the fact that samples studied in the laboratory were higher in concentration (based on comparisons of percentage light scattered from the infrared region. Compare Tables III and VIII). It could be anticipated from past knowledge of infrared response by algal suspensions that not only would a spectral signature shape become independent of concentration at some point, but also that the intensity of this signal would become independent of concentration. Two reasons explain this incongruity, i.e., that more massive concentrations may have a weaker infrared response than less concentrated ones: First, this study has shown that spectral response is highly dependent on gas vacuolation, and the act of collecting algal samples may have caused a significant number of gas vacuoles to collapse before spectra were measured in the laboratory. Secondly, changes in flake size or other alterations in physiology occurred in the lake. These, coupled with the concentrating effect of water currents, produced different conditions at the surface which were not duplicated in the laboratory. Caution is needed in assigning any absolute Chl *a* values to any particular spectral signature presented in this section. The spectral signatures can be taken only as broadly representative of concentration and are dependent on variables such as degree of gas vacuolation and minor changes in vertical stratification.

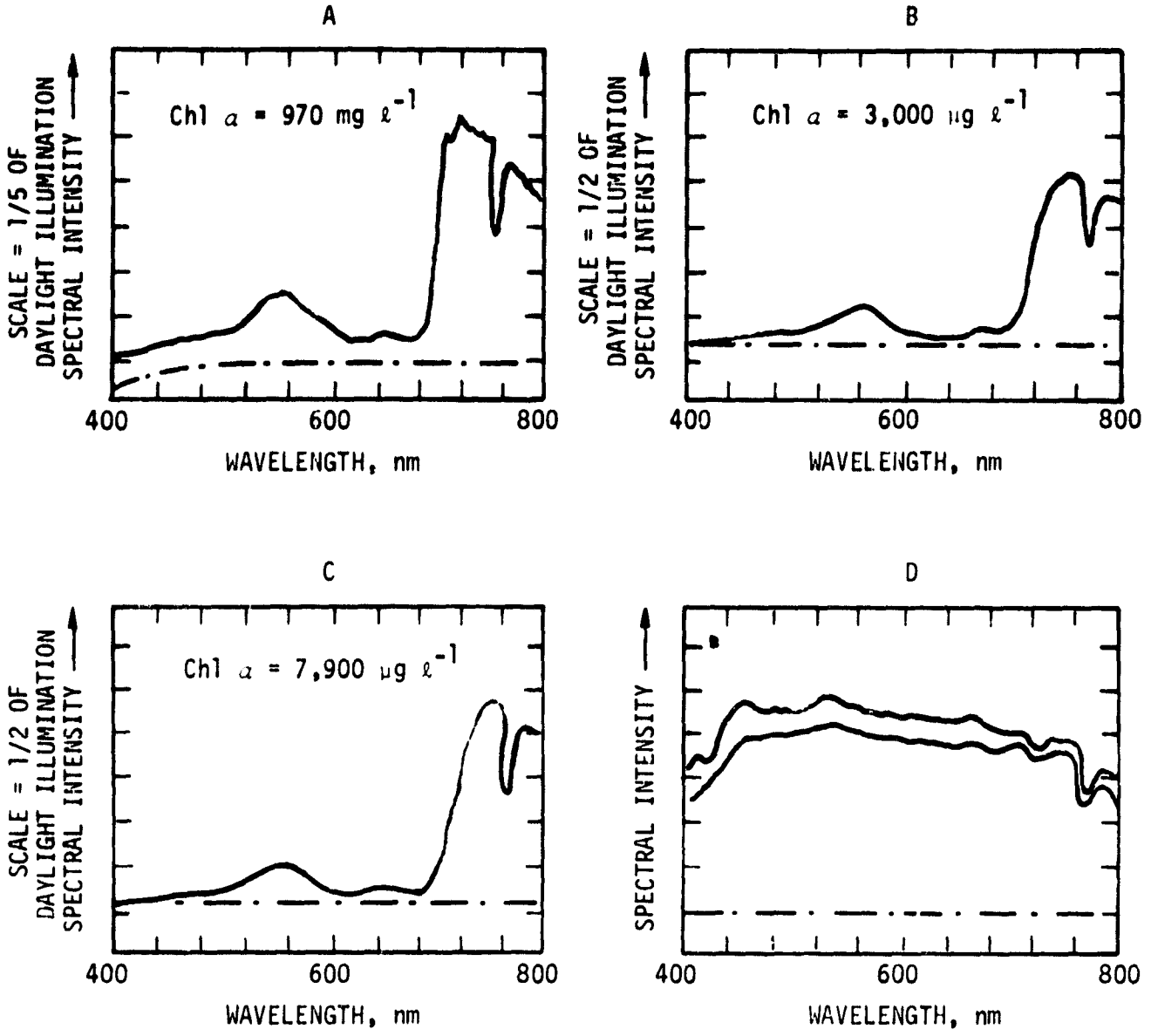

D - Daylight illumination at time of recording. Lower curve represents irradiance at time A. Upper curve at time B and C.

FIGURE 40. COMPARISON OF THE SPECTRAL REFLECTANCE CURVES OF *Aphanizomenon flos-aquae* AT THREE HIGH CONCENTRATIONS. (RECORDED *in situ* ON CLEAR LAKE, CA., 3 JULY 1975)

Note: These spectral curves were recorded using the Tectronix spectrometer. The dashed line at the bottom of each figure represents the baseline of the spectral response. Parts A and B-C are on a different energy scale, hence only general comparisons between A, B, and C can be made. The energy scale for daylight irradiance is double that of Figures B and C and five times that of Figure A. A, B, and C are representative only of a water body with surface microstructure. Scale for Figure D is 1 scale division = 1000 picowatts per nanometer.

TABLE VIII

REFLECTANCE VALUES AS A PERCENTAGE OF INCIDENT LIGHT
FOR SURFACE CONCENTRATIONS OF BLUE-GREEN ALGAE
MEASURED *in situ* AT CLEAR LAKE, CA., 3 JULY 1975

Spectral Curve	Reflectance as a % of Incident Light				
	440 nm	565 nm	625 nm	650 nm	730 nm
A 0.97 mg/ℓ Chl *a*	3.3	7.5	3.6	4.2	37.4
B 3.0 mg/ℓ Chl *a*	4.3	8.3	4.4	5.0	45.0
C 7.9 mg/ℓ Chl *a*	3.5	7.3	2.4	4.2	50.0

TABLE IX

VALUES FOR REFLECTANCE RATIOS (565/730, 625/730, 650/730) FOR SURFACE CONCENTRATIONS OF BLUE-GREEN ALGAE MEASURED *in situ* AT CLEAR LAKE, CA., 3 JULY 1975

Spectral Curve	Reflectance Ratios		
	565/730 nm	625/730 nm	650/730 nm
A 0.97 mg/ℓ Chl *a*	0.20	0.096	0.112
B 3.0 mg/ℓ Chl *a*	0.184	0.098	0.111
C 7.9 mg/ℓ Chl *a*	0.146	0.048	0.084

TABLE X

REFLECTANCE VALUES AS A PERCENTAGE OF INCIDENT LIGHT
FOR SURFACE CONCENTRATIONS OF BLUE-GREEN ALGAE
MEASURED *in situ* AT CLEAR LAKE, CA., 3 JULY 1975

Spectral Curve	Reflectance as a % of Incident Light				
	440 nm	565 nm	625 nm	650 nm	730 nm
[a] 970 µg/ℓ Chl *a*	3.3	7.5	3.6	4.2	37.4
[b] 170 µg/ℓ Chl *a*	2.9	8.3	3.9	4.7	11.8
[c] 50 µg/ℓ Chl *a*	3.3	8.5	4.1	4.3	7.8
[d] 25 µg/ℓ Chl *a*	3.4	8.8	4.3	4.0	4.0

TABLE XI

VALUES FOR REFLECTANCE RATIOS (565/730, 625/730, 650/730 FOR SURFACE CONCENTRATIONS OF BLUE-GREEN ALGAE MEASURED *in situ* AT CLEAR LAKE, CA., 3 JULY 1975

Spectral Curve	Reflectance Ratios		
	565/730 nm	625/730 nm	650/730 nm
[a] 970 µg/ℓ Chl *a*	0.20	0.1	0.11
[b] 170 µg/ℓ Chl *a*	0.70	0.33	0.4
[c] 50 µg/ℓ Chl *a*	1.1	0.53	0.55
[d] 25 µg/ℓ Chl *a*	2.2	1.075	1.0

Although direct comparisons between the signals recorded by the ISCO spectroradiometer in the laboratory experiment and the Tectronix spectrometer cannot be made easily, comparison of the percentage of incident light reflectance values in Table VIII with those of Table III indicates that substantial agreement exists between reflectance ratios derived from laboratory and lake studies.

Algal Spectral Signatures—Green Algae. Figure 39B-C comprises reproductions of photos taken over Perris and Silverwood reservoirs, respectively, on 12 September 1974. The arrows in each photo indicate significant features, including nuisances. Figure 39B (Perris reservoir) shows how color infrared film records the reflected light spectral signature of an intense growth of the shallow-water, shoreline-dwelling filamentous green alga, *Spirogyra*. The same can be said for the area designated in Figure 39C, only on this occasion the subject is the attached filamentous green alga, *Cladophora*.

Water truth measurements made at the time of aerial reconnaissance established that in each case the area identified by a pink tone represents a growth of potential nuisance algae. Chl *a* concentration was estimated to be ~50 mg/ℓ (Figure 41). However, within the designated area surface chlorophyll *a* levels were quite variable and within a few meters of shore were reduced by a factor of 10^4. The algae appeared healthy with no obvious sign of decay, although in parts of Silverwood reservoir other than those shown in Figure 39C the same algae, *Cladophora*, were badly decayed. In this case, the signature recorded on color IR film produced a white response.

Figure 39A shows the same area as in Figure 39B, two months earlier. Although a faint pink tone (indicating a high infrared response) can be seen near the shoreline, it is apparent that the surface scum was not nearly as extensive. Phytoplankton counts established that this algae increased in the water column of the closest sample site between June and September. Though the sample counts indicated only those attached algae which had broken away their rock strata, the evidence still suggests that the algae had reached a peak in their growth phase near the date at which the photo (Figure 39B) was taken. It is possible that decreased water level had some concentrating effect. In each case, the concentration of the surface algae was sufficient to form an opaque surface to incident light, similar to that used in laboratory studies. For this reason, it appears that each example represents the type of color tone observed when the density of a phytoplankton population is at a maximum, the scattering properties of water ($^1w_\lambda$) are a near total function of the phytoplankton and the spectral signature and reflectance ratios should be similar to those of laboratory studies.

The four-band imagery indicated that a spectral signature reminiscent of blue-green algal scums in Clear Lake (intensive infrared band, diminished visible bands—see Appendix) correspond with ground truth measurement of the areas designated in Figure 39B-C. However, Figure 39B-C demonstrates that the color to associated with green algae scums as noted in Figure 38A. (Note: color reproduction of the area in Figure 39C designated as *Cladophora* did not retain the true color of the original. Original positives which would be used in practice gave a much more intense pink tone.)

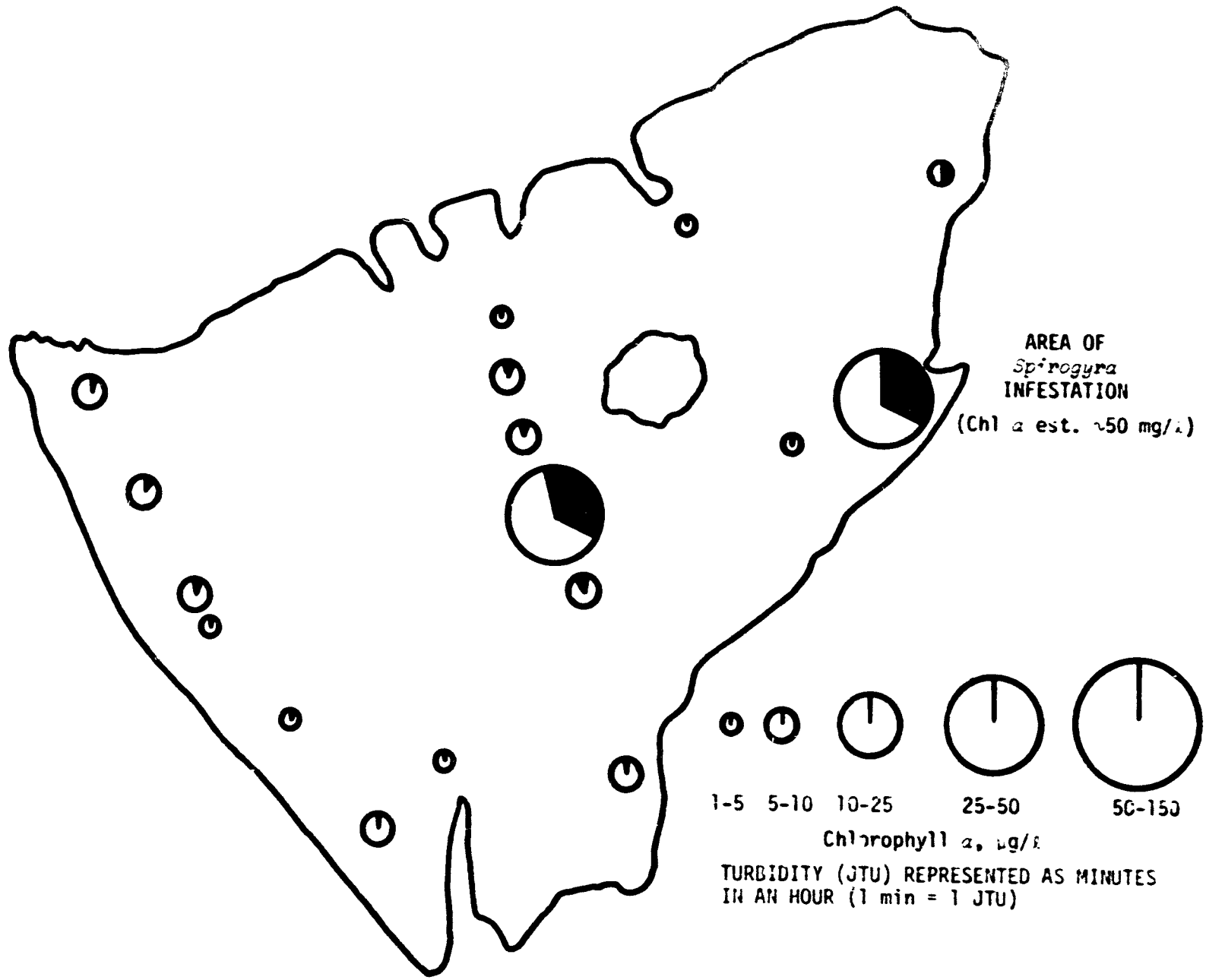

FIGURE 41. CHLOROPHYLL AND TURBIDITY IN PERRIS LAKE, 12 SEPTEMBER 1974

The color tone attributed to green algal scum as noted in the Southern California study is the first instance in these remote sensing studies where a distinct color tone could be ascribed to an alga of another taxonomic group. Since each case represented healthy algae, the color tone differences recorded are probably due to the structural differences of the algae, and not to a physical attenuation of the signature resulting from altered physiology or water absorption. At the same time, film characteristics and atmospheric attenuation may alter records of reflected light imagery. These alterations appear insignificant when imagery is taken under the same sun angle and atmospheric conditions, and when film character is corrected by color compensation. Hence, direct comparisons of color infrared imagery from Southern California and Clear Lake can be made. Also, aerial photography of ponds near Clear Lake supporting similar filamentous green algae has given similar results. The Tectronix instrumentation spectral signature of these green algal scums near Clear Lake had reflectance ratios 565/720 different from those of blue-green algae and a spectral reflectance curve almost identical to those observed in the laboratory study.

When color tone differences noted between algal groups were a function only of structural differences between the algae and the resultant reflected light spectral curve, laboratory studies indicated that duckweed (*Lemna*) should produce a color tone in color infrared film similar to that of green algae. This is because the shape of spectral signatures of green algae and of *Lemna* were almost optically identical (given that a similarly concentrated scum of this plant is found on the surface of a lake).

To test this hypothesis, imagery was taken of a sewage pond near Clear Lake, California, covered with a surface scum of *Lemna*. Figure 39C illustrates a color infrared photo of the pond with duckweed present. The pond supports the same healthy duckweed which was used in laboratory experiments and at the same concentration. Again color reproduction of the false color original did not register the true color of the original (a slight shift from pink to orange took place). Still a distinct color tone is apparent from that of the fiery red of blue-green algae. Original transparencies show a pink false color tone similar to that of Figure 39B.

The results show that false color tones of color infrared film which are the result of massive algal scums agree in substance with the observations of the laboratory study and that the results are reproducible. The unique color tones of nuisance scums of various plant material depend on cellular architecture and the resultant ratio of light backscattered from different wavelength bands. Blue-green algae are unique in the possession of gas vacuoles and the pigment phycocyanin-*c* which absorbs in the green and red wavelengths *in vivo*. This produces a very high reflectance in the infrared. Compared to any other waveband, green algae do not reflect infrared light as well as blue-green algae. This and the lack of phycocyanin-*c* produce a distinct color tone. *Lemna* has intracellular air spaces and a strong IR reflectance but lacks phycocyanin. The spectral signature produced is much the same as that for green algae, hence the color tone perceived is similar.

Debris in Water. During the 12 July 1974 aerial reconnaissance, photography captured a spectral response from Castaic Lake similar to a concentrated suspension of phytoplankton found near the surface of the

water. The response was similar in the sense that the film contrasts in the four-band imagery (intense infrared band, diminished visible bands, see the Appendix), were highly reminiscent of those known to correspond with the appearance of blue-green algal scums in Clear Lake. Ground truth determined that no excessively (i.e., > 0.5 mg/ℓ Chl *a*) large surface concentration of algae existed on Castaic Lake that day (see Chl *a* distribution—Figure 42), rather, the lake was covered with small bits and pieces of dead, buoyant cellulose material (debris = dead grasses, dust, twigs, dead leaves). Figure 38D reproduces a section of the original false color infrared photograph. A portion of the surface debris noted to occur on the lake is designated by arrows. The debris in this case exhibits a distinct orange color tone. In this sense, the spectral character of debris does not resemble the typical signal of any aquatic plant tested.

Studies have shown that for living trees, the reflectance of bark, twigs, and wood generally gives a neutral color tone in color infrared film. Cellulose fibers subject to the drying and cracking of the environment, however, become porous and fill with air. Debris floating in water may have many more air/water interfaces which serve to reflect infrared strongly and to some extent behave spectrally as gas-vacuolated phytoplankton. However, the lack of photosynthetic pigments causes a deviation in the light reflected from the visible region.

Surface Algal Concentration Based on an Infrared Band. Figure 38A-C illustrates how color tone in color infrared film varies when blue-green algal suspensions of different concentration are photographed. Figure 38A represents a portion of Clear Lake where, as previously noted, a large mid-summer bloom was present. Figure 38B also represents Clear Lake, but in this instance a small, overwintering population of *Aphanizomenon* is evident as a reddish patch (indicative of infrared response) in a corner of the figure. Chlorophyll *a* values (30 µg/ℓ) are substantially less than those found in nuisance scums. Consequently, the deep red tone also is absent. Figure 38C illustrates patchiness on Perris Lake on 12 September 1974. Water truth measurements (Figure 41) established that surface Chl *a* concentrations from the area exhibiting patchiness were 10 µg/ℓ, while outside this zone they were 4 µg/ℓ. In the designated area of Figure 38C, field observations showed visible colonies of the blue-green algae *Anabaena*. In this instance, these colonial algae represented approximately 50% of the biomass of the sample. Although it can readily be seen that a portion of the water mass is definitely richer in reflective particles, at the relatively low concentration of Chl *a*, the patch does not exhibit any reddish color tone whatsoever. Figure 38A-C demonstrates that progressive color tone changes occur with increasing concentration of blue-green algae, and that these easily recognized color tones provide a simple means of estimating approximately the amount of blue-green algal biomass present. Also, though it is apparent that algae can only be recognized when concentrations are relatively high, the lake-wide concentration of chlorophyll is obviously much lower than that observed within the patch. Clearly these photographic techniques provide some minimal information about phytoplankton presence in a wide range of lakes and trophic levels.

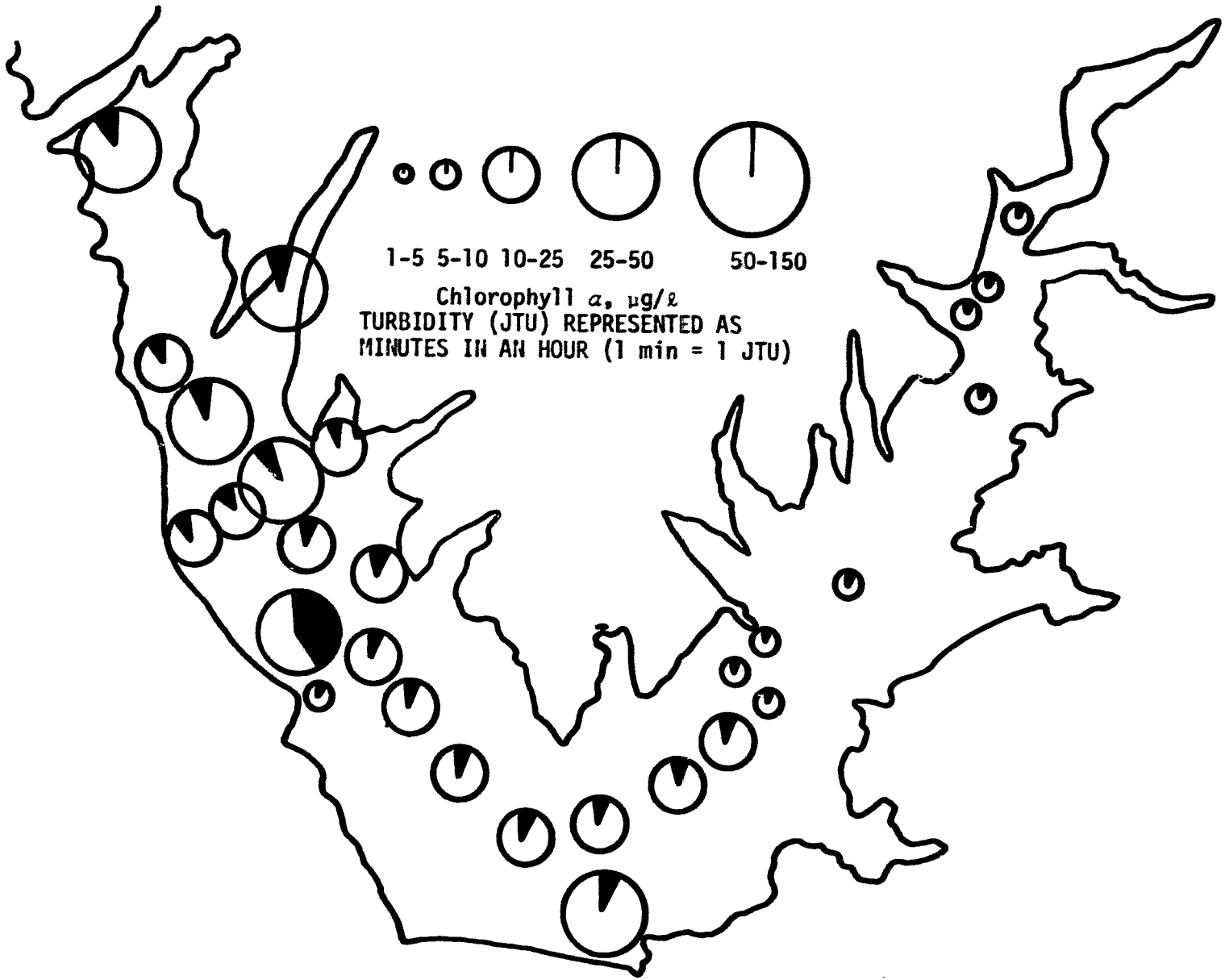

FIGURE 42. CHLOROPHYLL AND TURBIDITY IN CASTAIC LAKE, 12 JULY 1974

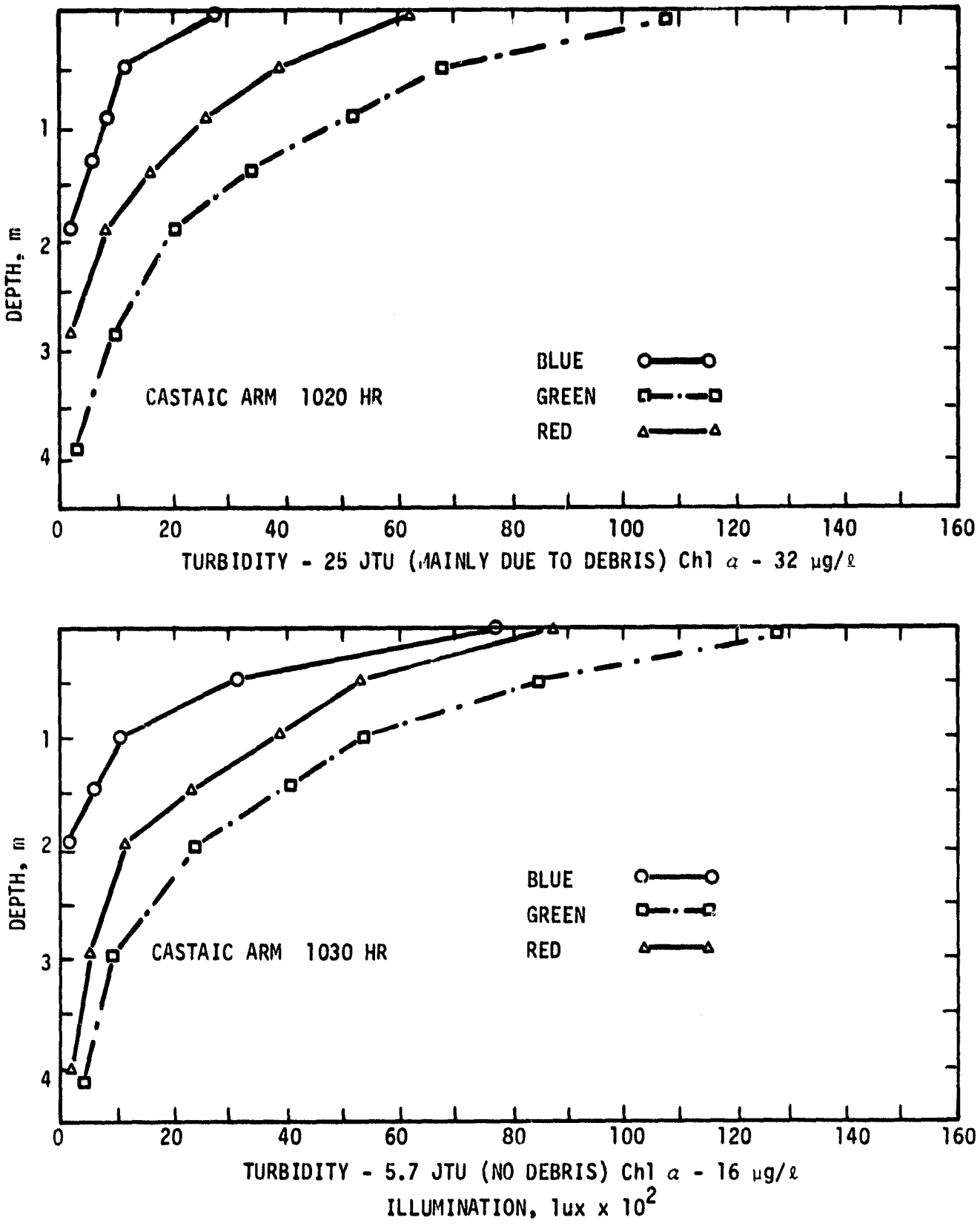

FIGURE 43. LIGHT EXTINCTION CHARACTERISTICS OF CASTAIC LAKE, 12 JULY 1974

To understand the changes in color tone which occur in Figure 38A-C, it is useful to define the changes in color tone as changes in the shape and intensity of the spectral signature from these areas of the photos. The photos were selected because they exhibit patches with essentially one color tone present, hence one spectral signature will nearly describe each photo. In many instances where remote sensing is used, this will not be the case and photointerpretation will depend on using the principles these examples bring to mind, perhaps all in one picture frame. Figure 44 illustrates data collected *in situ* at Clear Lake in June 1975 which demonstrates the changes in spectral signature which take place in the photos. Figure 44 is intended to serve as an aid in interpreting that imagery. Photographic coverage provided by NASA-Ames during the time the signatures of Figure 44 were collected showed that in the portion of the lake where Figure 44A-D was taken, microstructure existed comparable to that of Figure 38A, B, or C, respectively.

Figure 44A shows the typical signature of a massive blue-green algal scum and corresponds with the fiery red portion of Figure 38A. The shape of this signature is not only typical of concentrations of 0.97 mg/ℓ but represents a broad range of concentrations from as low as 0.6 mg/ℓ (as at the sampling point in the picture) to as high as 200 mg/ℓ used in the laboratory studies. Within this concentration range, changes in spectral signature shape and intensity do not show substantial changes and appear to be nearly independent of concentration.

Figure 44B and C shows both typical spectral signatures of moderate or "transitional" concentrations of blue-green algae. The term "transitional" is used for these intermediate concentrations of 50-167 µg/ℓ surface Chl *a*, for it can be seen that the shape of the spectral curve varies radically with concentration. This is unlike the stable spectral signature of massive algal blooms. Though the spectral signatures of Figure 47C are unique to those concentrations, within this concentration range the shape of the spectral signature has definite bounds. Hence the color tones which will be associated with these types of spectral signatures will appear more or less like those of Figure 38B which has a Chl *a* concentration in the transition zone. The spectral signature in Figure 44C perhaps comes the closest to being representative of Figure 38B for the concentration values are the most similar. In the transitional zone, the infrared response is significant, but not overwhelming as is the case with Figure 44A. Within the transitional zone the infrared predominates with increases in Chl *a*, hence increases in concentration produce more prominent shades of red in color infrared film. The color tone of Figure 38B is one of the lightest shades of red which can be observed, since the measured Chl *a* value places the concentration at the lower limits of the transition zone. By photointerpretation alone it would be difficult to tell whether the light red tone of an intermediate blue-green algal concentration indicates blue-green algae or whether it would come from a much more substantial population of green algae. In theory this is a problem, but in practice it is not. In drinking water reservoirs where water quality standards must be kept high, the appearance of anything in the water promoting a significant infrared response would warrant further attention.

Figure 44D is a spectral signature that is broadly representative of Figure 38C. Although Figure 44D is clearly unique to that Chl *a* level, within a range of concentrations the shape of the spectral signature

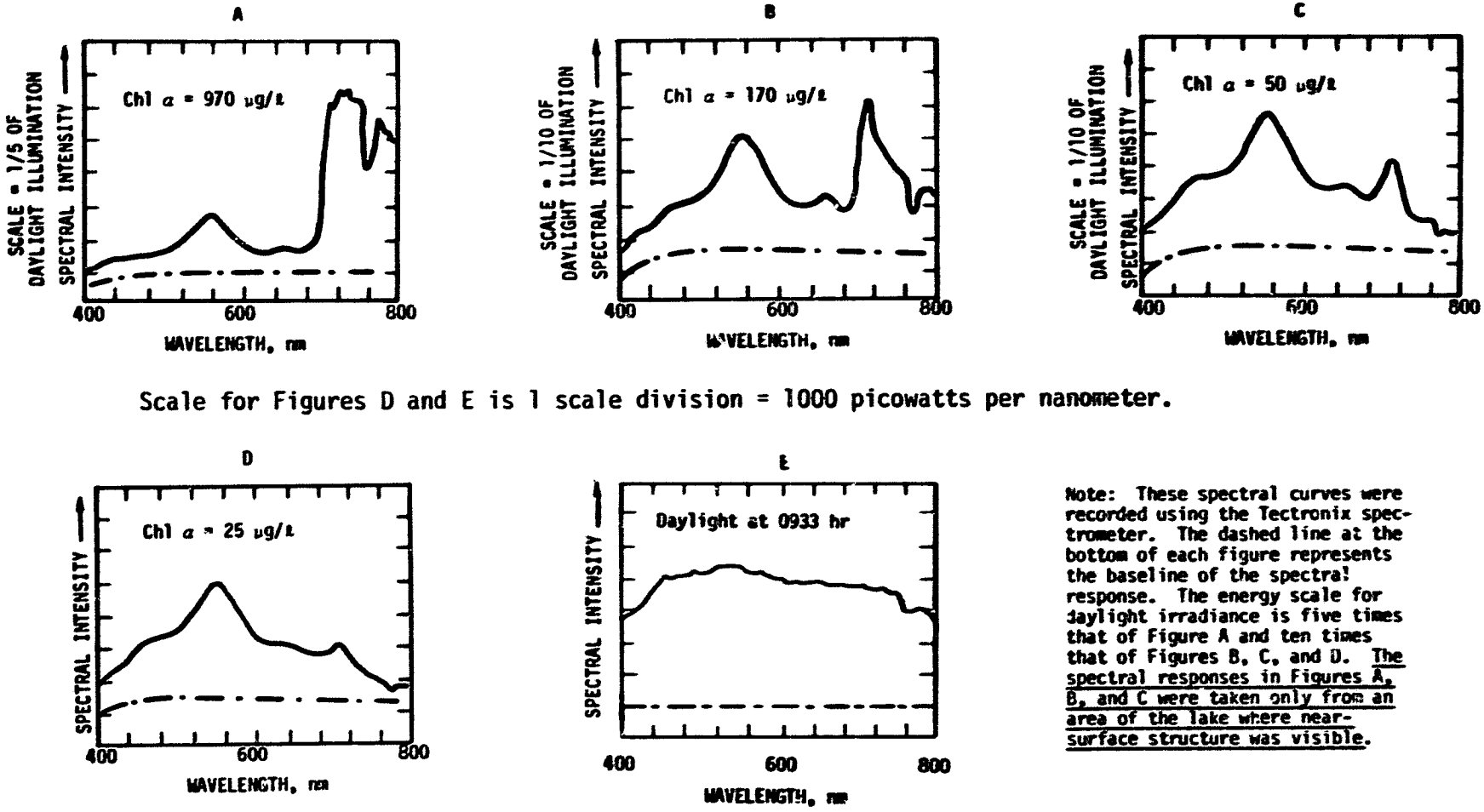

Scale for Figures D and E is 1 scale division = 1000 picowatts per nanometer.

Note: These spectral curves were recorded using the Tectronix spectrometer. The dashed line at the bottom of each figure represents the baseline of the spectral response. The energy scale for daylight irradiance is five times that of Figure A and ten times that of Figures B, C, and D. The spectral responses in Figures A, B, and C were taken only from an area of the lake where near-surface structure was visible.

FIGURE 44. COMPARISON OF THE SPECTRAL REFLECTANCE CURVES OF *Aphanizomenon flos-aquae* FOUND IN A NEAR-SURFACE FILM AT THREE CONCENTRATIONS. (RECORDED *in situ* UNDER DAYLIGHT ILLUMINATION ON CLEAR LAKE, CA., 3 JULY 1975 BETWEEN 0933 and 0955 HOURS)

(and reflectance ratios) is constant enough so that the resultant macrostructure will appear similar in color tone to that of Figure 38C. This will be a more or less white tone. From the appearance of the patch observed in Figure 38C which has been ascribed to the presence of blue-green algae in Lake Perris on 12 September 1974, it can be said that both photo and spectral signature 44D are in good agreement. The color infrared photo shows microstructure as white, indicating a broad response in at least the green, red and infrared wavelengths. In the appendix a breakdown of the spectral response by wavelengths indicates that the patch was in fact more visible in the green band of the 4-band camera, but by no means invisible in the red or infrared. The appearance of structure at such low concentrations as that recorded at the Southern California reservoirs is interesting, for it shows that highly reflective near-surface, large colonial blue-green algae induce the appearance of patchiness at very low population levels. However, in this instance the ability to predict chlorophyll level is not strictly related to the algae's infrared response, but rather to its high reflectance in all wavelengths and proximity to the surface. Not only low levels of blue-green algae will induce a white response in color infrared film, but also high concentrations of suspended sediment, green algae, and foam formations. Certainly problems in photointerpretation will inevitably arise from time to time, but as will be pointed out in the discussion these can be resolved by some other knowledge of spectral responses.

Our experience with photographic remote sensing leads us to believe that at or below a concentration of 10 μg/ℓ, the ability to recognize any structure with or without color tones is lost. It is also evident that at or above 10 μg/ℓ surface blue-green algal Chl *a* values, the reflectance peak in the infrared begins to appear (Figure 44D). The infrared reflectance by blue-green algae is a crucial factor in determining whether or not microstructure will be apparent in aerial photographs of water bodies. But at the same time spectral response by blue-green algae is dependent on the state of gas vacuolation. Also the delineation of blue-green algal Chl *a* concentration is dependent on the algae being very close to the surface in order that infrared light be reflected before it is absorbed. Since these factors must be taken into account in the work we have done so far, the spectral signatures presented in this section can be taken as only a broad measure of chlorophyll concentration.

Figure 45 also illustrates patchiness found in Perris Lake which could be ascribed to blue-green algae (*Microcystis aeruginosa*). This photograph was taken by closed-circuit television instrumentation over Perris Lake on 4 November 1974. During the November reconnaissance Chl *a* values were again low (10 outside and 18 μg/ℓ inside the patch), although it should be noted that field sampling did not touch on the exact area where film contrast is greatest. Figure 45 was taken solely in the infrared band and the structure is shown to promote the modest infrared response expected from blue-green algae. However, it can be stated that without water truth measurements and observations neither this phenomenon nor the concentration or species present would have been noted. Iris effects and blooming of land features, due to the fact that instrument gain controls had to be opened to fully pick out any features in the water, contributed to the problem as did poor resolution and lack of orientation within the picture scene.

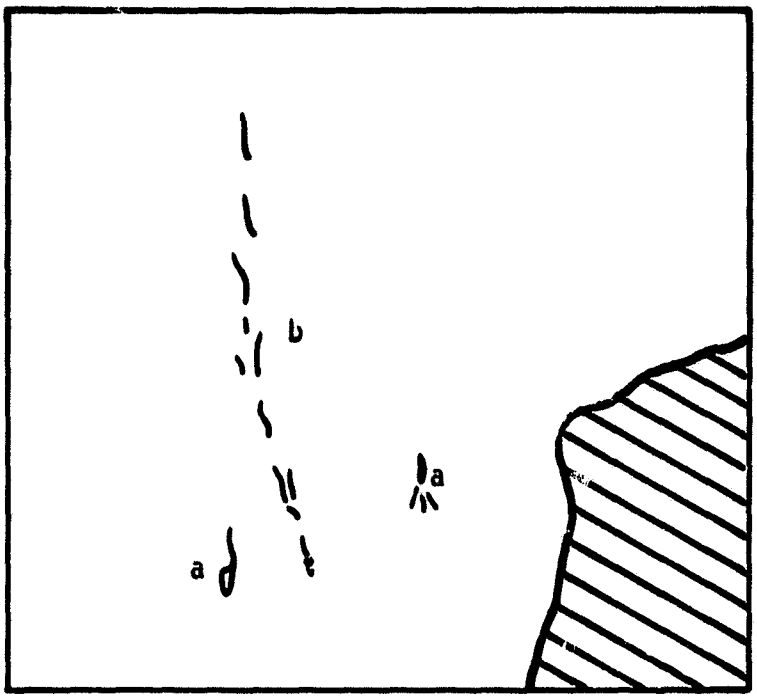

NEAR IR PHOTOGRAPH

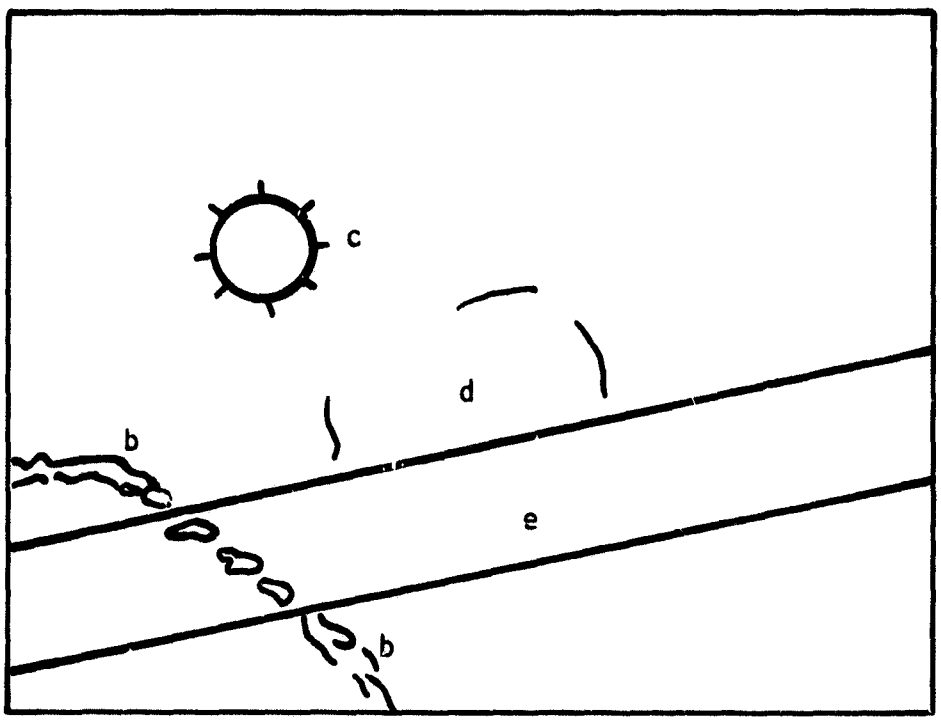

TV VIDEO IMAGE

a. Boats
b. Surface structure due to algae (decayed periphyton, *Spirogyra*)
c-e. Lens and other artifacts

FIGURE 45. KEY

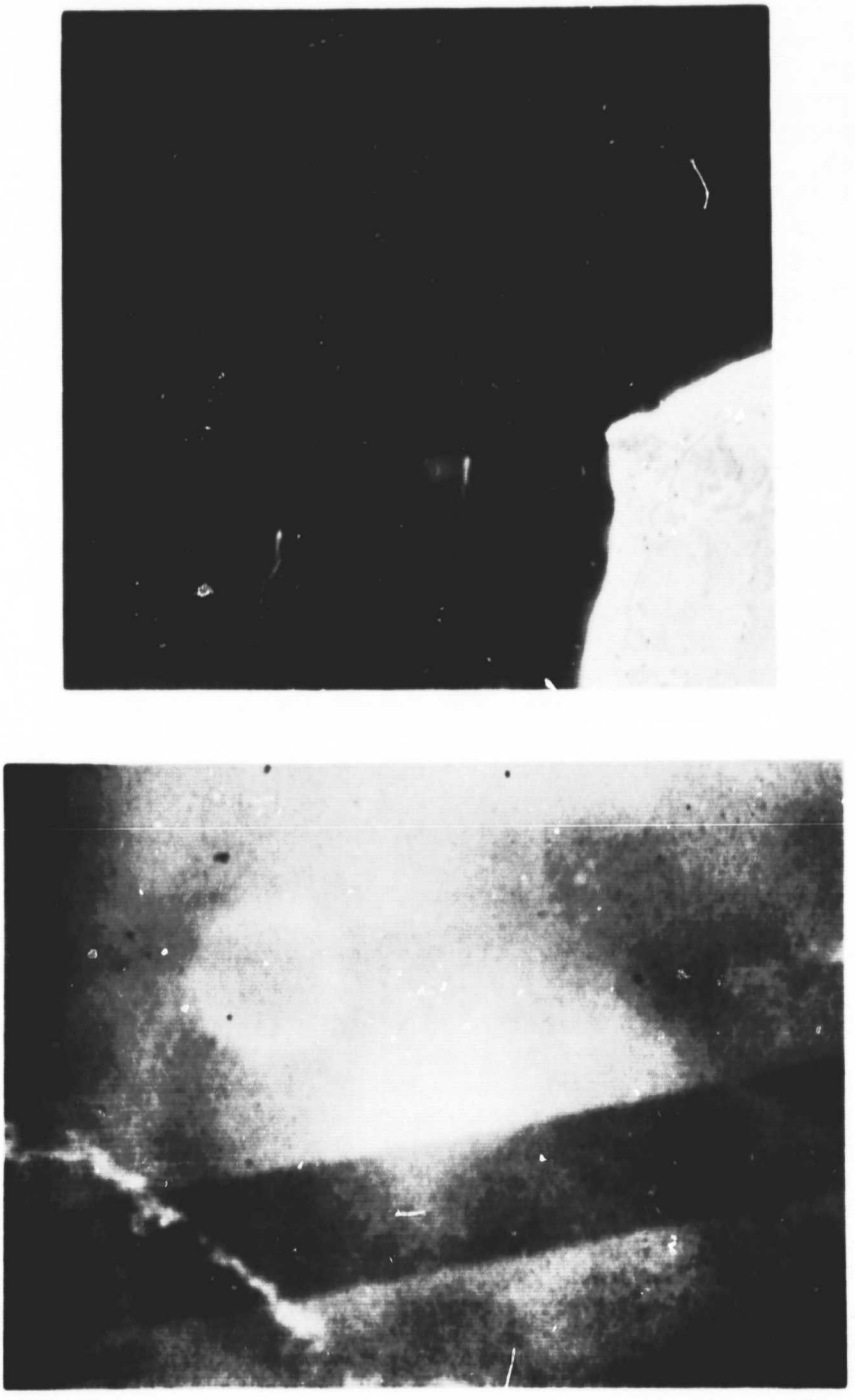

FIGURE 45. COMPARISON OF TV-VIDEO NEAR INFRARED IMAGERY WITH CONVENTIONAL IR PHOTOGRAPHY, PERRIS LAKE

Although the laboratory studies indicated that at most a fourfold difference in IR reflectance existed between blue-green algae and green algae, the results of the lake studies indicate that if the concentration of green algae is simply four times that of blue-green algae, patchiness comparable to that outlined previously for blue-green algae, does not exist. The study indicated that the probability of recording a significant infrared response from a concentration of planktonic green algae was far less than for blue-green algae. In Figures 1, 4, 41-42, 46-48, 54, and 60-61 the distribution of chlorophyll *a* and turbidity over the reservoirs at the time of aerial reconnaissance is shown for the entire range of sampling dates. These water quality measurements suggest that there is no simple relationship between the arrival of visible patchiness and suspended solid concentration. On the contrary, distinct threshold concentrations for the appearance of patchiness are dependent on the type of plankton in the water.

On no occasions in our study could patchiness be attributed to the appearance of planktonic green algae, diatoms, or dinoflagellates, despite the fact that during the test period in Southern California chlorophyll *a* levels measured from samples known to contain primarily these algae varied from 1 µg/ℓ to well over 100 µg/ℓ. Continuing studies of this subject on some highly eutrophic sewer ponds near Clear Lake showed that patchiness similar to that in Figure 38C became apparent only when green algal chlorophyll *a* levels approached 350 µg/ℓ. This suggests two important points. First, magnitudes of difference in chlorophyll *a* levels must exist between green algae and blue-green algae before equivalent patterning in color IR is apparent, and this can be explained only by taking into account reflectance capabilities and differences in stratification near the surface for the two algal types. Blue-green algae, being buoyant, will appear just below the surface whereas green algae will not. Second, although it is clear that at some point green algae, diatoms, and dinoflagellates will promote a significant infrared response, such a concentration appears to be out of the range of normal conditions, except for the instance of shoreline growth or "red tides" [48]. The significance of these statements to the personnel in charge of lake management becomes manifest when charting correlation between surface chlorophyll *a* measurements and the signs of patchiness. Figure 49 shows the breakdown of algal species present in the surface water as averaged for six stations over Perris Lake where the patchiness was noted, and over Castaic Lake where the spread of chlorophyll *a* levels was the greatest for the four reservoirs, during the four-month test period. As can be seen in Figures 48-50, patchiness at Lake Perris coincided with a minor blue-green algal bloom in September and occurred just prior to a minor bloom in November. In each case, lake observations established that the portion of the lake exhibiting patchiness had blue-green algae. Chlorophyll *a* levels were more than 100 µg/ℓ in Castaic Lake in September and November (Figures 46 and 47) but no patchiness was detected. Figure 51 confirmed that for all surface samples collected, only green algae were present. Imagery showed that both arms of the lake were just very dark, indicating that reflectance in any waveband was simple and below that which could cause a substantial deviation in the response of the film.

A second interesting point respecting green algae was made during lake observations. During the October and November sampling dates, a bloom of the green alga *Mougeotia* was noted on Lake Perris. *Mougeotia* is a

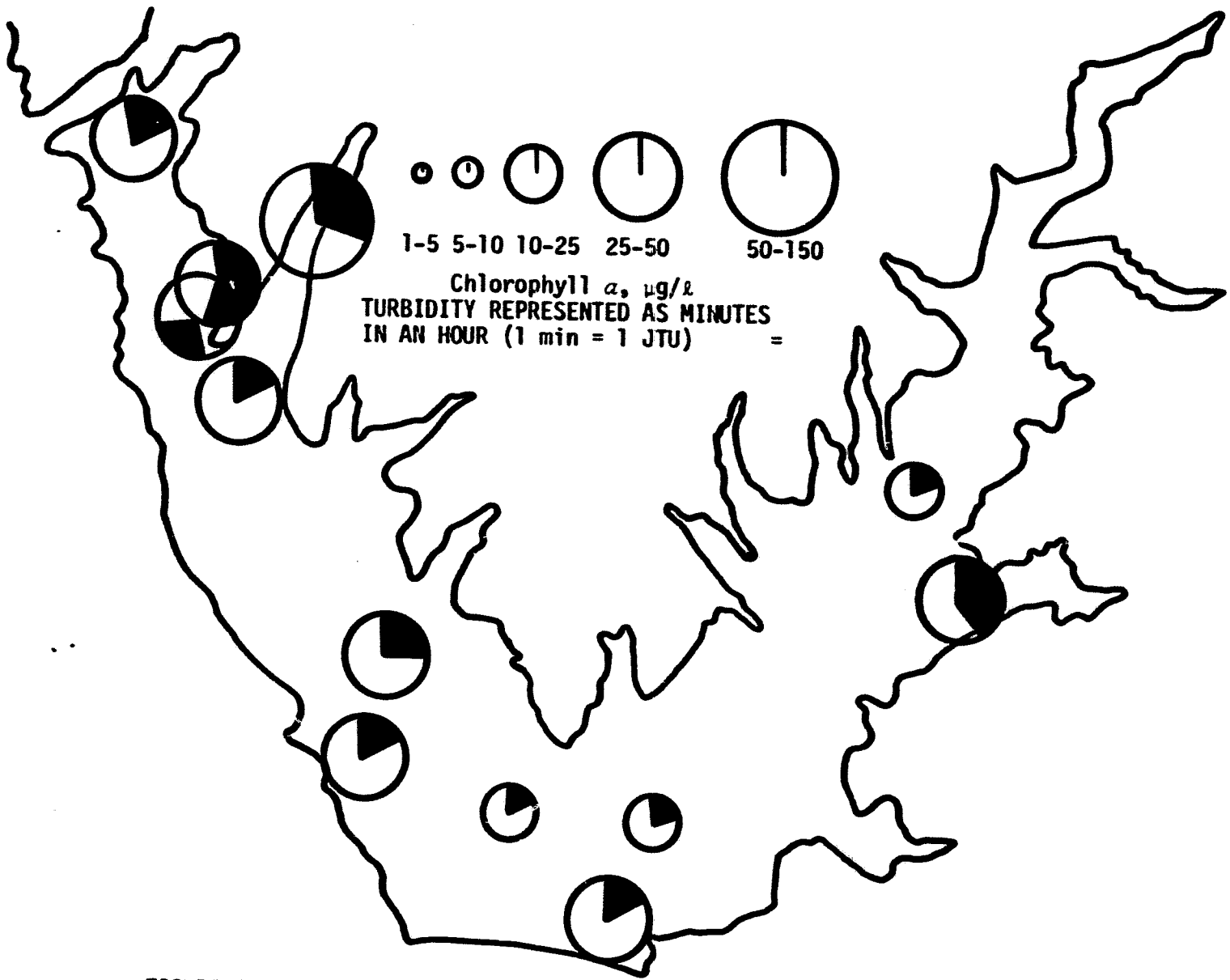

FIGURE 46. CHLOROPHYLL AND TURBIDITY IN CASTAIC LAKE, 12 SEPTEMBER 1974

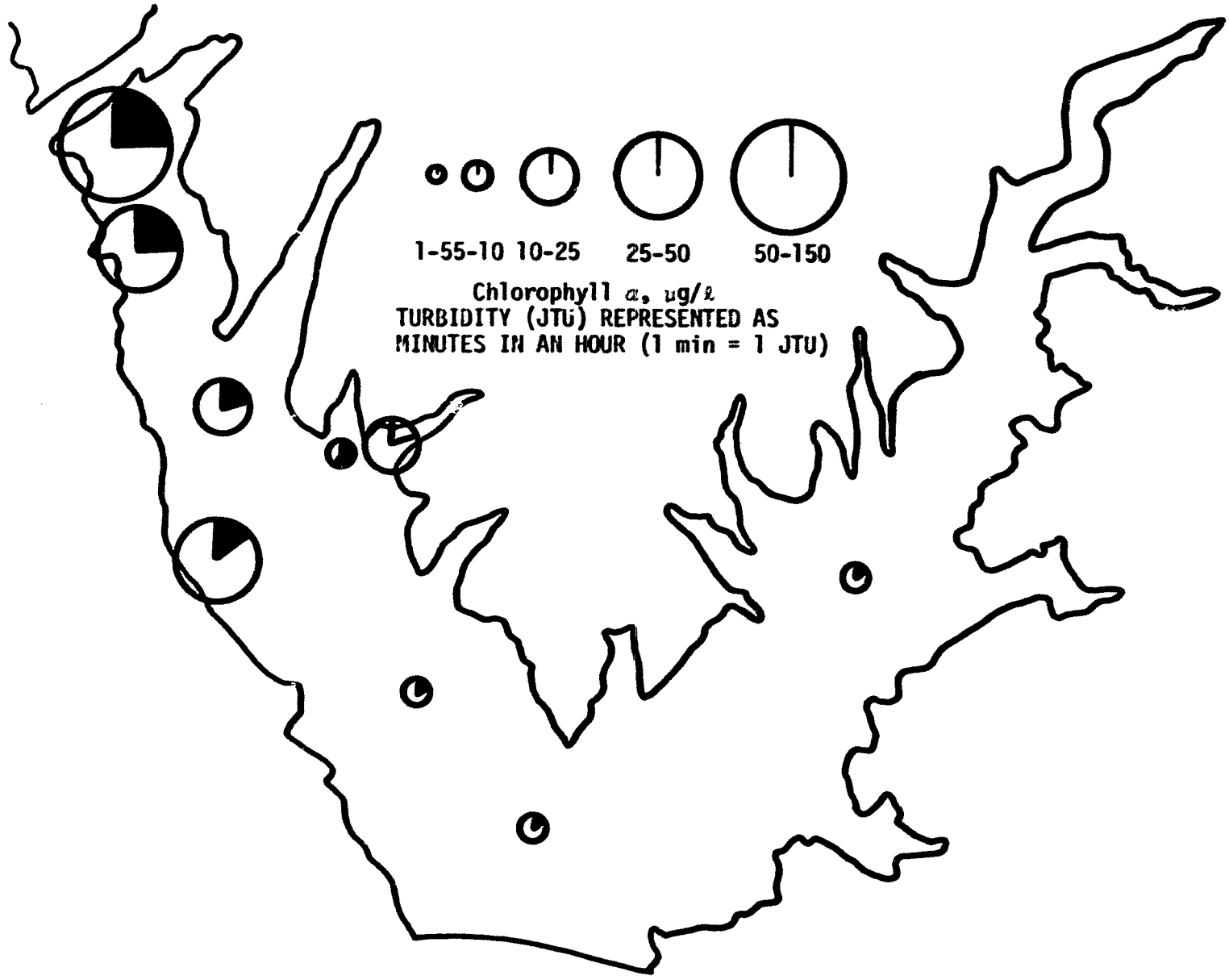

FIGURE 47. CHLOROPHYLL AND TURBIDITY IN CASTAIC LAKE, 2 NOVEMBER 1974

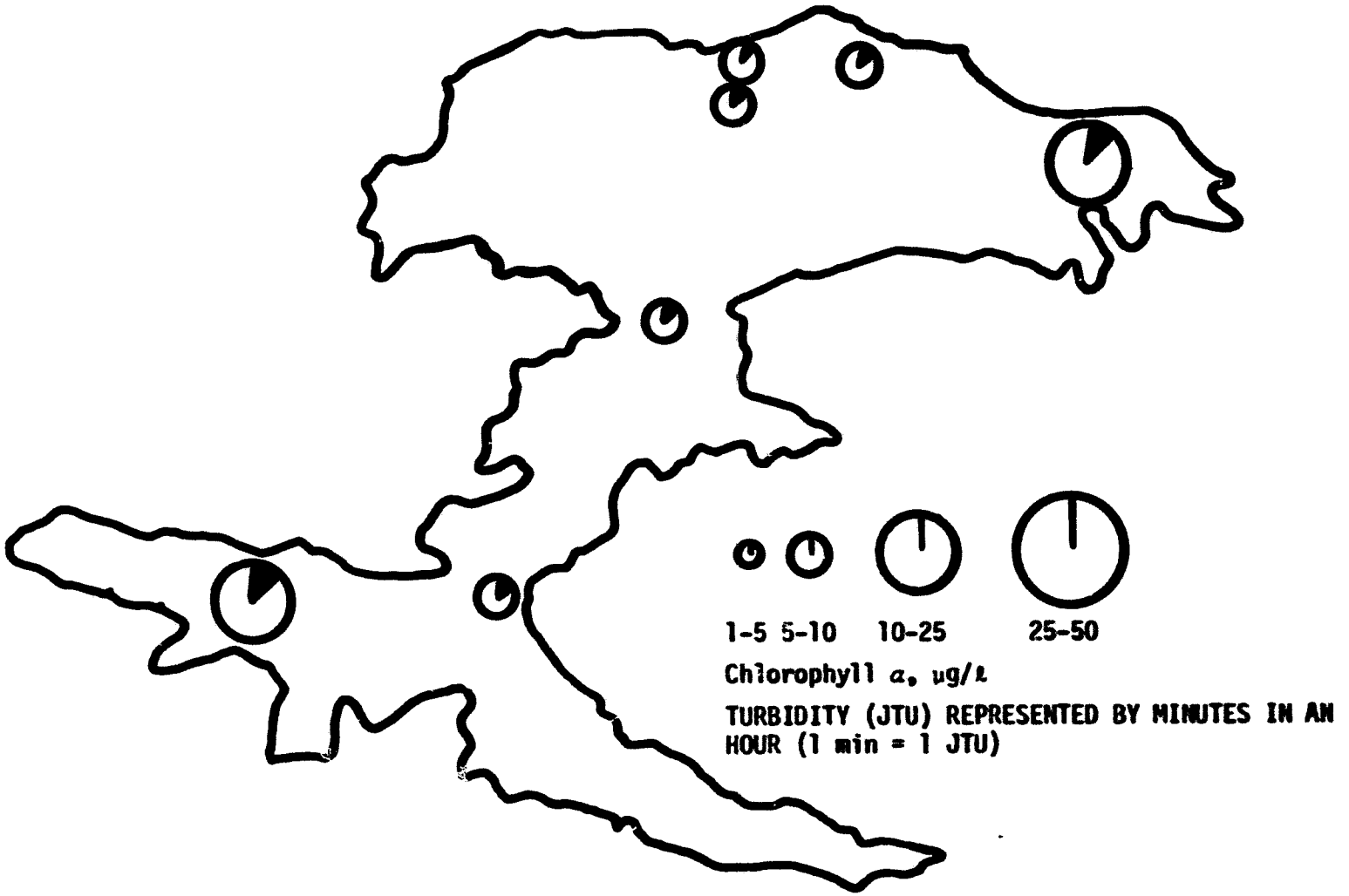

FIGURE 48. CHLOROPHYLL AND TURBIDITY IN SILVERWOOD LAKE, 4 OCTOBER 1974

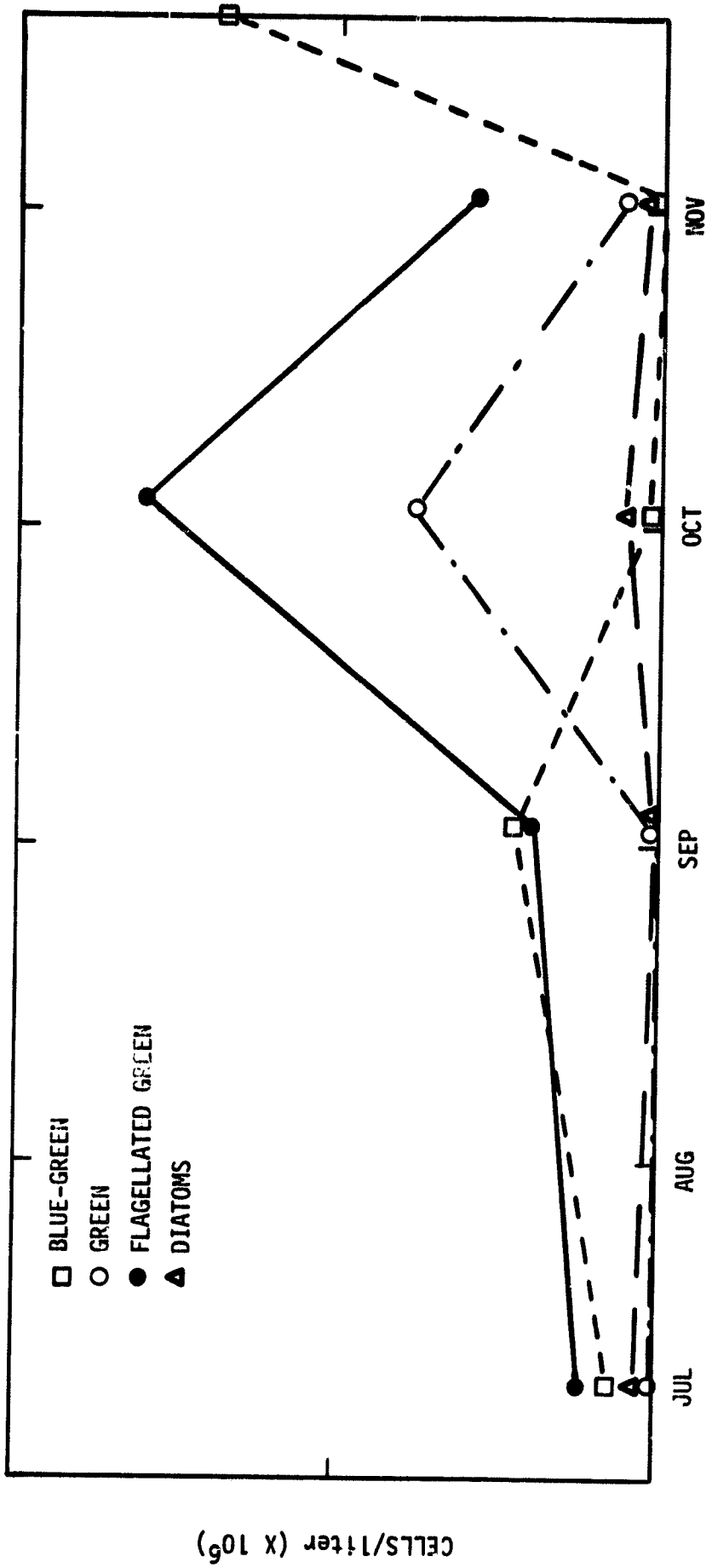

FIGURE 49. PERRIS LAKE ALGAL COUNTS FOR SURFACE SAMPLES

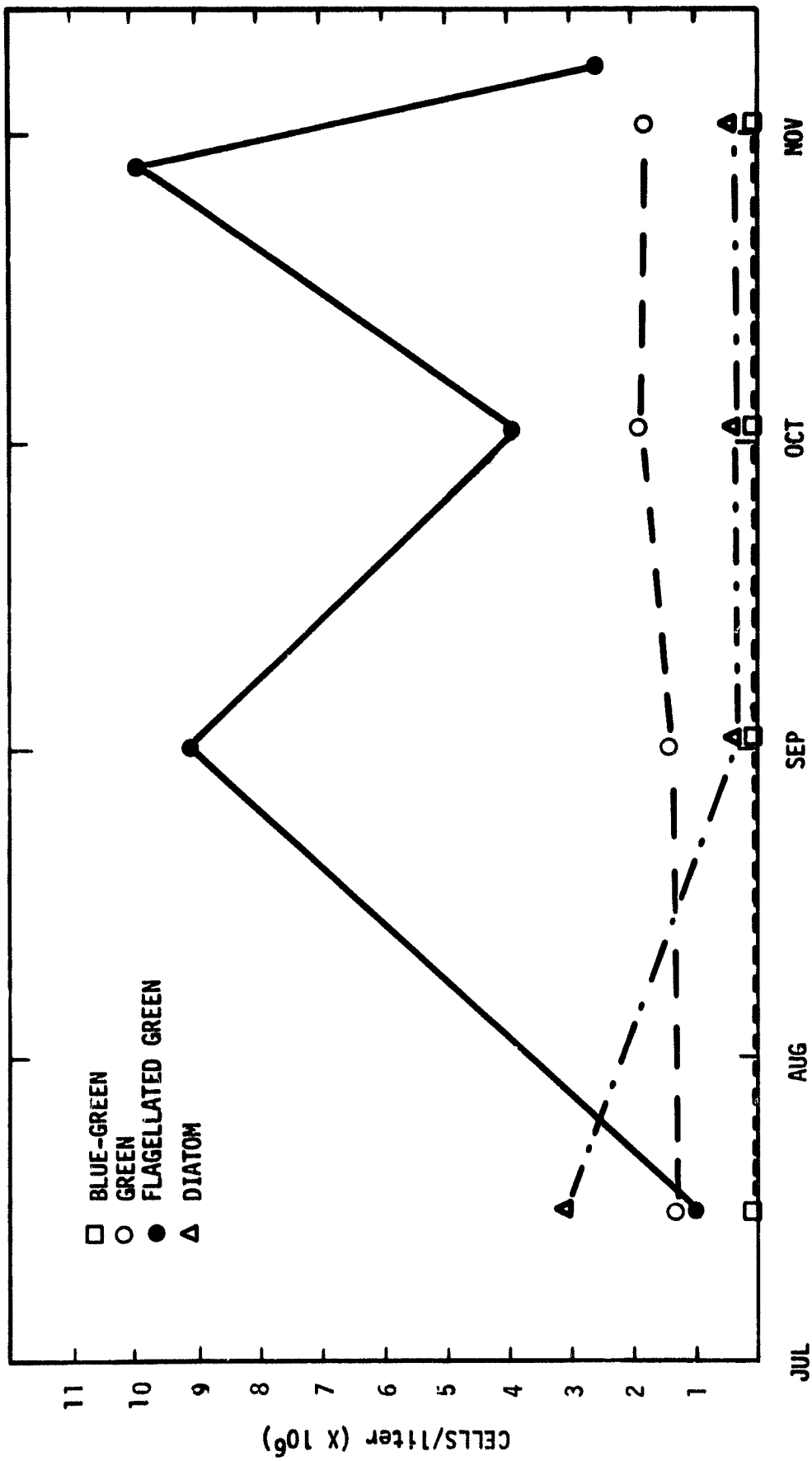

FIGURE 50. CASTAIC LAKE ALGAL COUNTS FOR SURFACE SAMPLES

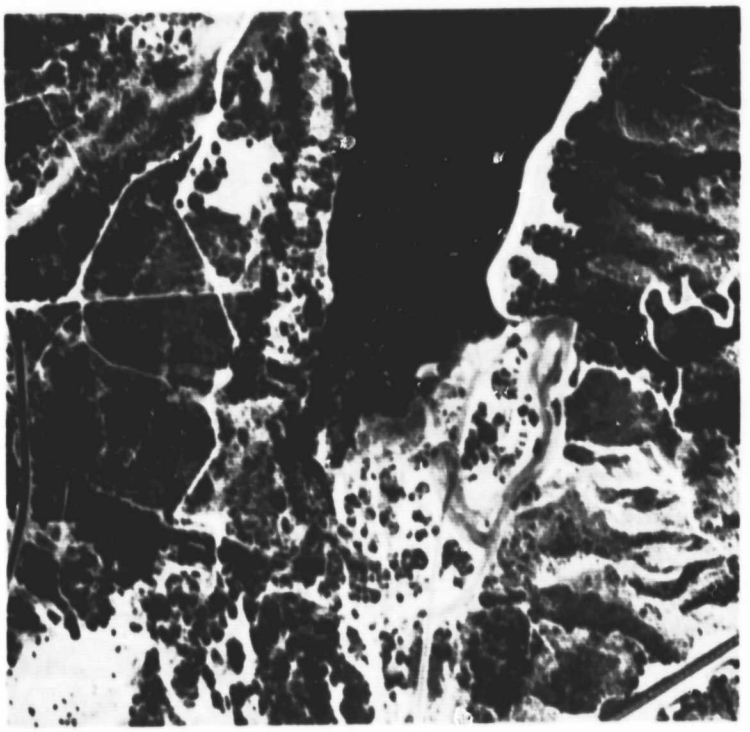

A

12 SEP 74

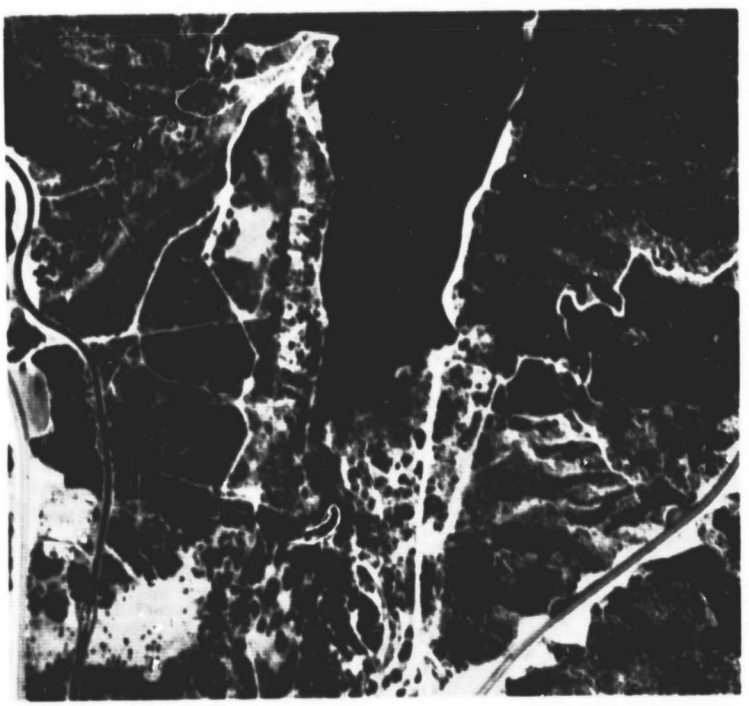

B

11 JUL 74

FIGURE 51. *Cladophora* IN SILVERWOOD LAKE

filamentous green alga known to form surface mats. These were evident in the lake at the time of aerial reconnaissance, but no patchiness could be associated with the areas of high *Mougeotia* concentration. Concentrations in this instance were still substantial (10-25 µg/ℓ Chl *a*).

Together, the two points above illustrate that by simple photographic interpretation it may be possible to predict general types of algal composition in surface waters, and that to some extent the appearance of surface patchiness is specific to nuisance blue-green algae. Under no circumstances, however, can the chlorophyll *a* model based on infrared response, as outlined in previous pages, be applied when the phytoplankton is not a blue-green gas vacuolated alga.

Macrophytes and Periphyton. Figure 39B-D illustrates a second important feature of remote sensing in aquatic environments. Attached growths such as *Spirogyra*, *Cladophora*, and *Lemna* often cause problems in lake management because they obstruct navigation or break loose and cause filter clogging. Decaying scums may also cause visual unpleasantness and malodor. Remote sensing offers a rapid, simple means of detecting the extent and growth rate of these nuisances. Outside the colored zone which corresponds to a surface scum, light and dark areas of contrast are apparent in Figure 39B. Lake observations established that the darker areas correspond to areas of sub-surface algae (1-3 m deep). Normally, high infrared reflectance does not occur from this depth because the infrared band has been absorbed. Visible light penetrating to the bottom is largely absorbed by the attached plants or algae. Lighter areas adjacent to the dark patches correspond to areas with less algae, consequently a greater benthic reflectance of visible light. As the edge of sub-surface shelf is reached, reflectance in all bands drops off and the image appears dark.

Figures 38A-B and 54A-B show the change in extent of growth over two summer months. Lighter areas not infested at the time of aerial reconnaissance can be delineated as potential sites for aufwuchs invasion. Estimates of standing crop and percent shoreline infestation of benthic algae or macrophytes can aid user agencies in planned use development. A more extensive approach to the use of remote sensing technology in monitoring this type of nuisance aquatic phenomena has recently been published [12].

Sediments. Highly turbid waters were observed by aerial reconnaissance on three of the four reservoirs and were linked with two phenomena: turbidity associated with water flows from the California State Aqueduct, and shoreline erosion at Pyramid and Castaic lakes. Shoreline erosion tended to increase in the afternoon with noticeably strong westerly winds. Sediment plumes regulated by flow operations were assigned density units corresponding to water turbidity in the plumes, and erosions correlated well in the red band of the four-band multispectral camera (see Appendix). Depending on the nature of the object, plume or shoreline erosion, turbidity appeared well delineated from the rest of the water body. The plume vanished shortly after flow was cut off, indicating that particle size was possibly large and producing quick sedimentation (Figure 53A). Shoreline erosion fanned out from the shore and particles remained in suspension a great deal longer (Figure 53B), possibly indicating smaller particle size. The Appendix illustrates the correlation between wavelength response and turbidity. At no time could a distinct color tone, in color

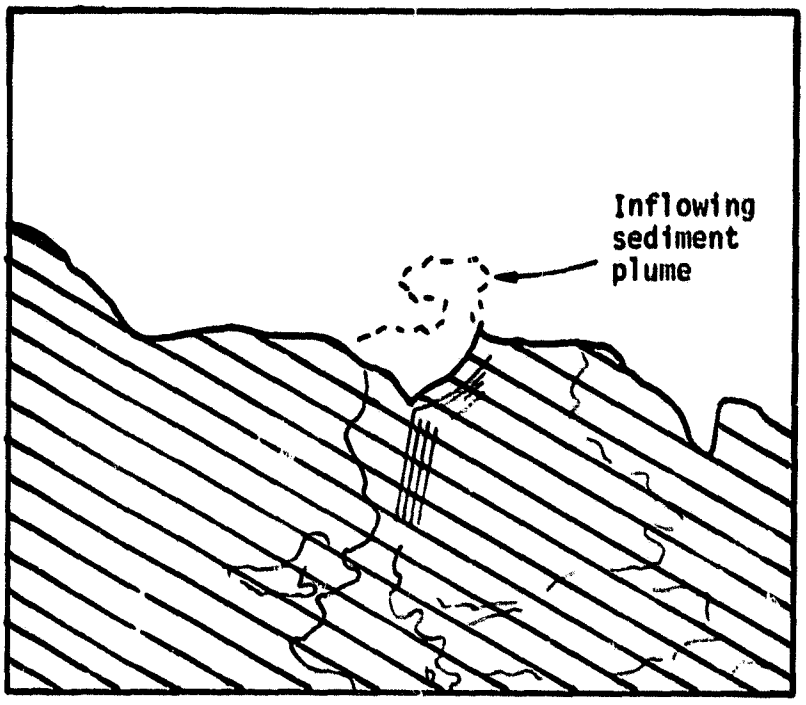

A

SEDIMENT PLUME—SILVERWOOD RESERVOIR
11 JULY 1974

B

SHORELINE EROSION—CASTAIC RESERVOIR
12 SEPTEMBER 1974

FIGURE 52. KEY

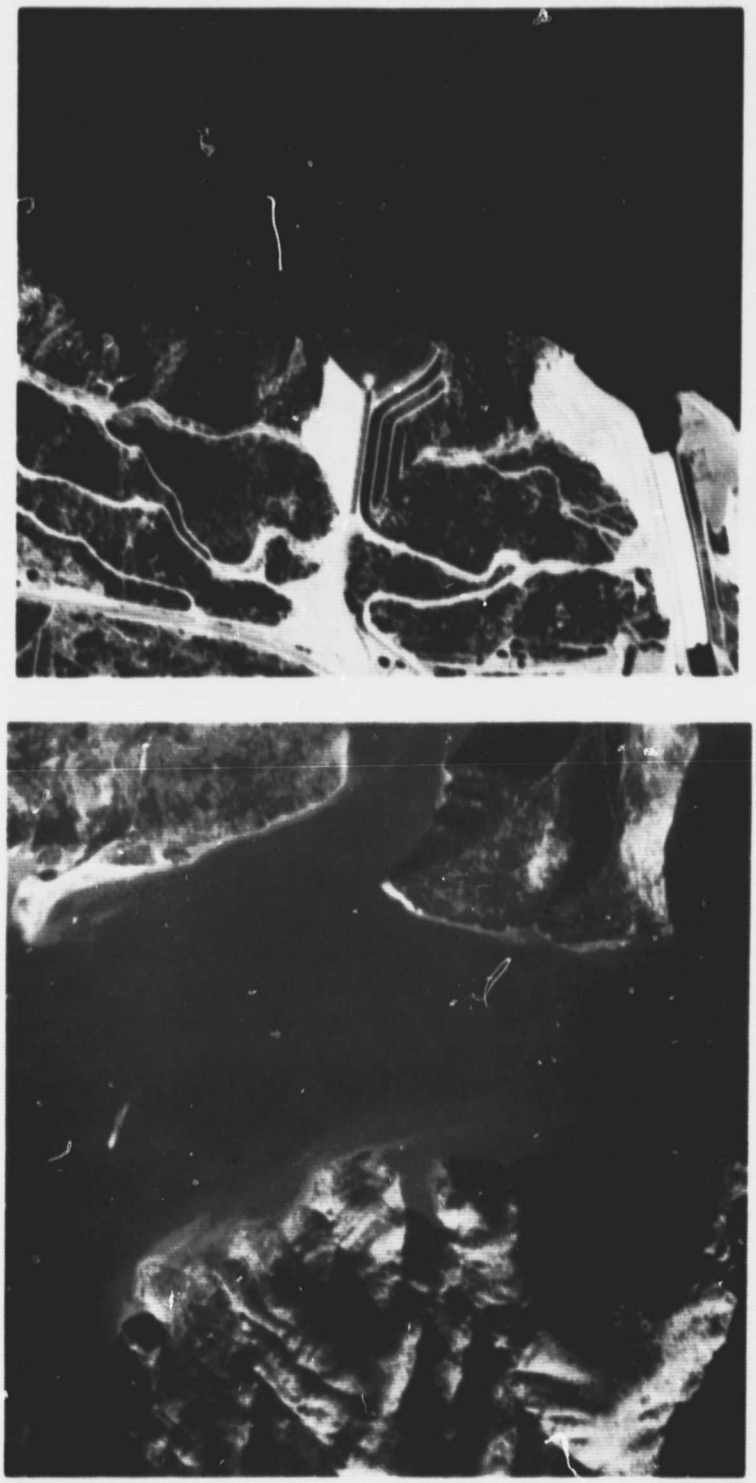

A

B

FIGURE 52. SEDIMENT PLUME (SILVERWOOD) AND LATERAL SHORELINE EROSION (CASTAIC)

A

SILVERWOOD LAKE

B

CASTAIC LAKE

FIGURE 53. WIND-INDUCED SHORELINE EROSION IN SILVERWOOD (A) AND CASTAIC (B) LAKES

IR film, be associated with any of the suspended sediment concentrations; on the contrary, even the heaviest concentrations gave a rather dull, neutral tone (gray-blue) in contrast to distinct colors associated with biomass.

Figure 53A-B also illustrates two instances where sediment induced patchiness. In both, one feature is apparent: the sediment patches start at an obvious point source such as an eroding shoreline or a water inlet. This indicates that sediment often appears in this fashion rather than as turbulence produced bottom stirring (a non-point source of sediment). Sediment plumes such as those in Figure 53A-B have an obvious shape which is not at all reminiscent of phytoplankton patchiness. Therefore, on some occasions the dispersion or movement of particles in water can serve to identify particle type.

Water Clarity. Another water quality parameter, that of light penetration in water, was measured during aerial reconnaissance dates. Since water clarity is both desirable from the point of view of water recreationists and lake management personnel (highly transparent water means few nuisance algae are present), it would be useful if techniques could be developed whereby water clarity was measured automatically by remote sensing techniques. Also, since light responds unevenly to different types of suspended particles in water, the extinction profiles for light as a function of depth can be useful in determining particle character and concentration [11]. The following discussion summarizes the important results noted during the study.

Figure 54 has depth profiles of light penetration at stations 5 and 9 on Perris reservoir on 11 July 1974. A slight increase from 2 to 5 mg/ℓ chlorophyll *a* surface concentration was recorded and a noticeable increase in colonial algae was apparent to the naked eye. Since turbidity was essentially constant at these two stations, the decrease in light transmission can only be attributed to the phytoplankton in the water. Though the surface biomass levels changed only slightly (and DWR depth sampling at six stations in the lake showed little stratification over the entire lake), the depth of the photic zone dropped substantially. Figure 54 shows that blue and red light are absorbed preferentially to green light, and may serve as an indication of photosynthetic pigments.

Although a marked increase in particulate composition could be observed by eye, as mentioned, no patchiness was detected on film. This seems to be due to the fact that only weak reflecting green algae were in the lake at the time.

Figure 55A and B from Silverwood and Castaic reservoirs, on 11 and 12 July 1974, respectively, also indicates this phenomenon. Although the profiles were taken at different times of the day, the sun angle was nearly equivalent (35 deg). Note how the slope of blue light extinction has changed radically from that in Figure 54.

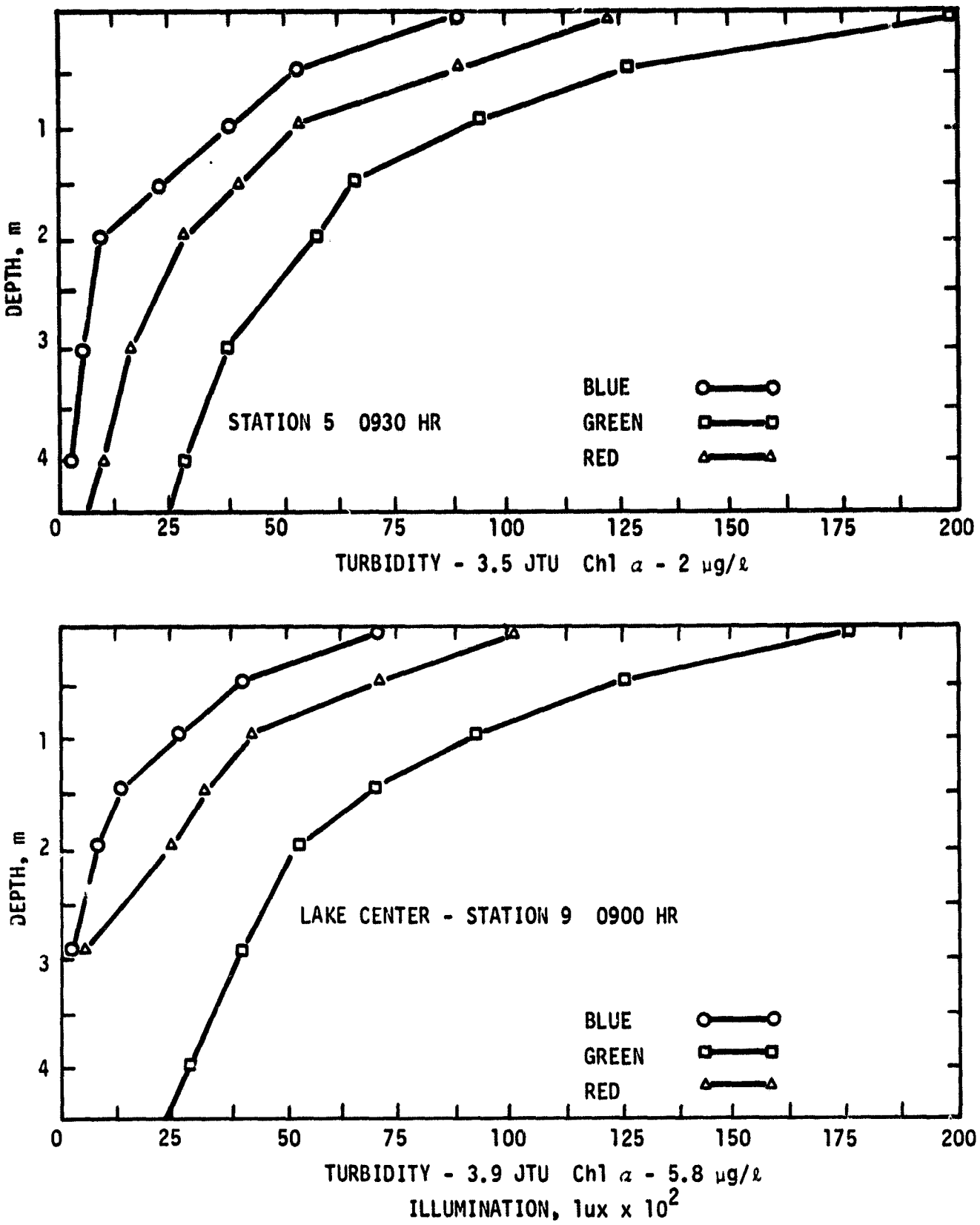

FIGURE 54. LIGHT EXTINCTION CHARACTERISTICS OF PERRIS LAKE, 11 JULY 1974

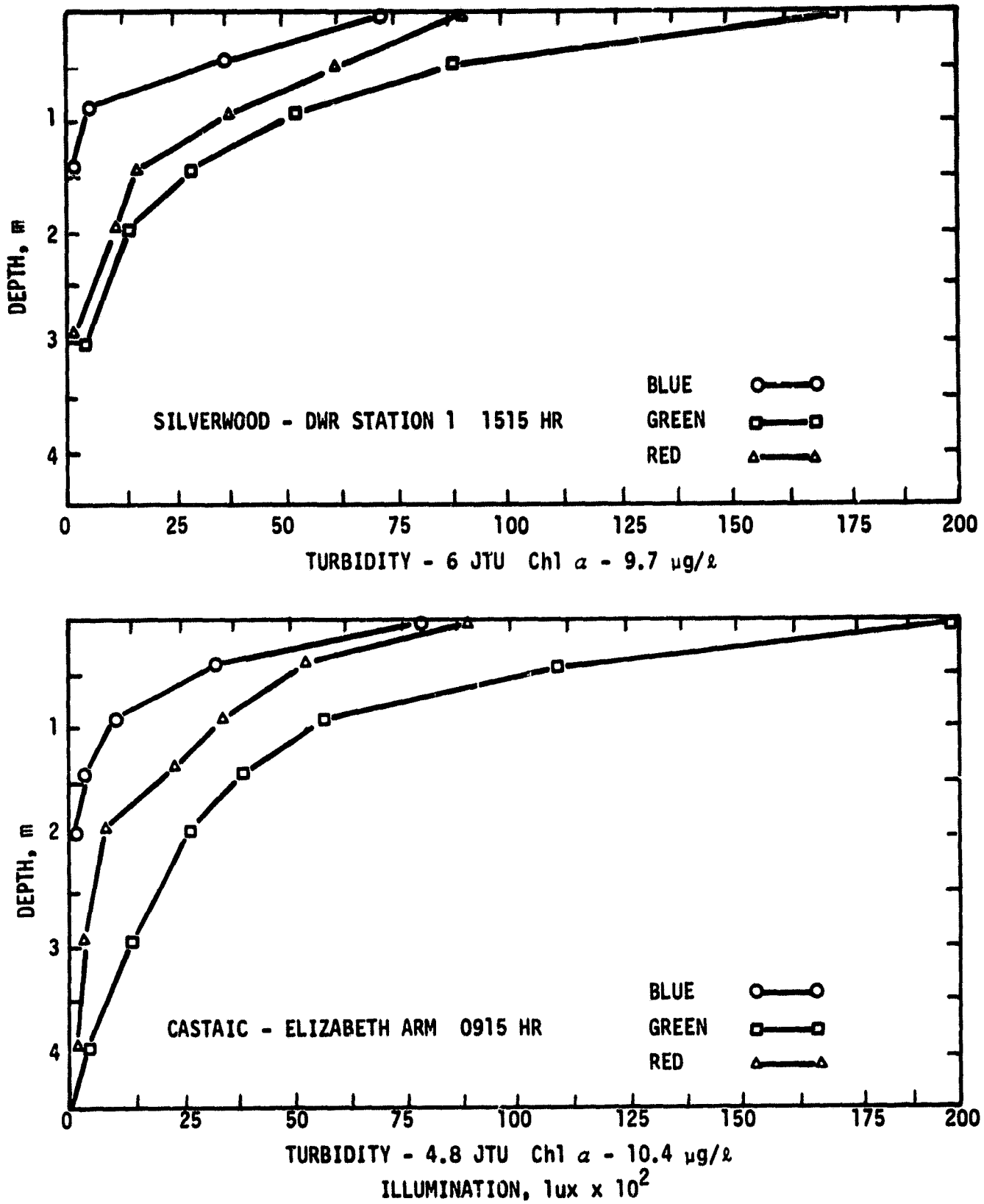

FIGURE 55. LIGHT EXTINCTION CHARACTERISTICS OF SILVERWOOD LAKE, 11 JUNE 1974, AND CASTAIC LAKE, 12 JUNE 1974

VII. DISCUSSION

Nowadays it is quite common to use aerial remote sensing for rapid, synoptic measurements of large-scale environmental phenomena. Symposium proceedings, articles in scientific journals, and those in the popular press appear regularly [3, 4, 6, 10-14, 28, 29, 31-34, 43, 47, 49, 50-73]. At least for different types of static vegetation such as forests, marshes and grasslands [e.g. 53, 64, 68, 74], different species [e.g. 53] and even the state of health of the population can be assessed. For mobile vegetation—generally phytoplankton—only very generalized remarks have been possible due to lack of simultaneous water truth. This is particularly so with Skylab and with oceanic phytoplankton [67]. Sediment, however, has proved amenable to semi-quantitative remote sensing since it is often routinely measured by conventional means [57, 62].

A unifying feature of these reports is the experimental nature of remote sensing projects, together with a constant search for applications of this powerful technique. A few workers with longer experience of the technique have developed their methods so that now economic considerations dictate the use of remote sensing instead of, or at least in conjunction with, conventional measurements. R. N. Colwell and his students in the Department of Forestry, University of California at Berkeley have been able to predict the number of board-feet of certain types of timber using remote sensing, at less cost than conventional forestry ground sampling [74]. SERL studies in Southern California reservoirs were designed for a similar purpose. Could the cost of lake monitoring be reduced by using aerial remote sensing? Could lake monitoring using remote sensing be made even more useful?

Our initial laboratory studies with natural populations demonstrated that different algal types could be distinguished by their characteristic reflectance spectral signatures. This was perhaps to be expected given the high concentrations of algae used, but nevertheless these were natural populations. More unexpected were the aerial reflectance signatures producing distinct color tones for the different types of algae, macrophytes, and debris which cause reservoir management problems. These colors were a apparent at concentrations lower than those used in our laboratory experiments. It appears that the water absorbance is insufficient to obscure all algal reflectance in the near-surface water. The integral reflectance for this short water column then resembles that of a membrane filter through which a similar column of water has been passed. Thus, given a sufficient concentration of algae in the surface or near-surface waters, remote sensing can usually identify approximate type and concentration using color tone on false infrared film. In addition, shallow water periphyton and macrophytes can be assayed, as has been found previously [12]. The aerial identification of sediment eroding from the newly-formed shoreline was predictably easy, since sediment is known to have a distinct color tone in four-band photography (0.3-1 μm).

Four-band color or instantaneous remote sensing using the TV-video system is of less direct value to the reservoir manager, since it is more difficult to interpret the patterns of algae on the lake surface than to notice the color tone of a photograph. However, rapid identification may be vital for the efficient deployment of copper sulfate dispensers or algal

harvesters, especially in the Los Angeles area where reservoirs are far apart. The unavailability of a Polaroid-type color IR film was a serious handicap. The TV-video single waveband system proved useful in predicting the onset of a small bloom of *Microcystis* (Figure 45) prior to its detection by conventional methodology. Although the TV camera was useful in this case, the overall performance of this imaging system when dealing with biomass levels found in reservoirs was poor. The resolution of the television camera was the biggest drawback. For a common television video-camera, there are only approximately 500 line scans. In a 9x9-inch photograph of comparable size, there are approximately 17,000 lines for the same area. The result is that common TV video-camera sensing systems are limited to a resolving power of 5 meters at a scale of 1/10,000, while a comparable photograph has a resolving power of 30 cm. The problem can be defined as recognizing patchiness or microstructure typical of blue-green algae. Since the structure is often obvious only briefly and in a limited area, resolution is essential. There were also some problems with the spatial orientation with the TV camera, which produced imagery with a different perspective from that of the typical airborne 9x9 photographic cameras.

In a well-designed, well-managed reservoir algal concentrations in the upper waters would usually be at levels too low to be detected by remote sensing. Thus any sign of algae, either from development of red or pinkish tone in false color IR film or in patchiness with possible microstructure in the NIR band of four-band photography or video, is a warning that problems may be arising. Periphytonic nuisance growths or macrophytes such as duckweed or water hyacinths develop quite slowly and could easily be detected by most types of remote sensing and controlled conventionally. In contrast, phytoplankton blooms—especially those of blue-green algae—develop rapidly. In high summer too much time may pass between flights, production of the processed photographs, and the action. It should be realized that most algal blooms are basically mechanical accumulations of already grown algae, rather than sudden overnight growths [3, 71-76]. For blue-green algae various conditions [44, 71] allow the algae to float to the surface and to remain there as a nuisance. On other occasions, as in the notorious Lake Zurich algal bloom, the breakdown of the summer thermocline may bring to the surface previously unnoticed deep-dwelling populations [77, 78]. In all these cases remote sensing would detect the algae, but so would simple visual observation or normal visitor use of the reservoir.

In the case of the initial growth or accumulation of a patch of blue-green algae in an unused corner or sidearm prior to its development in the whole reservoir, remote sensing provides a unique method of detection. In Lake Perris, however, the main corner for algal accumulation has been the main boat ramp, which can scarcely be described as unused! In Castaic Lake there were no incidences of algal accumulation in sidearms, although considerable debris was found there. For both Silverwood and Perris lakes, attached periphyton were a potential problem easily observed by remote sensing, although few complaints were received about their presence [79].

The color tone typical of highly concentrated scums of green algae is pink, and that of a moderate concentration of blue-green algae (40 µg/ℓ Chl *a*) is a faint red. What criteria can be used to distinguish a large concentration of green algae from a moderate concentration of

blue-green algae? To answer this question, it is first necessary to establish the amount of green algae which would produce a pink tone. The Southern California study has shown that a minimal amount of white structure is evident in the water when a concentration of predominantly blue-green algae has a chlorophyll *a* level of 10 µg/ℓ. Since blue-green algae constituted only about 50% biomass in samples taken from the area showing structure, it is assumed that their chlorophyll *a* concentration alone is approximately 5 µg/ℓ. A comparison between the chlorophyll *a* levels then known to produce (blue-green) structure at Perris Lake (12 September 1974) and those known not to cause (green) patchiness at Castaic Lake (4 November 1974) shows that at least a 20-fold increase in green algal plankton populations would be necessary to produce comparable structures. Recent aerial studies on sewage ponds near Clear Lake have established that only at green algal chlorophyll *a* concentrations of 350 µg/ℓ does an equivalent minimal amount of structure begin to appear. The conclusion is that a nearly 70-fold increase in green algal concentration would be necessary for an equivalent structure to be present. Given this context, the question seems rather esoteric as far as lake management personnel are concerned, for a 70-fold increase in the population of green algae (4 µg/ℓ going to 280 µg/ℓ, for instance) would be quite evident from just a casual glance at the lake.

Another problem in using remote sensing for monitoring water quality is presented by changeable weather. Bad weather—particularly morning mist or clouds—reduced coverage for the Southern California reservoirs. Smog did not affect operations, however. Conventional measurements were less limited by cloud cover, although mist usually prevented sampling. Beyond that was the problem of how wind affects water circulation patterns. Patchiness, especially microstructure, resulted from active algal movement, water currents, and light. However, in a lake or reservoir where biomass levels are low, patchiness is easily lost during periods of windy weather. On the night of 2 October 1974, extremely calm conditions prevailed over Lake Perris (Table XII). Winds measured at nearby March Air Force Base were only two knots, from 319 deg true north, up until 1000 hours on the following day. The lake itself was littered with balls and patches of detached shoreline aquatic growths (mainly highly decayed *Spirogyra* with unidentified macrophytes and filaments of the green alga *Mougeotia*). The balls and patches were sufficiently large to anticipate their being visible in the photographs. Figure 55 shows the relatively high morning chlorophyll *a* levels, but the *Spirogyra* was so badly decayed that it appeared white to the eye. It was apparent that a great deal of chlorophyll *a* had been lost to the environment and that chlorophyll *a* may not be a good measure of biomass present.

By noon, the winds had increased to 10 knots from 300 deg true north. The afternoon run showed little surface structure and decreased chlorophyll *a* levels (Figure 56). The lack of surface patterns indicated a more uniform vertical and horizontal distribution. It is at this point that resolution of patchiness or microstructure is lost totally, even if high concentrations of algae are involved [5]. Afternoon video-sensing picked up some of this extraneous drifting matter at a corner of the lake (Station 6), although much of the morning's patchiness was gone. Similar results could be anticipated if blue-green algae were present. Hence in any remote sensing monitoring program flight times and dates will have to be chosen carefully to coincide with calm periods if the maximum amount of useful information is to be

TABLE XII
WIND DATA – PERRIS LAKE

Day	Time	Direction degrees	Magnitude knots
11 Jul 74	0957	300	4
	1555	300	10
12 Jul 74	0957	160	1
	1555	300	8
11 Sep 74	0957	110	2
	1555	320	13
12 Sep 74	0957	---	Calm
	1555	300	10
13 Sep 74	0957	---	Calm
	1555	320	9
2 Oct 74	0957	310	2
	1555	300	10

Measured at true North: 15 deg off magnetic center

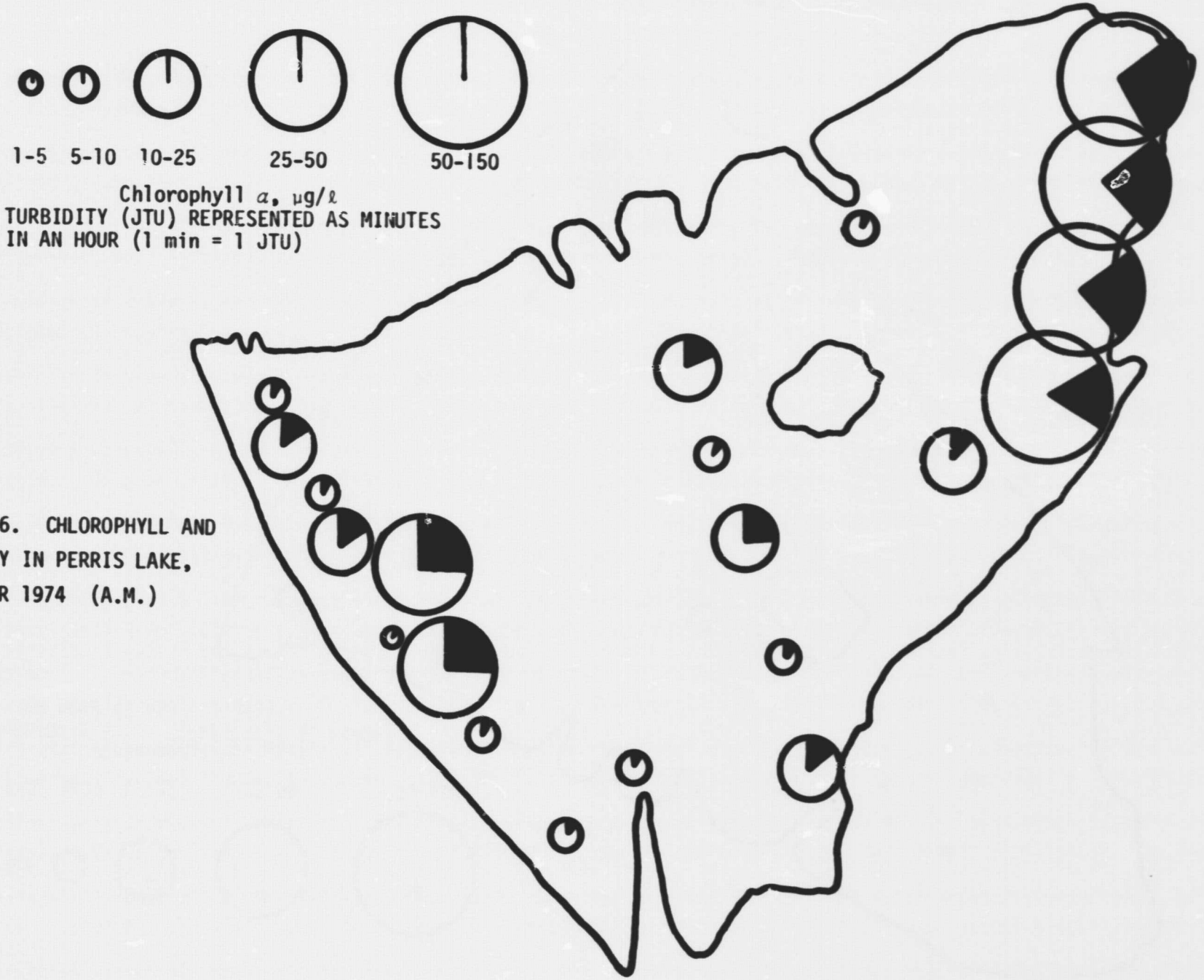

FIGURE 56. CHLOROPHYLL AND TURBIDITY IN PERRIS LAKE, 2 OCTOBER 1974 (A.M.)

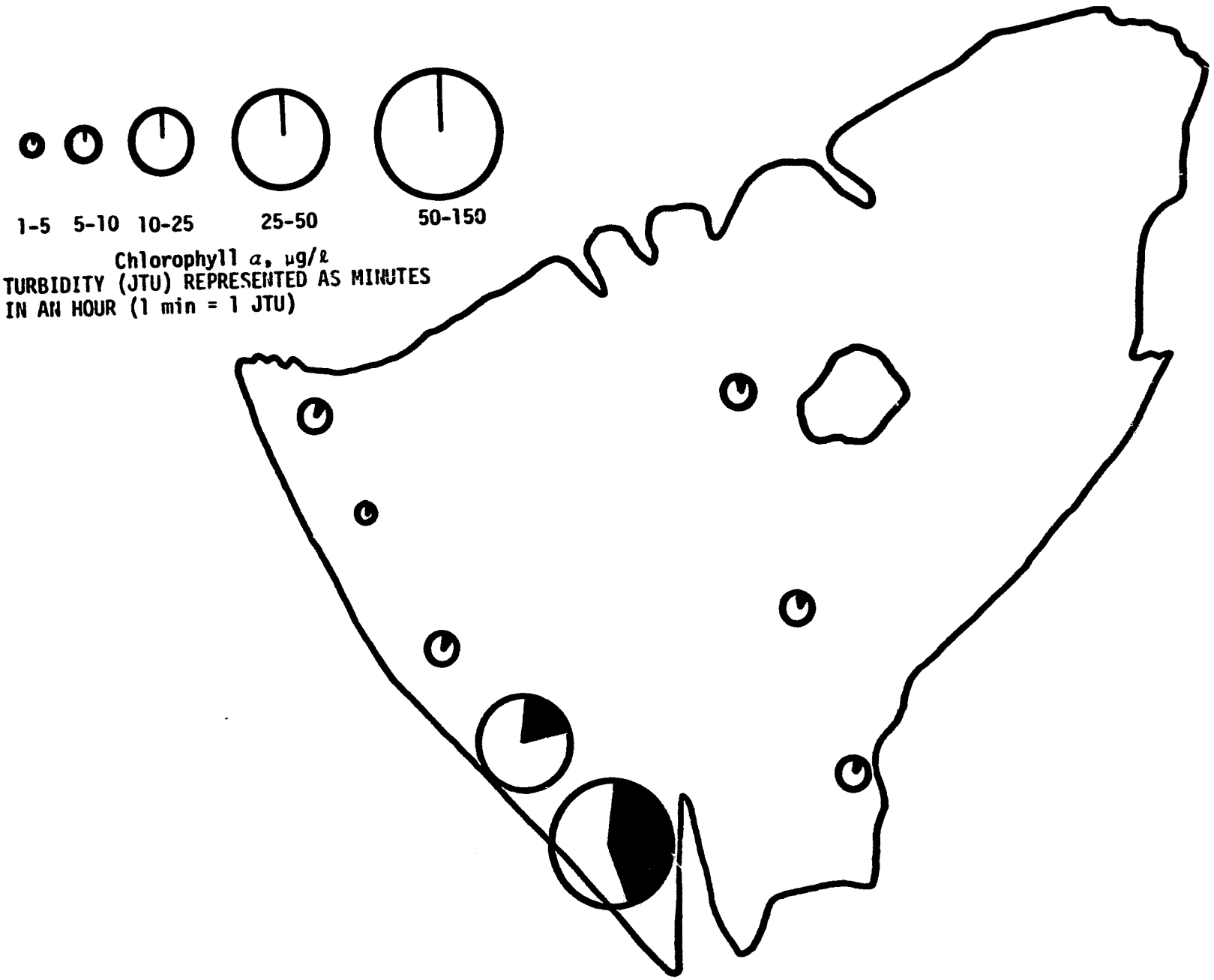

FIGURE 57. CHLOROPHYLL AND TURBIDITY IN PERRIS LAKE, 2 OCTOBER 1974 (P.M.)

obtained. The most favorable time of day is usually early morning before winds have picked up (i.e., 0700-0900 hours).

APPENDIX

VISUAL DENSITY UNIT CONTRAST VALUES VS. WAVEBAND VARIABLE FOR PICTURE SCENES SHOWING DISTINCT AQUATIC SPECTRAL SIGNATURES

(Note: No attempt has been made to determine the statistical significance of the values presented here. Rather, the table summarizes the type of information which can be obtained by analyzing aerial photography by simple, straightforward techniques which anyone unfamiliar with modern densitometry could follow. The data presented have been selected as being exemplary of the wide range of conditions present on-site during the study dates. Correlations noted are based upon the simple technique noted in the methods section, and hence can only be considered generalized statements.)

S = Silverwood C = Castaic P = Perris Py = Pyramid

Date (1974)	Sta.	Object in View	Turbidity JTU	Chl a µg/ℓ	Waveband		Correlation
					Red IR	Green Blue	
7/11	S-2	Turbidity Plume	18	9.9	11 1	11 6	Good general correlation between increased density units in the green and red wavebands and increased turbidity. Over the range of turbidity encountered, the spectral response appeared to increase linearly. No increase in reflectance could be ascribed solely to variations in Chl a at the levels encountered, although they may contribute to increased contrast associated with turbidity. No attempt was made to determine statistical significance.
7/12	C-26	Shoreline Erosion	7.2	11.5	5 0	3 0	
9/12	C-8	Shoreline Erosion	36	37	15 1	15 10	
7/12	C-24	Shoreline Erosion	6.7	11.5	4 0	3 0	
7/12	Py-1	Shoreline Erosion	32	2.8	14 0	14 8	

APPENDIX (continued)

Date (1974)	Sta.	Object in View	Turbidity JTU	Chl *a* µg/ℓ	Waveband		Correlation
					Red IR	Green Blue	
7/12	C-6	Heavy Debris	25	32.3 wet weight of debris 12.5 g/ℓ	1 15	5 5	Correlation between increased amounts of biomass in the form of debris and IR contrast. No such contrast in the case of dead biomass in the form of detached *Spirogyra*. No comparison between the wet weight of *Spirogyra* and debris can be made, as debris retains more water on filtration; but in each case, biomass appeared massive.
7/12	C-9	Light Debris	6.5	16.7 wet weight of debris 5.0 g/ℓ	7 10	1 1	
9/12	P-16	Detached *Spirogyra*	20	51	12 5	15 0	
9/12	P-17	*Spirogyra* Concentration	20	est. 50,000	5 15	5 0	Correlation between increase in biomass and increased contrast in IR waveband, but correlation does not appear linear. Increased reflectance due to bottom effects primarily in the visible wavebands.
9/12	P-16	Clear water outside algal growth-bottom reflectance	6	5.0	15 0	15 0	
9/12	P-3	Blue-green algal patches	4	7.5	2 3	3 3	
9/12	P-4	Clear water outside patch	5	4.5	0 0	0 0	

APPENDIX (continued)

Date (1974)	Sta.	Object in View	Turbidity JTU	Chl *a* µg/ℓ	Waveband		Correlation
					Red IR	Green Blue	
9/12	P-9	Outside Patch	5	9.5	0 0	0 0	See previous page.
11/2	C-7	No Patchiness	13	74.9	0 0	0 0	

REFERENCES

1. Bondurant, D.C. and R.H. Livesey. "Reservoir Sedimentation Studies," Paper presented at International Symposium of Man-Made Lakes, Knoxville, Tennessee, May 3-7, 1971. Proceedings edited by Ackermann, W.C., G.F. White, and E.B. Worthington, Man-Made Lakes: Their Problems and Environmental Effects, Washington, D.C., American Geophysical Union, 1973.

2. Lundquist, C.E. "Applied Remote Sensing of Water Pollution," Paper presented at Earth Resources Observation and Information Analysis System Conf., Tullahoma, Tennessee, March 26-28, 1973. Proceedings edited by F. Shahroki, Remote Sensing of Earth Resources, Vol. II, pp. 1121-1135, University of Tennessee Space Inst., 1973.

3. Horne, A.J. The Ecology of Clear Lake Phytoplankton, Clear Lake Algal Research Unit Special Report, 116 pp., 1975.

4. Roohe, E. "The Primary Production in Lakes: Some Results and Restrictions of the ^{14}C-Method," RAPP Proc. Verb. Cons. Int. Explorer Mer., 144:122-128, 1958.

5. Horne, A.J. and R.C. Wrigley. "The Use of Remote Sensing to Detect How Wind Influences Planktonic Blue-Green Algal Distribution," Verh. Int. Ver. Limnol., 19:784-791, 1975.

6. Wrigley, R.C. and A.J. Horne, "Remote Sensing and Lake Eutrophication," Nature, 250:213-214, 1974.

7. Goldman, C.R., R.C. Richards, H.W. Paerl, R.C. Wrigley, V.R. Oberbeck, and W.I. Quaide. "Limnological Studies and Remote Sensing of the Upper Truckee River Sediment Plume in Lake Tahoe, California — Nevada," Remote Sensing of Environment, 3:49-67, 1974.

8. California Department of Water Resources, The California State Water Project in 1968, Appendix C; Description and Status, Bulletin 132-68, Sacramento, p. 3, 1968.

9. Hergenrader, G.L. and M.J. Hammer. "Eutrophication of Small Reservoirs in the Great Plains," in Ackermann, W.C., G.F. White, and E.B. Worthington, Man-Made Lakes: Their Problems and Environmental Effects, Washington, D.C., Amer. Geophys. Union, 1973.

10. Grew, G.W. "Signature Analysis of Reflectance Spectra of Phytoplankton and Sediment in Inland Waters," Paper presented at Earth Resources Observations and Information Analysis System Conf., Tullahoma, Tennessee, March 26-28, 1973, Proceedings edited by Shahroki, F., Remote Sensing of Earth Resources, Vol. II, pp. 1147-1172, Univ. of Tennessee Space Insti., 1973.

11. Bressette, W.E. and P.E. Lear. "The Use of Near-Infrared Reflected Sunlight for Biodegradable Pollution Monitoring," Paper presented in Proceedings of Second Conference on Environmental Quality

REFERENCES (continued)

Sensors. National Environmental Research Center, Las Vegas, Nevada, October 10-11, 1973.

12. Wezernak, Lyzenga and Polcyn. "Cladophora Distribution in Lake Ontario (IFYGL)," EPA Ecological Research Series, EPA-660/3-74-028, National Environmental Research Center, December 1974.

13. Clarke, G.L., G.G. Ewing and C.J. Lorenzon. "Spectra of Backscattered Light from the Sea Obtained from Aircraft as a Measure of Chlorophyll Concentration," Science, 167:1119-1121, 1970.

14. Wezernak, C.T., *et al.* "Remote Sensing Studies in the New York Bight," Tech. Report #109300-S-F, Environmental Research Institute of Michigan, 1975.

15. Ruttner, Franz. Fundamentals of Limnology, Univ. Toronto Press, 1963.

16. Talling, J.F. and D. Driver. "Some Problems in the Estimation of Chlorophyll *a* Phytoplankton," in Doty, M.S. (Ed.), Proc. Conf. Primary Productivity Measurement, Marine Freshwater, USAES TID-7633, pp. 142-146, 1963.

17. Malan, O.G. "Color Balance of Color IR Film," Photogrammetric Eng., 40:3, 311-316, 1974.

18. Naftzger, H.J. Spectral Signatures of Aquatic Phenomena, Ph.D. Thesis, University of California, Berkeley, California, (In Preparation).

19. Horne, A.J. and C.R. Goldman. "Nitrogen Fixation in Clear Lake, California, I. Seasonal Variation and the Role of Heterocysts," Limnol. Oceanogr., 17:678-692, 1972.

20. Horne, A.J., J.E. Dillard, D.K. Fujita, and C.R. Goldman. "Nitrogen Fixation in Clear Lake, California, II. Synoptic Studies on the Autumn *Anabaena* Bloom," Limnol. Oceanogr., 17:693-703, 1972.

21. Photography Through the Microscope, Eastman Kodak Co., Rochester, New York, 1970.

22. Heller, R.C. "Imaging with Photographic Sensors," from Remote Sensing with Special Reference to Algae and Forestry, Natl. Acad. Sciences, Washington, D.C., 1970.

23. Klebahn, H. "Gasvakuolen, ein bestandteilderzellen der Wasserblütebildenden Pycochromacein," Flora, Jena, 80:241-282, 1895.

24. Holter, M.R. "Imaging with Non-Photographic Sensors," from Remote Sensing, Natl. Acad. Sciences, Washington, D.C., 1970.

25. Hutchinson, G.E. A Treatise on Limnology Vol. I, New York: John Wiley, 1957.

REFERENCES (continued)

26. Whitney, L.V. "Transmission of Solar Energy and the Scattering Produced by Suspensoids in Lake Waters," Trans. Wis. Acad. Sci. Arts, Lett., 31:201-221, 1938.

27. Benson, M.L., W.G. Sims, G. Hildebrandt, and H. Kenneweg. "The Truth about False Colour Film," Photogrammetric Record, 6:446-651, 1970.

28. Van Domelen, J.F. Photographic Remote Sensing – A Water Quality Management Tool, Ph.D. Thesis, Univ. of Wisconsin, Madison, Wisconsin, 1974.

29. Ross, P.S. "Simple Multispectral Photography and Additive Color Viewing," Photogrammetric Eng., 39:377-384, 1973.

30. Gates, D.M. "Physical and Physiological Properties of Plants," from Remote Sensing, Natl. Acad. Sciences, Washington, D.C., 1970.

31. Yentch, Charles S. "The Influence of Phytoplankton Pigments on the Color of Sea Water," Deep-Sea Research, 7:1-9, 1960.

32. Silvestro, F.B. and K.R. Piech. Project Aqua-Map II Development of Aerial Photography as an Aid to Water Quality Management, Cal. No. V.T.-2614-O-1, Cornell Aeronautical Laboratory, Buffalo, New York, 1969.

33. Arvesen, J.C., E.C. Weaver, and J.P. Millard. "Rapid Assessment of Water Pollution by Airborne Measurement of Chlorophyll Content," Joint Conference on Sensing of Environmental Pollutants, Palo Alto, California, November 8-10, 1971. AIAA Library, 750 3rd Avenue, New York, New York 10017.

34. Duntley, S.Q. "Detection of Ocean Chlorophyll from Earth Orbit," Scripps Institute of Oceanography, Paper presented at 4th Annual Earth Resources Program Review, Houston, Texas, January 17-21, 1972.

35. Gramms, L.C. and W.C. Boyle. "Reflectance and Transmittance Characteristics of Several Selected Green and Blue-Green Algae," Report #5, Institute for Environ. Studies, Remote Sensing Program, Univ. of Wisconsin, July 1971.

36. Horne, A.J. and H.J. Naftzger. Spectral Reflectance by Blue-Green Algal Blooms, (In Preparation).

37. Wolley, J.T. "Reflectance and Transmittance of Light by Leaves," Plant Physiol., 47:656-662, 1971.

38. Coleman, S.W. and E. Rabindwitch. "Evidence of Photoreduction of Chl *in vivo*," J. Phys. Chem., 63:30-34, 1959.

REFERENCES (continued)

39. Walsby, A.E. "The Structured Function of Gas Vacuoles," Bact. Revs., 36:1-31, 1972.

40. Walsby, A.E. "Pressure Relationships of Gas Vacuoles," Proc. Roy. Soc. Lond. B., 178:301-326, 1971.

41. Govindjee and B.Z. Braun. "Light Absorption, Emission and Photosynthesis," in Stewart, W.D.P. (Ed.), Algal Physiology and Biochemistry, Univ. of Calif. Press, Berkeley, pp. 346-379, 1974.

42. Walsby, A.E. "A Portable Apparatus for Measuring Relative Gas-Vacuolation, the Strength of Gas Vacuoles and Turgor Pressure in Planktonic Blue-Green Algae and Bacteria," Limnol. Oceanogr., 18:653-658, 1973.

43. Govindjee and B.Z. Braun. "Light Absorption, Emission and Photosynthesis," Scientific American, 231:68-88, 1974.

44. Reynolds, R.C. "Growth, Gas Vacuolation and Buoyancy in a Natural Population of Blue-Green Algae," Freshwater Biol., 2:87-106, 1972.

45. Gausman, H.W. "Leaf Reflectance of Near-Infrared," Photogrammetric Eng., 40:183-191, 1974.

46. Powell, T.M., P.J. Richerson, T.M. Dillon, B.A. Agee, B.J. Dozier, D.A. Godden, and L.O. Myrup. "Spatial Scales of Current Speed and Phytoplankton Biomass Fluctuations in Lake Tahoe," Science, 189:1088-1090, 1975.

47. Horne, A.J. and R.C. Wrigley. Remote Sensing of Large Blue-Green Algal Blooms in Clear Lake, California, (In Preparation).

48. Horne, A.J., P. Javornicky, and C.R. Goldman. "A Freshwater 'Red Tide' on Clear Lake, California," Limnol. Oceanogr., 16:684-689, 1971.

49. Lewin, R.A. Physiology and Biochemistry of Algae, New York: Academy Press, 1962.

50. Yost, E. and S. Wenderoth. "Coastal and Estuarine Applications of Multispectral Photography," Paper presented at 4th Annual Earth Resources Program Review, Houston, Texas, January 17-21, 1972.

51. NASA, Third Earth Resources Technology Satellite-1 Symposium, 1973.

52. ERIM, Tenth International Symposium on Remote Sensing of Environment, 1975.

REFERENCES (continued)

53. Hefner, J., W. Brown and F.J. Wobber. "Aerial Photography for Wetland Management," Photogr. Appl. Sci. Technol. Med., November 1974.

54. Rango, A., J.R. Graves and R.J. DeRycke. "Observations of Arctic Sea Ice Using the Earth Resources Technology Satellite (ERTS-1)," Arctic, 26:337-339, 1973.

55. Welch, R.I., A.D. Marmelstein and P.M. Maughan. Aerial Spill Prevention Surveillance During Sub-Optimum Weather, Environmental Protection Agency Report EPA-R2-73-243, 56 pp., 1973.

56. Soules, S.D. "Sun Glitter Viewed from Space," Deep-Sea Research, 17:191-195, 1970.

57. Pionke, H.B. and B.J. Blanchard. "The Remote Sensing of Suspended Sediment Concentrations of Small Impoundments," Water Air Soil Poll., 4:19-32, 1975.

58. Colwell, J.E. "Vegetation Canopy Reflectance," Remote Sensing Envir., 3:175-183, 1974.

59. Strong, A.E. "Remote Sensing of Algal Blooms by Aircraft and Satellite in Lake Erie and Utah Lake," Remote Sensing Envir., 3:99-107, 1974.

60. Moore, G.K. and M. Deutsch. "ERTS Imagery for Ground Water Investigations," Ground Water, 13:214-226, 1975.

61. Deutsch, M. and F. Ruggles. "Optical Data Processing and Projected Applications of ERTS-1. Imagery Covering 1973 Mississippi River Floods by the NOAA-2 Satellite," Wat. Resources Bull., 10:1040-1049, 1974.

62. Wiesnet, D.R., D.F. McGinnis and J.A. Pritschard. "Mississippi River Floods by the NOAA-2 Satellite," Wat. Resources Bull., 10:1040-1049, 1974.

63. Alexander, S.S., J. Dan and D.P. Gold. "Use of ERTS-1 Data for Mapping Strip Mines and Acid Mine Drainage in Pennsylvania," Symp. on Significant Results from ERTS-1, Proc. Natl. Aeronautics and Space Admin., 1, Section A, pp. 569-575, 1973.

64. Colwell, R.N. "ERTS-1 Applications to California Resource Inventory," ERTS-1 Symp. Sept. 29, NASA, pp. 7-20, 1973.

65. Barnes, J.C., J.B. Clinton and D.A. Simmes. "Use of Satellite Data for Mapping Snow Cover in the Western United States," Symp. on Management and Utilization of Remote Sensing Data, Am. Soc. Photogrammetry, pp. 166-176, 1973.

REFERENCES (continued)

66. Hirsch, A. "NOAA's New York Bight Marine Ecosystems Analysis Project: An Interdisciplinary Study of the Marine Environment," Mar. Sci. Technol., 8:29-34, 1974.

67. Stevenson, R.E. "Observations from Skylab of Mesoscale Turbulence in Ocean Currents," Nature, 250:638-40, 1974.

68. Klemas, V., D. Bartlett, R. Rogers and L. Reed. "Coastal and Estuarine Studies with ERTS-1 and Skylab," Remote Sensing Envir., 3:153-174, 1974.

69. Yentsch, C.S. "Remote Sensing for Productivity in Pelagic Fisheries," Nature, 244:307-308, 1972.

70. Walker, J.E. and D.B. Dahm. "Measuring Environmental Stress," Envir. Sci. Technol., 9:714-719, 1975.

71. Bressette, W.E. and D.E. Lear, Jr. "The Use of Near-Infrared Reflected Sunlight for Biodegradable Pollution Monitoring," EPA, Paper presented at 2nd Envir. Qual. Sensors Conf., 1973.

72. Bressette, W.E. "The Use of Near-Infrared Photography for Aerial Observation of Phytoplankton Blooms," Paper presented at 2nd Ann. Conf. Remote Sensing of Earth Resources, 1973.

73. Wrigley, R.C., S.A. Klooster, M.J. Leroy, A.J. Horne and H.M. Anderson, Field Measurement of Algal Blooms by Infrared Reflectance, (In Preparation).

74. Colwell, R.N., Univ. of Calif., Dept. of Forestry, Berkeley, Ca., per. comm.

75. Fogg, G.E. "Observations on the Snow Algae of Signy Island, S. Orkney Islands, Antarctica," Proc. Roy. Soc. Lond. B, 252:279-287, 1967.

76. Seliger, H.H., J.H. Carpenter, M. Loftins and W.D. McElroy. "Mechanisms for the Accumulation of High Concentrations of Dinoflagellates in a Bioluminescent Bay," Limnol. Oceanogr., 15:234-245, 1970.

77. Thomas, E.A. "The Process of Eutrophication in Central European Lakes," in Eutrophication: Causes, Consequences, Correctives, Proc. of a Symp. 1969, National Academy of Sciences, pp. 29-49.

78. Reynolds, C.R. "Growth and Buoyancy of *Microcystis aeruginosa* in a Shallow Eutrophic Lake," Proc. Roy. Soc. Lond. B, 184:29-50, 1971.

79. Horne, A.J. and J.F. Elder. The Limnology of Lake Perris — A New Reservoir in a Semi-Arid Zone, (In Preparation).